

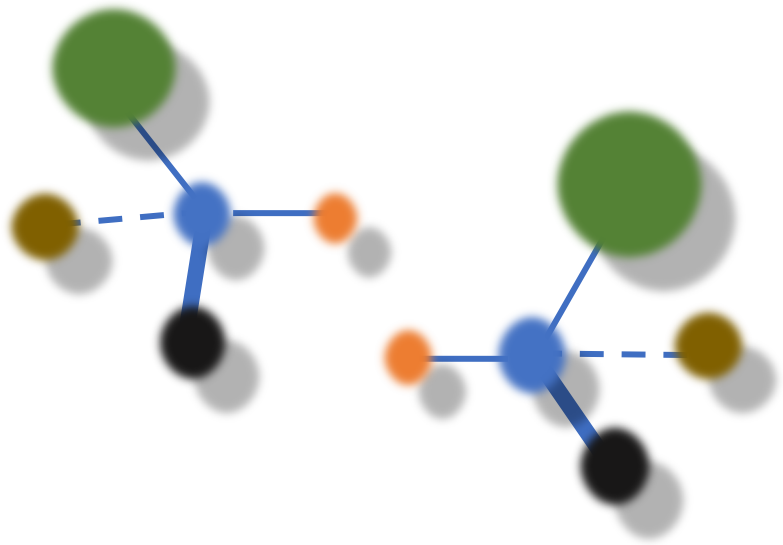


中国科学院近代物理研究所  
Institute of Modern Physics, Chinese Academy of Sciences



中国科学院大学  
University of Chinese Academy of Sciences

# Collectivity and chirality in neutron deficient $^{119}\text{Cs}$ , $^{119}\text{Ba}$ , and $^{118}\text{Cs}$ nuclei



*Kuankuan Zheng (郑宽宽)*  
IMP, CAS

*Costel Petrache*  
IJCLab, Université Paris-Saclay

*Chirality and Wobbling in Atomic Nuclei, July 10 - July 14, 2023, Huizhou, China*

## **Motivation**

- Chirality

## **Experimental setup**

## **Results and discussion**

- Isomer
- Chirality

## **Summary**



# Chirality

- ◆ It is a **common phenomenon** in nature.
- ◆ It is a simple **symmetry property** of an object or system which cannot be superimposed onto its mirror image.
- ◆ It can occur in a **static** or **dynamic** regime.

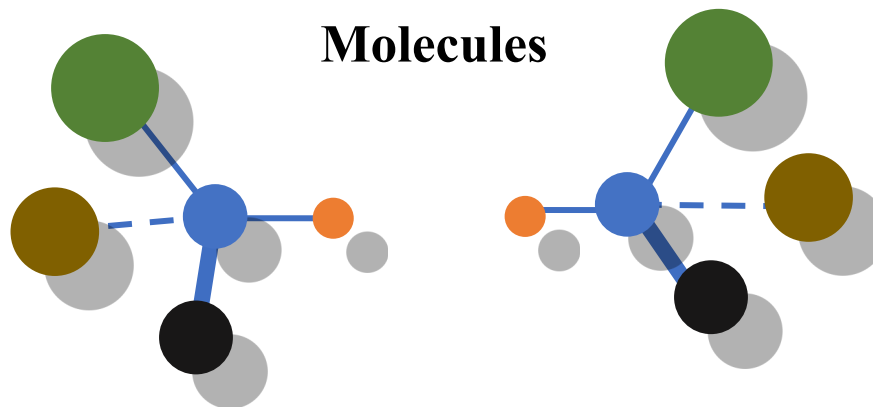
## Chiral symmetry

## Chiral symmetry breaking (chirality)

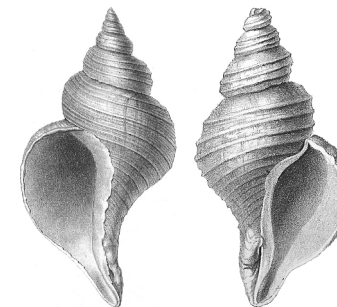
### Hands



### Molecules



### Shells of sea snail



It should be pointed out that the chirality in nature is often **static**.

How about in nuclei ???

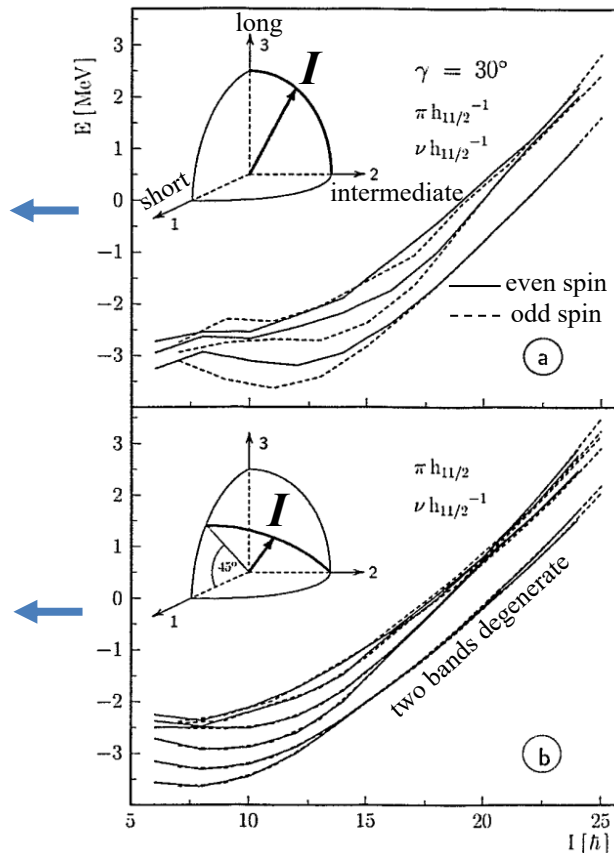
# Nuclear Chirality

Chirality in nuclei was proposed in 1997 by Frauendorf and Meng.

Collective core ( $\mathbf{R}$ ); Quasi-proton ( $\mathbf{j}_\pi$ ); Quasi-neutron ( $\mathbf{j}_\nu$ ); Total angular momentum ( $\mathbf{I}$ ).

**Band head:**  $R=0$ ;  
 $\mathbf{I}$  is parallel to the 3-axis.  
**Rotation:**  $R \neq 0$ ;  
 $\mathbf{I}$  moves into the 2-3 plane.

**Band head:**  $R=0$ ;  
 $\mathbf{I}$  lies in the 1-3 plane.  
**Rotation:**  $R \neq 0$ ;  
 $\mathbf{I}$  points to 3D.

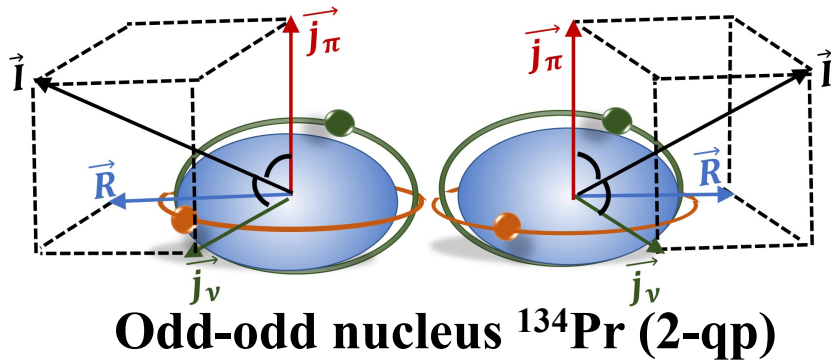


The nuclei exhibit the chirality when two conditions are satisfied, **axial-asymmetry** and **dynamic regime**: triaxial shape, and rotating around an axis out of the principal planes of the intrinsic reference system.

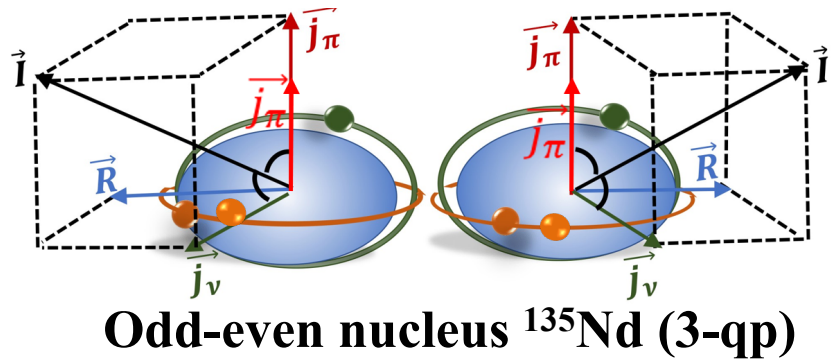
**Chiral operator:**  $\chi = \text{TR}(\pi)$   $\longrightarrow$  **Time reversal + rotation**

Nuclear Physics A, 617(2):131–147, 1997

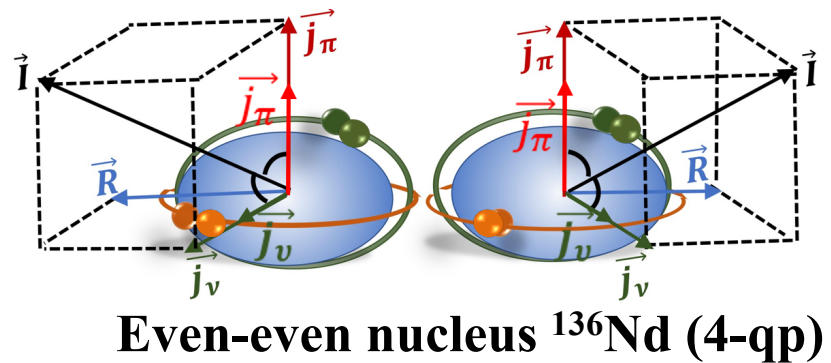
# Nuclear Chirality



Odd-odd nucleus  $^{134}\text{Pr}$  (2-qp)



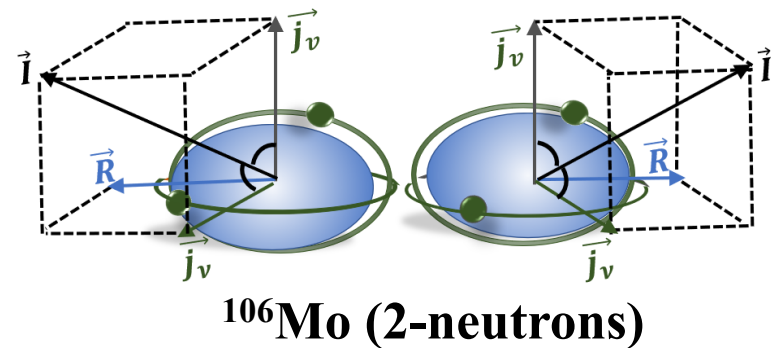
Odd-even nucleus  $^{135}\text{Nd}$  (3-qp)



Even-even nucleus  $^{136}\text{Nd}$  (4-qp)

The chiral phenomenon is spread over the different systems in **odd-odd, odd-even, even-even** nuclei with **complicated configurations**.

For a configuration with only neutrons? **yes**



$^{106}\text{Mo}$  (2-neutrons)

The chirality is generated by a neutron  $h_{11/2}$  particle and a mixed ( $d_{5/2}$ ,  $g_{7/2}$ ) hole aligned to the short and long axes, respectively.

For a configuration with only protons?

C. M. Petrache Phys. Rev. C 97, 041304(R). S. Zhu Phys. Rev. Lett. 91, 132501. S.J. Zhu Eur. Phys. J. A 25, s01, 459–462 (2005).

# Motivation

The primary motivation is to study the evolution of the nuclear structure and exotic phenomena towards the proton drip line in the 120 mass region.

Nuclei of interest:  $^{119}\text{Cs}$ ,  $^{118}\text{Cs}$ , and  $^{119}\text{Ba}$ .

 To study the properties of **collective rotational bands** from low to very high spin and to identify and extract the half-lives of the **isomeric states**;

 To search for **chiral doublet bands** and other exotic phenomena in the proton-rich deformed nuclei.

# Experimental Setup

**FOCAL PLANE**

**MARA**

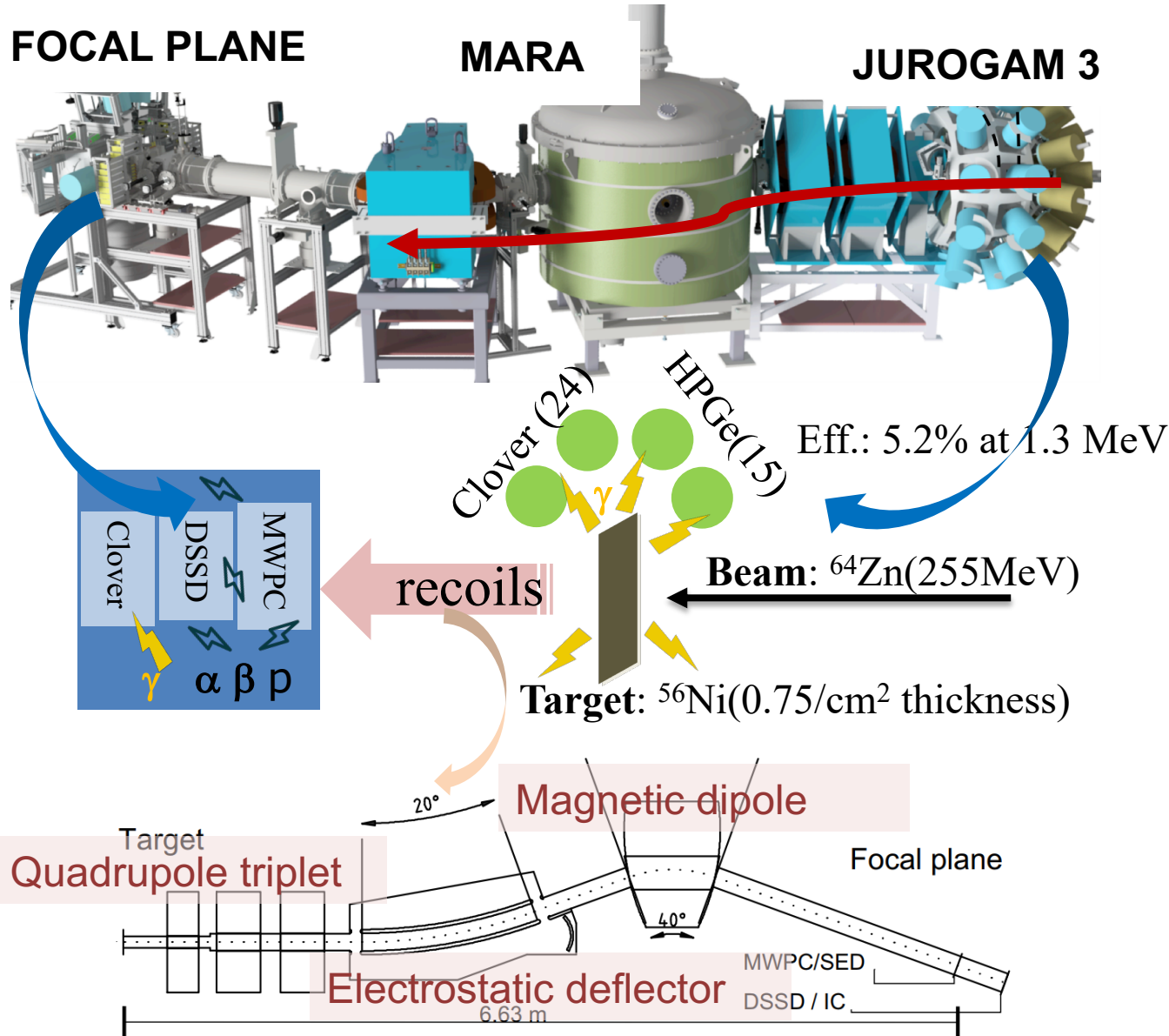
**JUROGAM 3**

**Location:** JYFL;

**Beam:**  $^{64}\text{Zn}$ , 255 MeV, 2-3 pA;

**Target:**  $^{58}\text{Ni}$  (self-supporting enriched), 0.75 mg/cm<sup>2</sup> ;

**Populated nuclei:**  
 $^{119}\text{Cs}$  (150 mb),  
 $^{119}\text{Ba}$  (20 mb) ,  
 $^{118}\text{Cs}$  (40 mb).



# Data analysis

Data: **700 Gb**

**350 files**

**$4 \times 10^{10}$  prompt  $\gamma$ -ray (fold  $\geq 3$ )** by JUROGAM 3 array.

Trigger: **Total Data Readout** data acquisition system.

Time-stamped: **100 MHz** clock with the time resolution of **10 ns**.

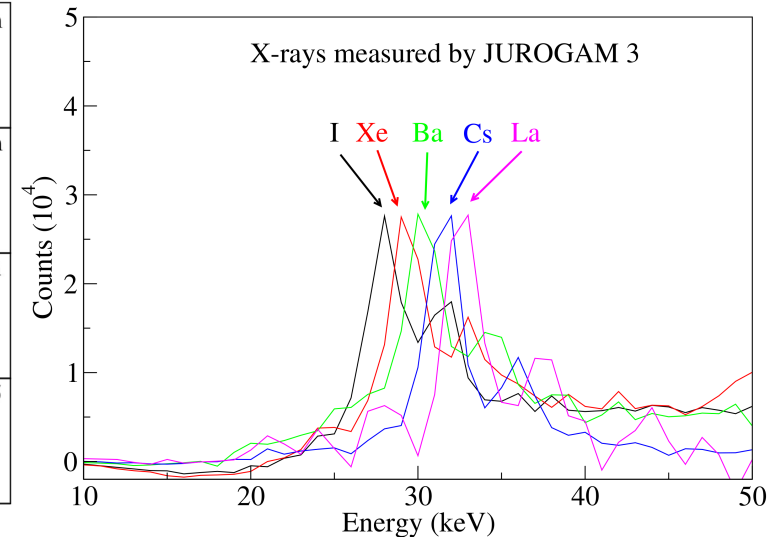
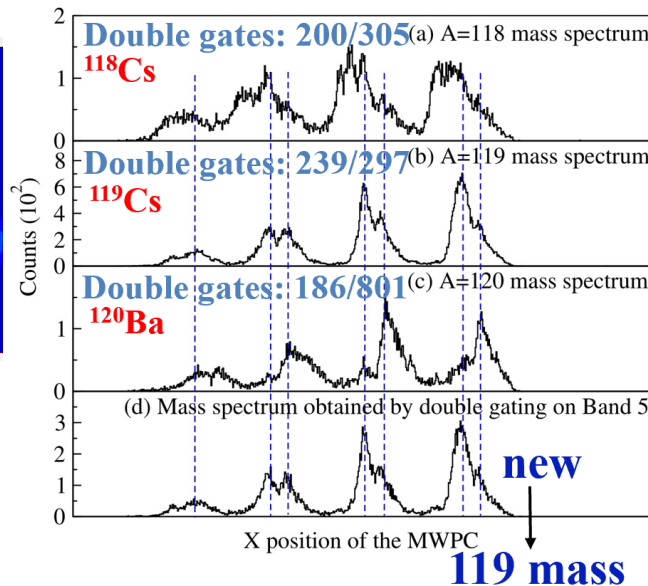
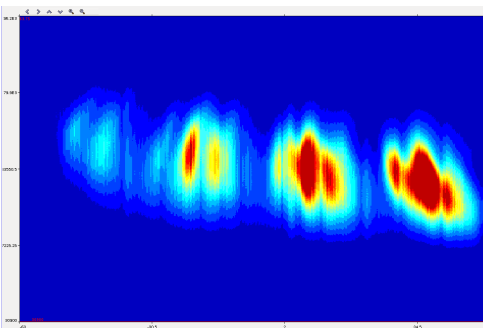
Analysis: the **GRAIN** and **RADWARE** packages.

- 1 Setting of the low-energy thresholds, **energy calibrations**, gain matching, and **efficiency calibrations**
- 2 Doppler shift correction, add-back
- 3 Analysis of the  $\gamma\gamma\gamma$ ,  $\gamma\gamma\gamma + \mathbf{recoil}$ , prompt  $\gamma\gamma$  (target position) + delayed  $\gamma$  (focal plane) coincidences
- 4 Assignment of multipolarities by using  $\mathbf{R}_{\text{DCO}}$  and  $\mathbf{R}_{\text{ac}}$

# Results: The assignment of the bands to nuclei

The assignments of the bands to  $^{119}\text{Cs}$ ,  $^{119}\text{Ba}$ , and  $^{118}\text{Cs}$  are based on:

- 1. The mass 119 and 118 detected at the MARA focal plane** in coincidence with transitions detected in JUROGAM 3;
- 2. The 31 and 32 keV  $K_{\alpha}$  X rays** of cesium and barium nuclides detected in prompt coincidence with in-band transitions.



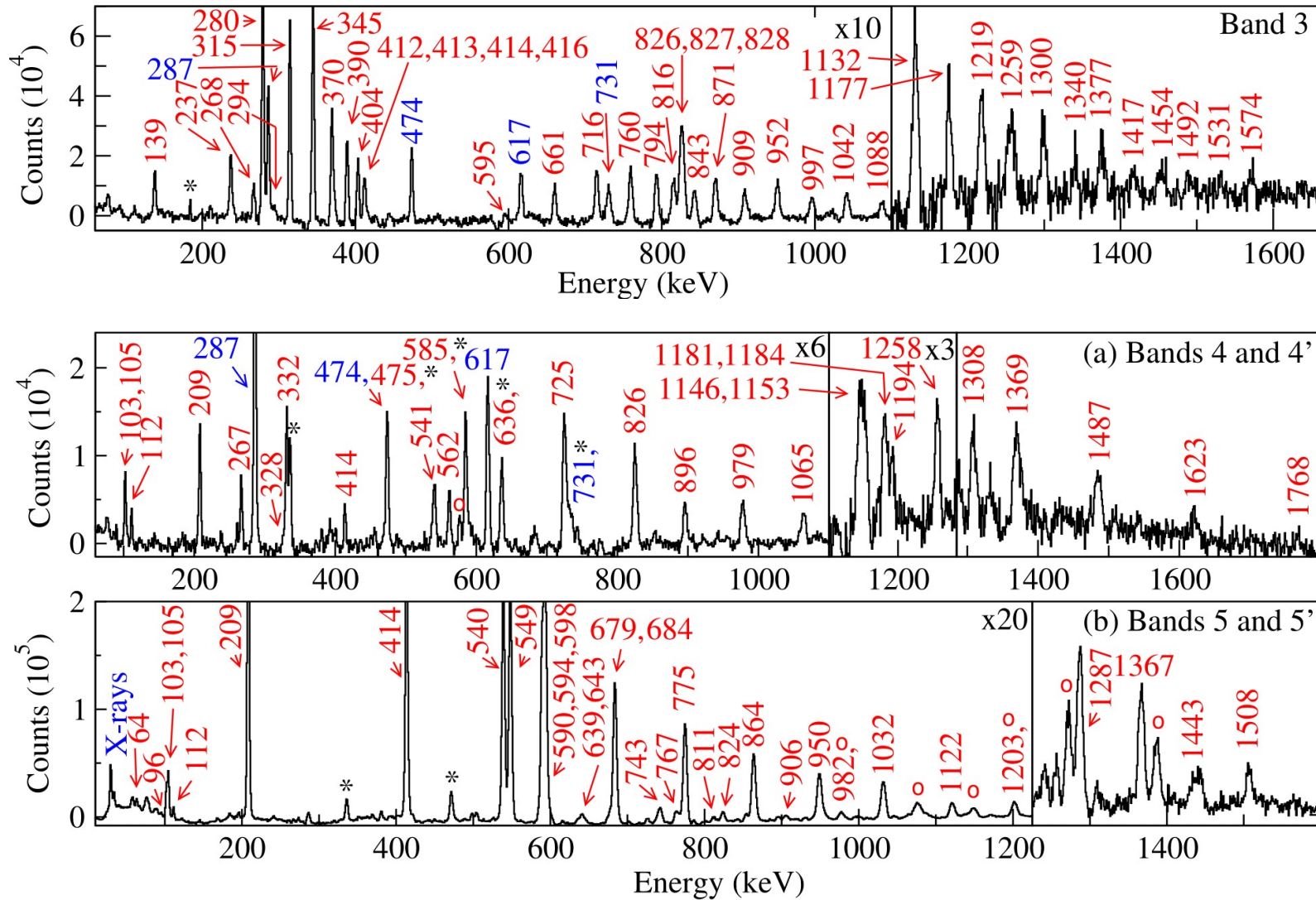
Combining information on the mass spectra and on the X-rays, we could assign new bands.







# Results: examples of energy spectra of $^{119}\text{Cs}$

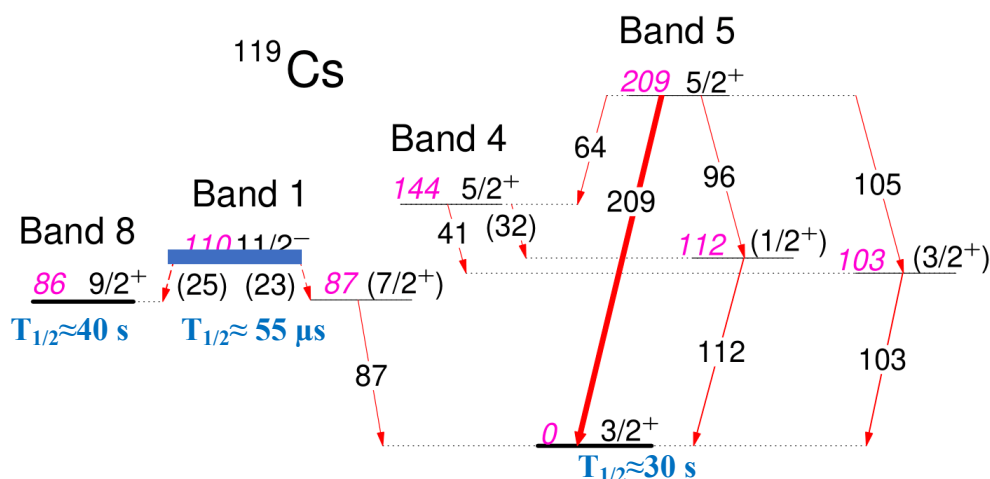


K. K. Zheng, C. M. Petrache, et al. Phys. Rev. C104 (2021) 044305

# Results: Towards complete spectroscopy of $^{119}\text{Cs}$

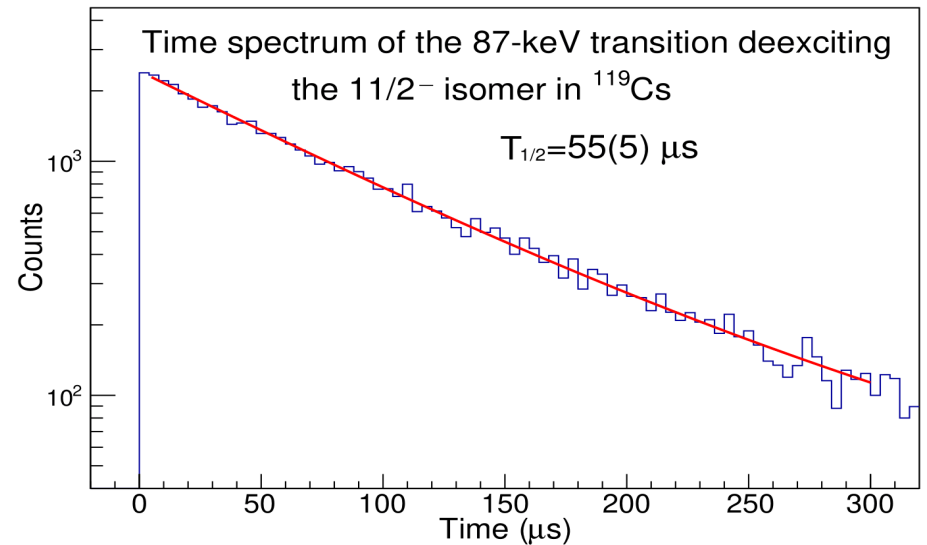
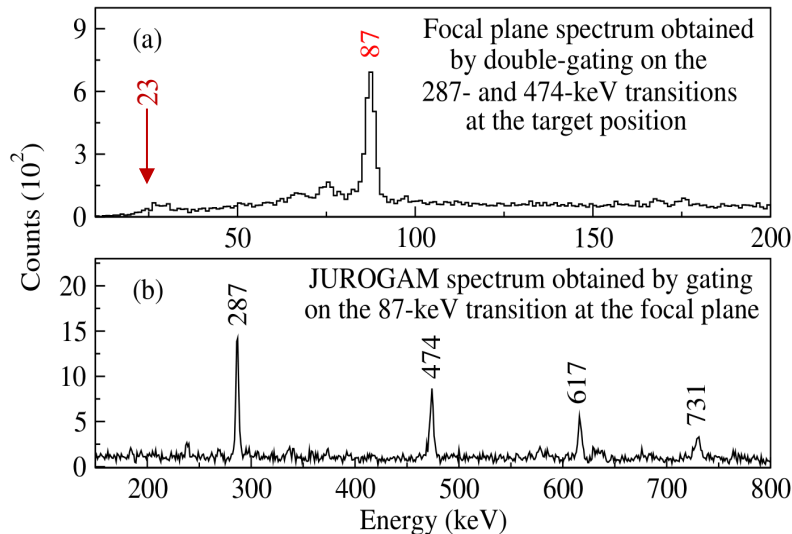
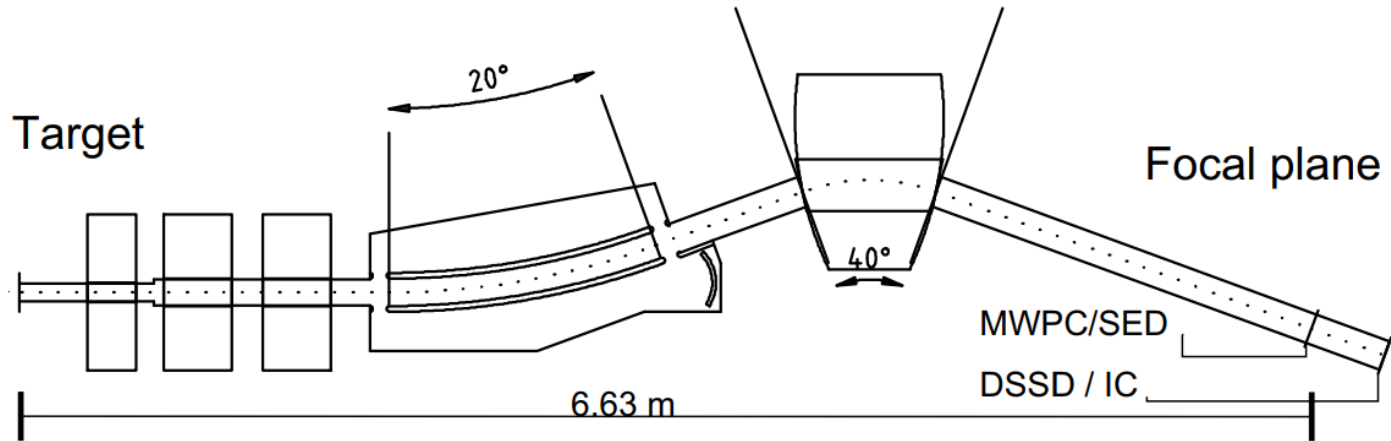
- The extension of the known bands to very **high spin** (B1 35/2-67/2) (B8 29/2-63/2);
- Identifying **eight new rotational bands**;
- All bands are interconnected by multiple transitions, thus **fixing their relative intensities**;
- **Spins and parities** are determined for most of the observed bands;
- The **configurations** of the observed bands are assigned based on **PNC-CSM calculations**.

The several new bands observed in  $^{119}\text{Cs}$  lead to one of **the most complete level schemes** of proton-rich Cs nuclei



- **Low-lying states:**  
Long-lived  $9/2^+$  (40 s) and  $3/2^+$  (30 s) isomer were known;  
**Ground state:**  $9/2^+ \rightarrow 3/2^+$  Fixed by the 209-keV (B5), 738-keV (B6-B4) four parallel cascades (105-103, 41-103, 96-112, (32)-112);  
**New isomer:**  $11/2^-$  (order (23)-87 or 87-(23)).

# Results: isomeric states of $^{119}\text{Cs}$



The extracted lifetime of the  $11/2^-$  state is  **$T_{1/2} = 55(5) \mu\text{s}$** .

# Results of PNC-CSM calculations of $^{119}\text{Cs}$

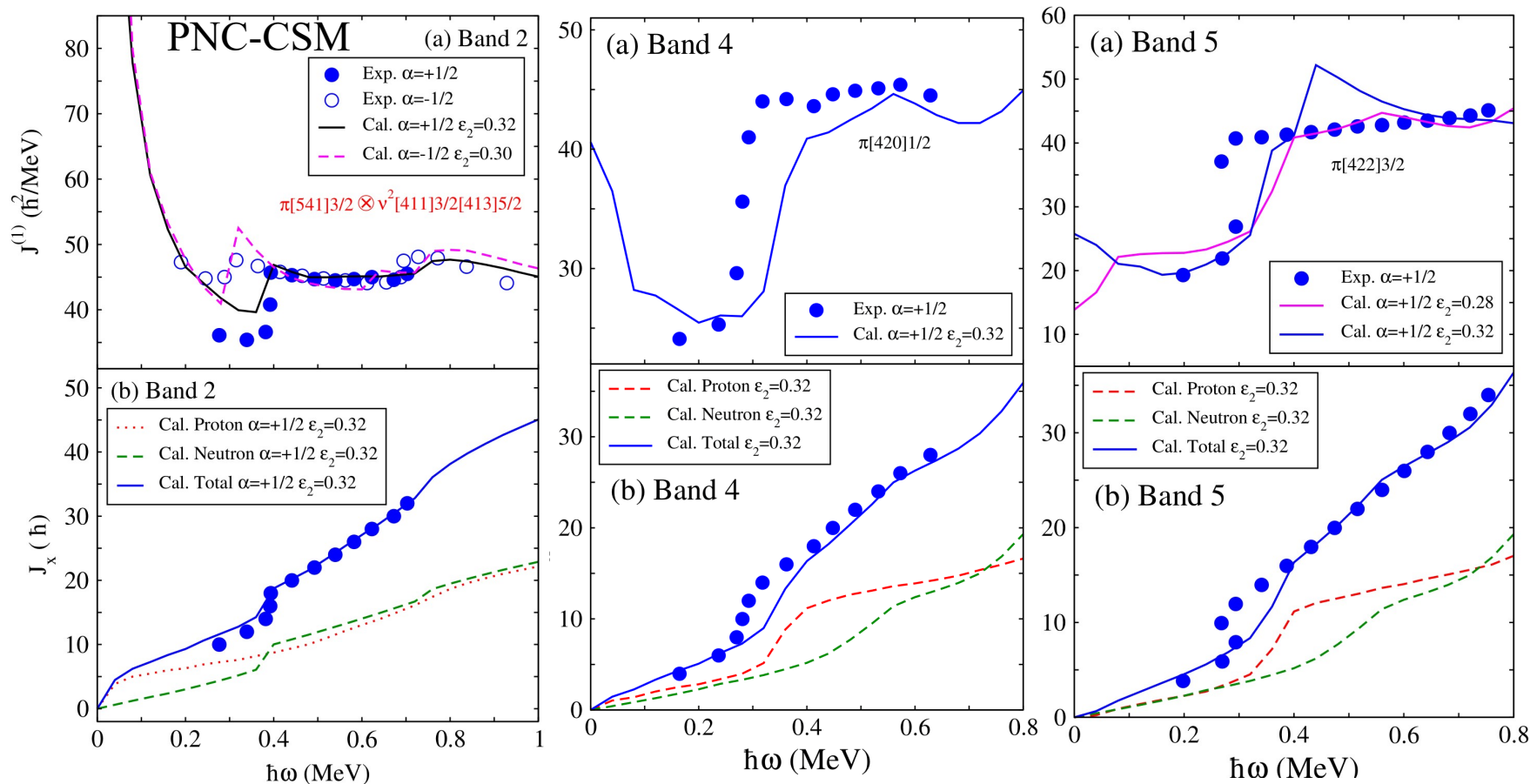
**PNC-CSM**: particle number conserving cranked shell model

This model was recently used to successfully describe the band structure in rare-earth nuclei.

- 1 The calculations have been performed assuming **axially symmetric shape**.
- 2 The parameters  $\kappa$  and  $\mu$  taken from Ref. [D. R. Inglis, Phys. Rev. 103, 1786 (1956)].
- 3 Effective monopole pairing strengths of **0.8 MeV for protons and 0.6 MeV for neutrons**.
- 4 The deformation parameters  $\varepsilon_2 = 0.32$  for most prolate bands, Band 2 ( $\alpha = -1/2$ ) ( $\varepsilon_2 = 0.30$ ) and Band 3 ( $\varepsilon_2 = -0.17$ ).

Z. H. Zhang, Phys. Rev. C 101, 055506 (2020)

# Results: examples of PNC-CSM calculations of $^{119}\text{Cs}$



**Assign** the  $\pi[541]3/2^- \otimes \nu[411]3/2^+[415]5/2^+$ ,  $\pi[420]1/2^+$  and  $\pi[422]3/2^+$  **configurations** to Bands 2, 4 and 5, respectively.

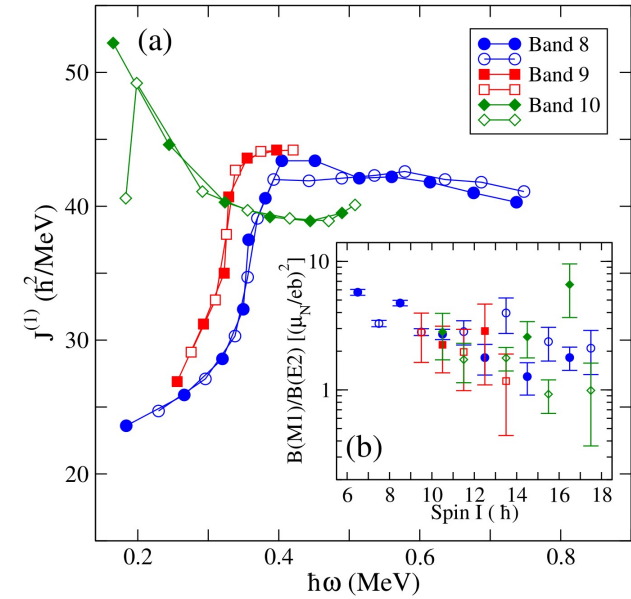
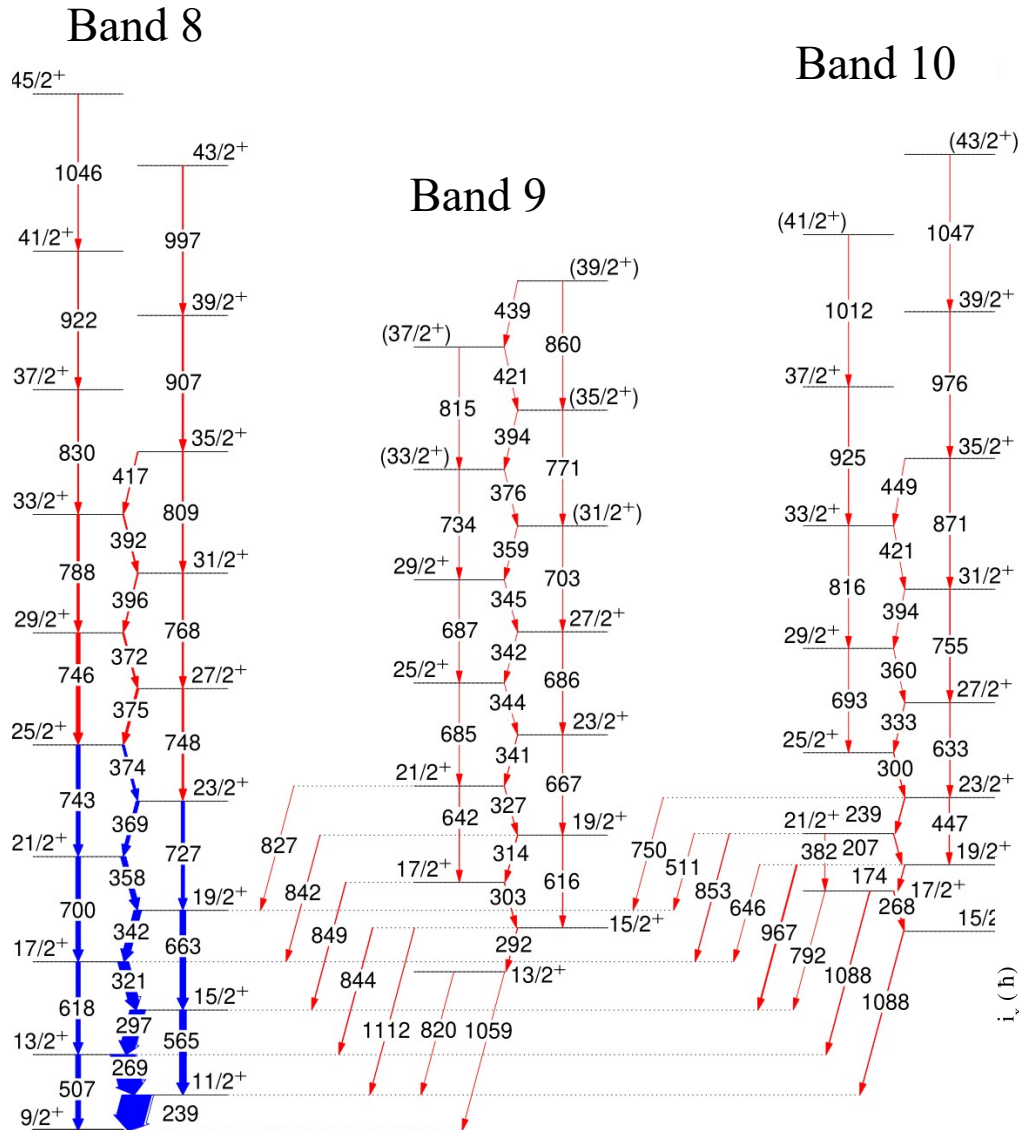
**Identify the nature of upbending (backbending).**

# Configurations of $^{119}\text{Cs}$

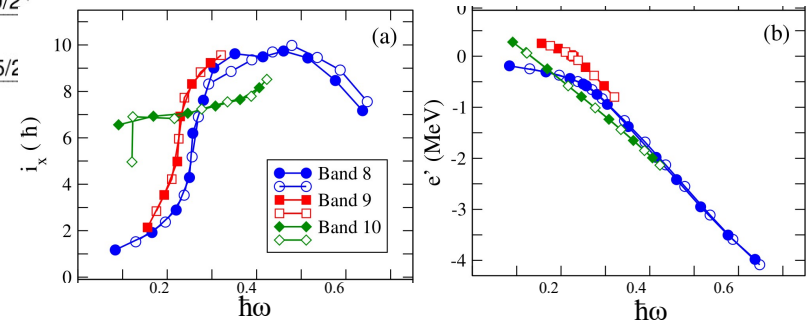
Band	Configuration	1 <sup>st</sup> crossing ( $\hbar\omega$ )	2 <sup>nd</sup> crossing ( $\hbar\omega$ )	$\pi$	$\varepsilon_2$
1	Mixed $\pi[541]3/2^--[550]1/2^-$	$v^2h_{11/2}$ (0.45)	$v^2(g_{7/2}d_{5/2})$ (0.70)	-	0.32
2	Mixed $\pi[541]3/2^--[550]1/2^-$ ( $\alpha=1/2$ )	$v^2(g_{7/2}d_{5/2})$ (0.36)		-	0.32
2	Mixed $\pi[541]3/2^--[550]1/2^-$ ( $\alpha=-1/2$ )	$v^2(g_{7/2}d_{5/2})$ (0.30)	$v^2(g_{7/2}d_{5/2})$ (0.70)	-	0.30
3	$\pi[505]11/2^-$	$v^2h_{11/2}$ (0.38)		-	-0.17
4	$\pi[420]1/2^+(\alpha=1/2)$	$\pi^2h_{11/2}$ (0.26)	$v^2h_{11/2}$ (0.40)	+	0.32
4'	$\pi[420]1/2^+(\alpha=1/2)$ $\otimes \pi^2(h_{11/2}) \otimes v^2(h_{11/2})$			+	0.32
5	$\pi[422]3/2^+(\alpha=1/2)$	$\pi^2h_{11/2}$ (0.26)	$v^2h_{11/2}$ (0.50)	+	0.32
5'	$\pi[422]3/2^+(\alpha=1/2) \otimes v^2(h_{11/2})$			+	0.32
6	$\pi[541]3/2^-(\alpha=1/2) \otimes v^2(h_{11/2}g_{7/2})$			+	0.32
7	$\pi[420]1/2^+(\alpha=1/2)$ $\otimes \pi^2(h_{11/2}) \otimes v^2(g_{7/2}d_{5/2})$			+	0.32
8	$\pi[404]9/2^+$	$\pi^2h_{11/2}$ (0.36)		+	0.32
9	$\pi[404]9/2^+$	$\pi^2h_{11/2}$ (0.30)		+	0.32
10	$\pi[541]3/2^- \otimes v^2(h_{11/2}g_{7/2})$			+	0.32



# Proton based revolving chiral bands in $^{119}\text{Cs}$

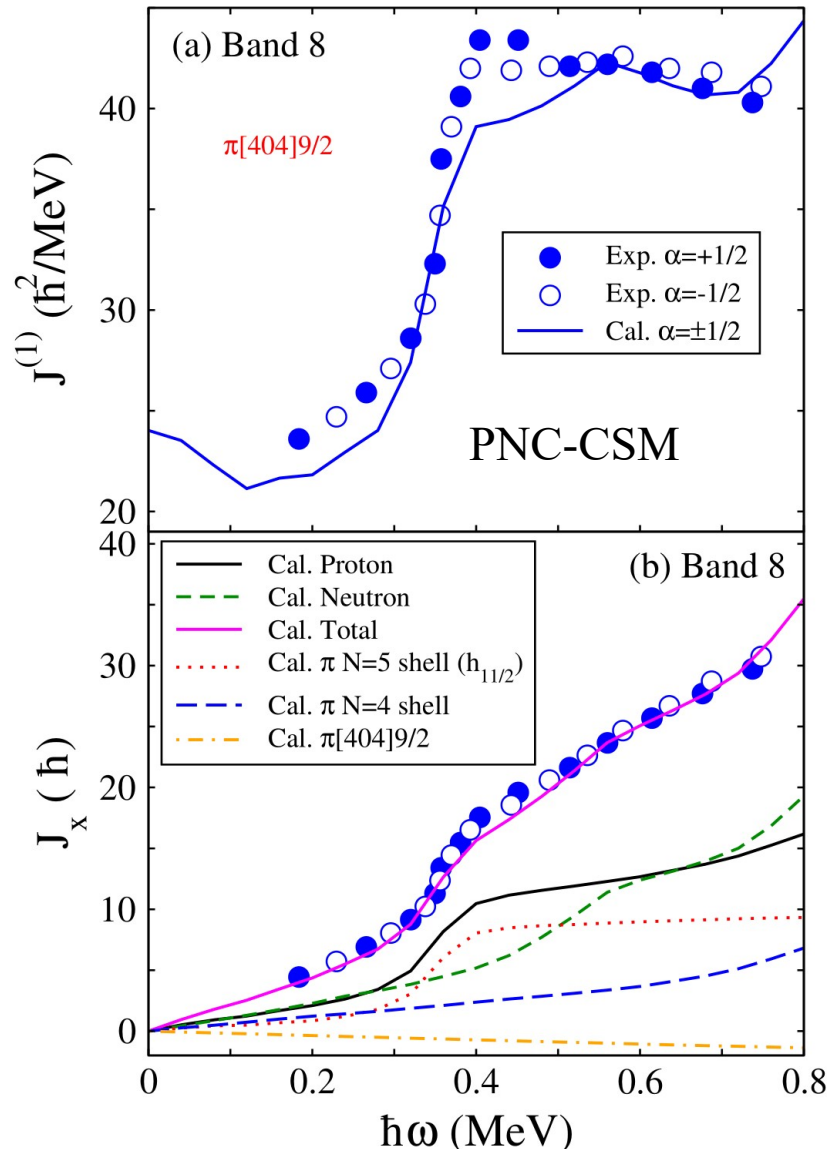


Bands 8, 9 are nearly degenerate, have similar moments of inertia and  $B(M1)/B(E2)$  ratios of reduced transition probabilities.



Chiral character ?

# Proton based revolving chiral bands in $^{119}\text{Cs}$



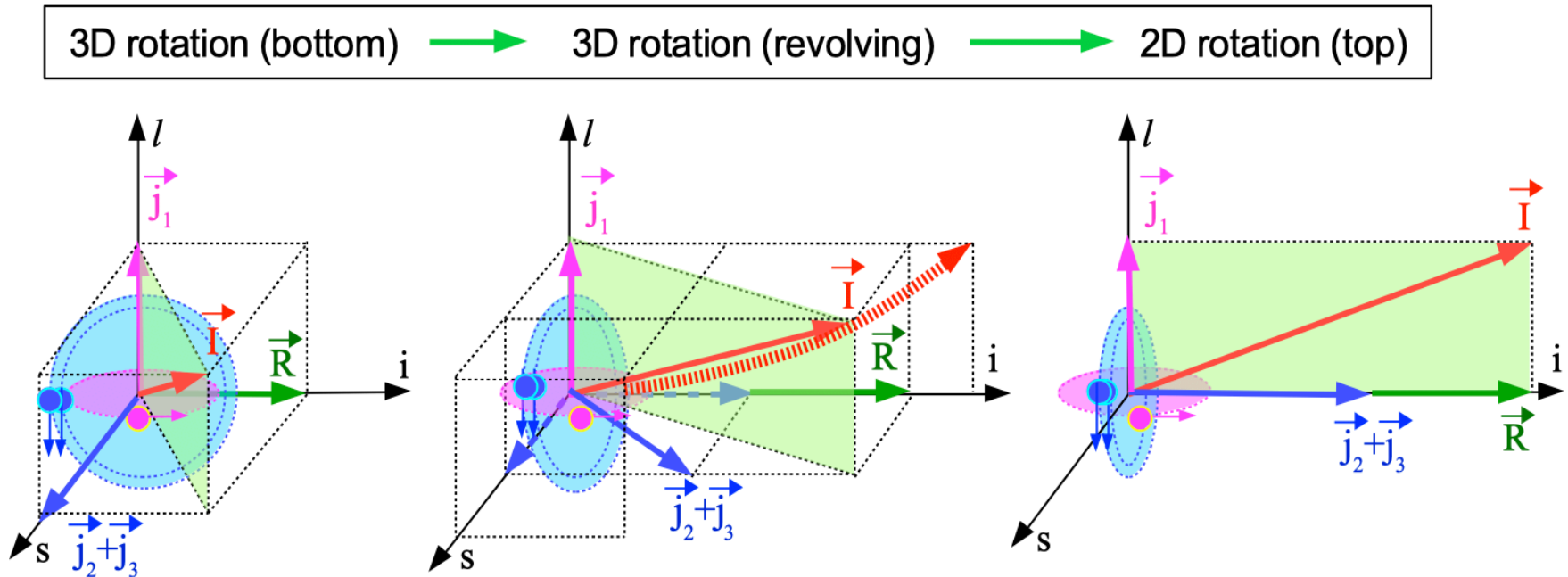
Bands 8, 9 are built on the **three-proton configuration** in the backbending region, one in the **high- $\Omega$  [404]9/2** orbital and two in **low- $\Omega$   $h_{11/2}$**  orbitals.

As for the contribution from the [404]9/2 orbital, it keeps nearly constant with rotational frequency, which means that this orbital **keeps aligned along the long axis**.

The gain of angular momentum is  $8\hbar$ , indicating the alignment of a pair of  $h_{11/2}$  particles, and the negligible contribution of the strongly-coupled [404]9/2 proton orbital.



# Proton based revolving chiral bands in $^{119}\text{Cs}$



Gamma band with Chiral character

We observed for **the first time such chiral doublet band:**

the configuration is formed by only protons;

the total angular momentum is revolving in 3D;

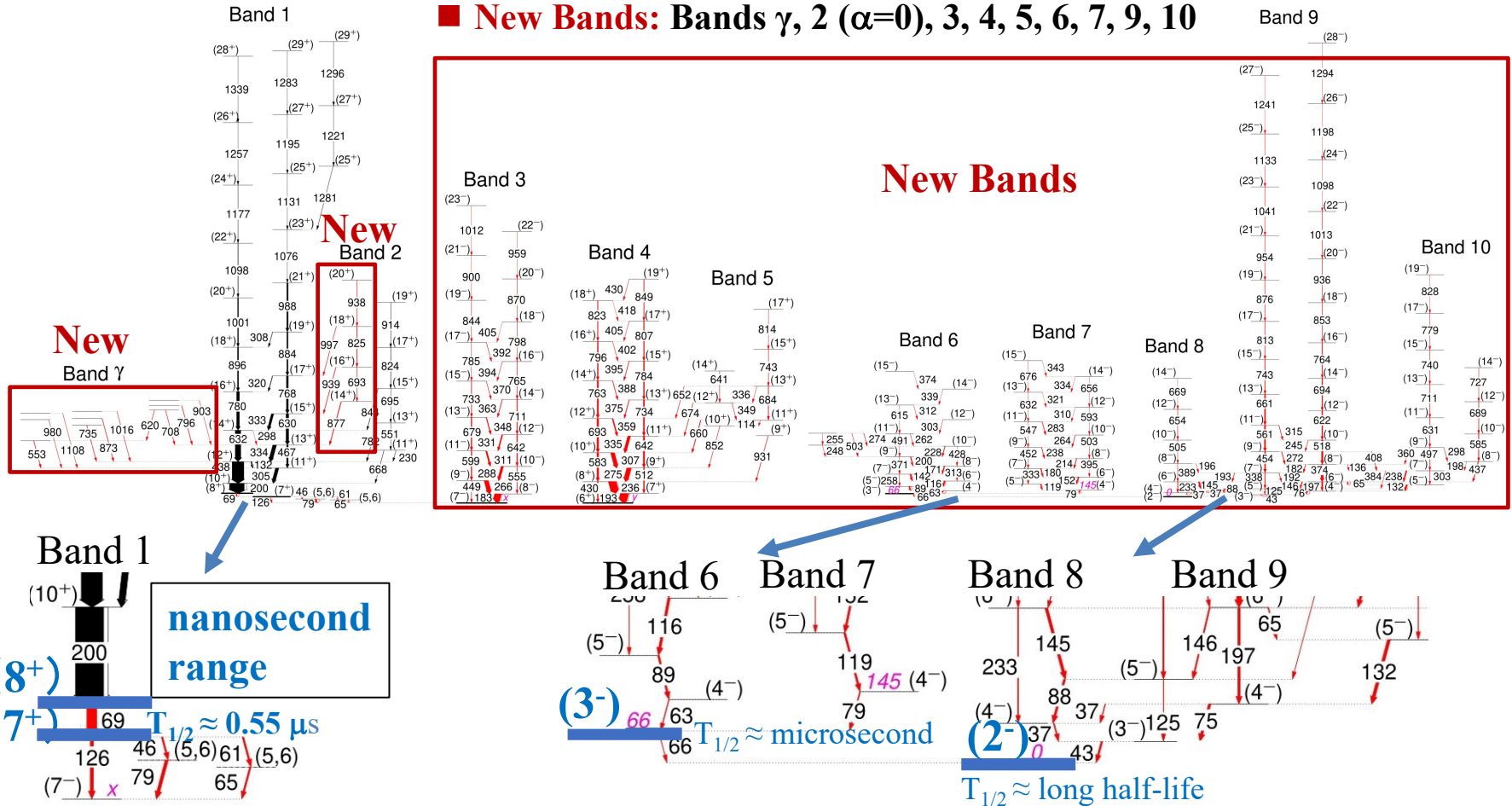
the triaxiality is not maximum ( $10^\circ$ - $15^\circ$ );

one proton keeps aligned along the long axis, while the other two are changing their orientation.

K. K. Zheng, C. M. Petrache, et al. EPJ A 59 (2022) 50

# Results: Rich band structure in $^{118}\text{Cs}$

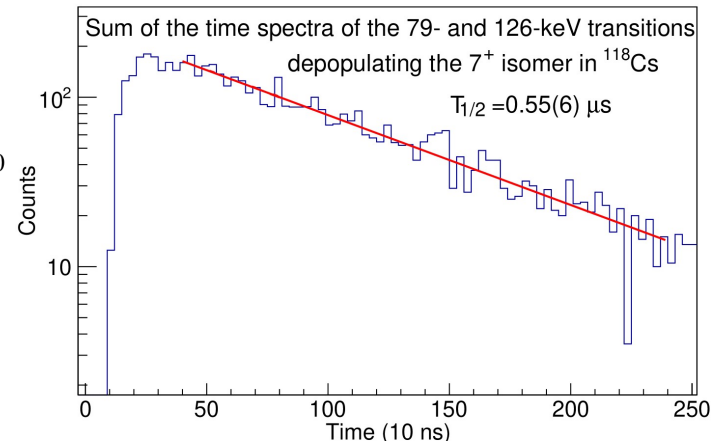
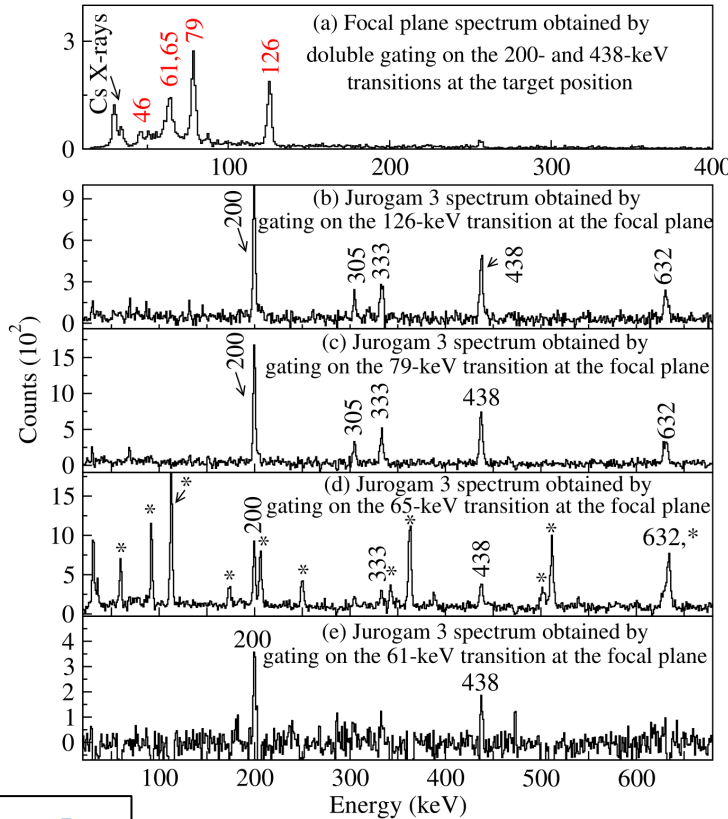
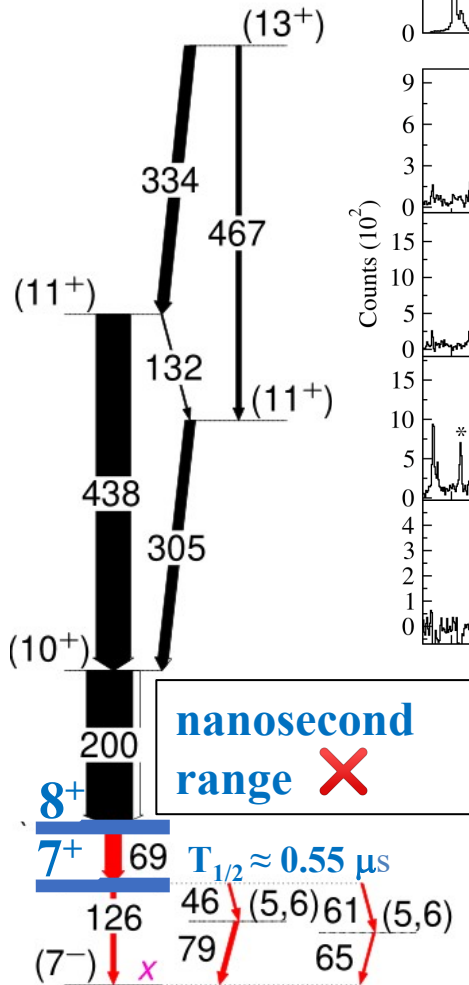
- **Known Bands:** Band 1, Band 2 ( $\alpha=1$ )
- **New Bands:** Bands  $\gamma$ , 2 ( $\alpha=0$ ), 3, 4, 5, 6, 7, 9, 10



● We reported **ten new bands**, **low-lying states**, several **isomeric states**, which leads to the **largest set of proton-neutron excitations of odd-odd Cs nuclei close to the proton drip line.**

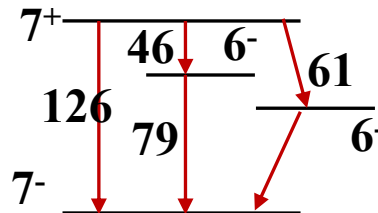
# Results: isomeric states of $^{118}\text{Cs}$

Band 1



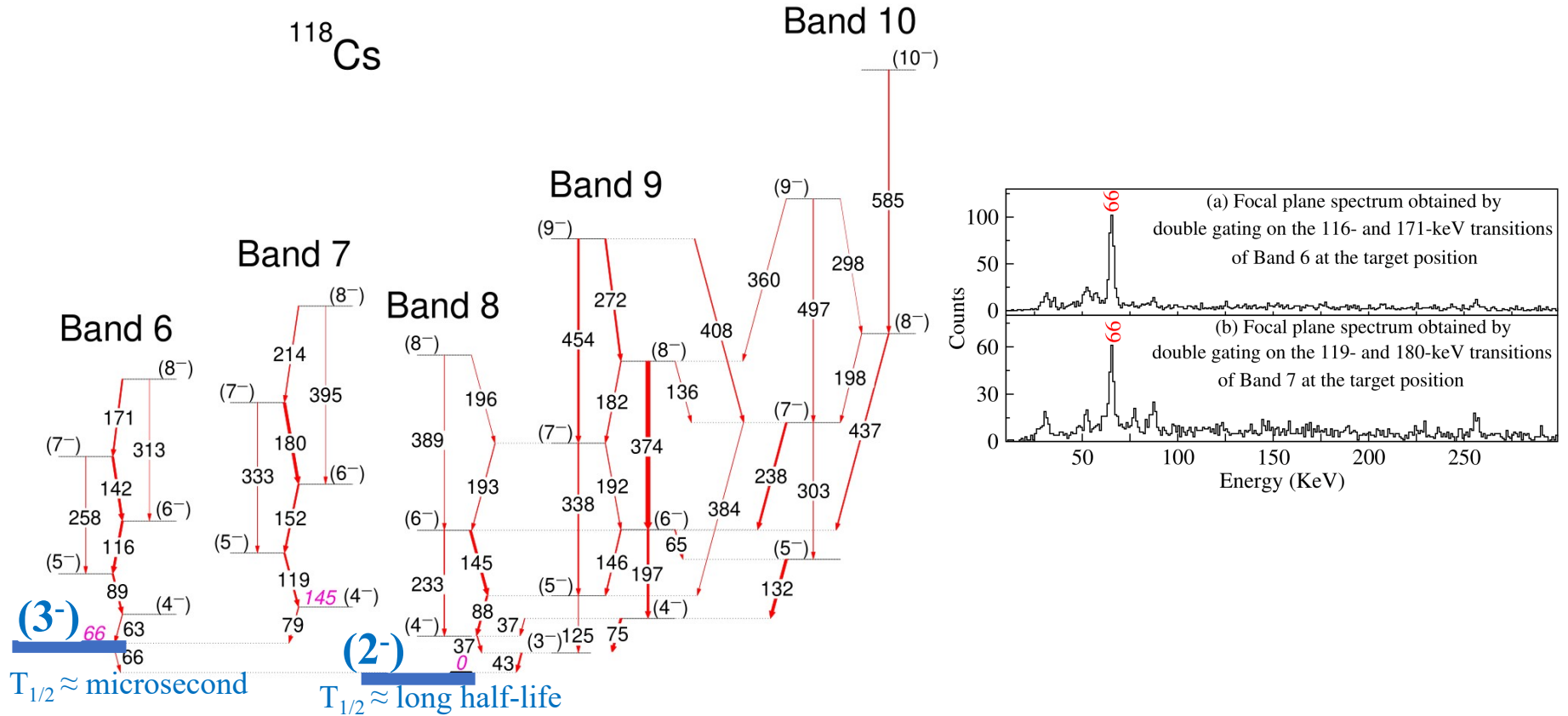
We extracted a half-life of  $T_{1/2} = 0.55(6) \mu\text{s}$  from the fit of the time spectrum of the 66-keV transition.

$$\text{Weisskopf estimate: } \frac{1}{T_{1/2}^W} = \sum_k \frac{I_\gamma(1+\alpha_k)}{T_k^W}$$



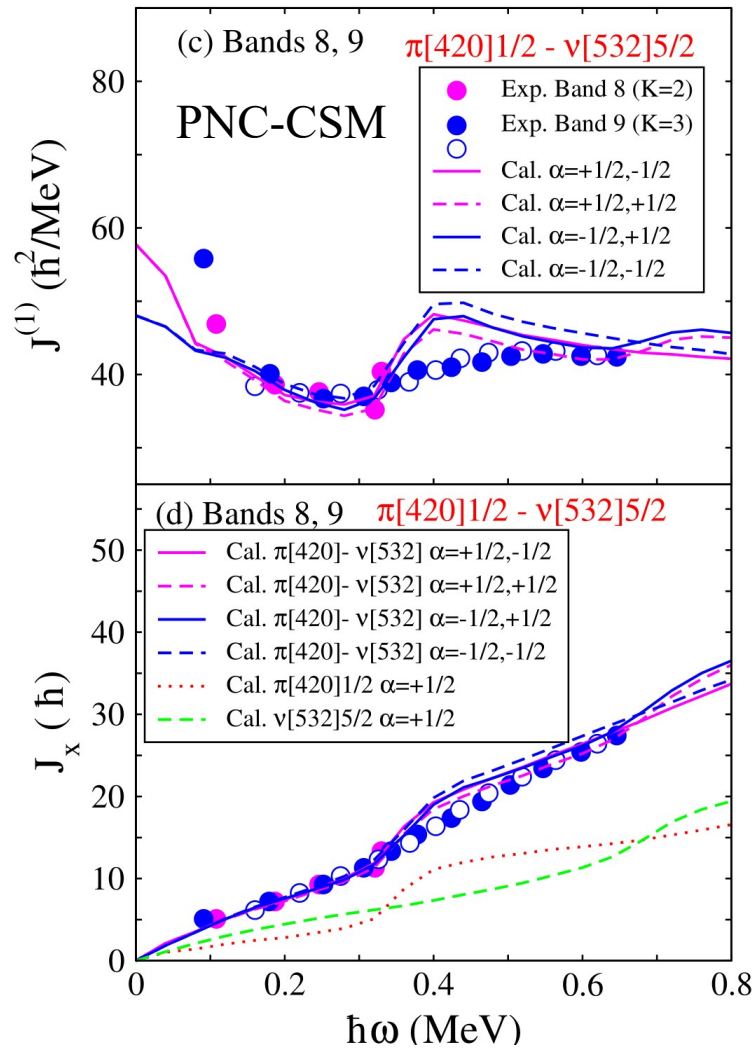
$T_{1/2} = 0.43 \mu\text{s}$

# Results: isomeric states of $^{118}\text{Cs}$



**Two long-lived isomers** have been identified: a **66-keV transition** detected at the MARA focal plane depopulates one of them, indicating a **half-life in the microsecond range**, while **no depopulating transitions** have been identified for the other, indicating a **much longer half-life**.

# Results of PNC-CSM calculations of $^{118}\text{Cs}$



Bands 1,2 :  $\pi[541]3/2 \otimes \nu[532]5/2$

Band 3:  $\pi[404]9/2 \otimes \nu[532]5/2$

Band 4:  $\pi[404]9/2 \otimes \nu[411]3/2, \nu[413]5/2$

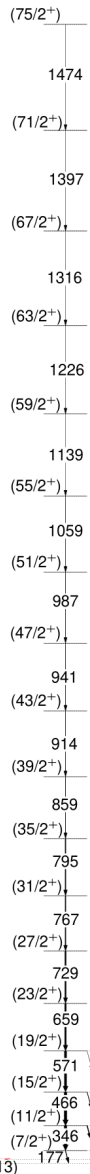
Band 6:  $\pi[541]3/2 \otimes \nu[411]3/2$

Bands 7, 10:  $\pi[422]3/2 \otimes \nu[532]5/2$

Bands 8, 9:  $\pi[420]1/2 \otimes \nu[532]5/2$

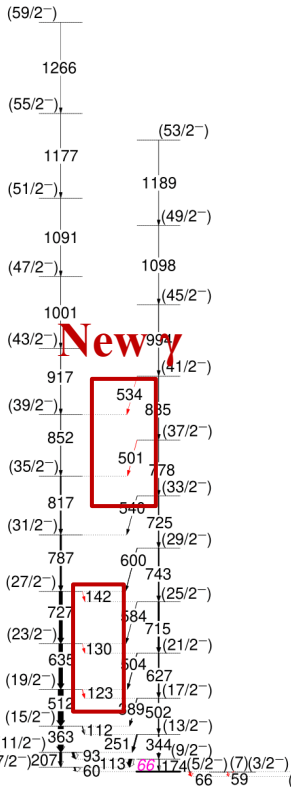
# Results: Neutron excitations in $^{119}\text{Ba}$

Band 2



$^{119}\text{Ba}$

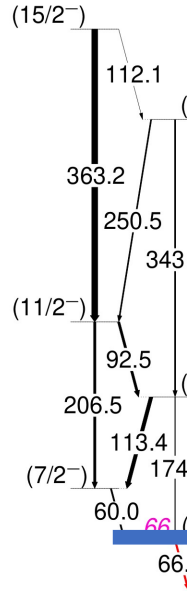
Band 1



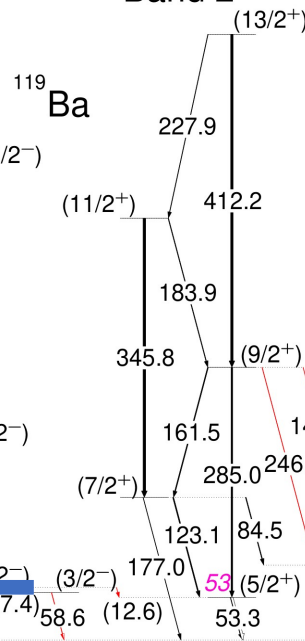
- Identified a new positive-parity band and several low-lying states.

- Identified an isomeric state  $5/2^-$  (B1).

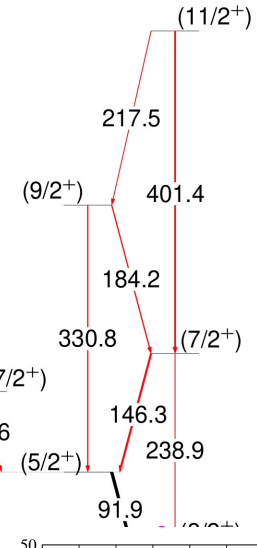
Band 1



Band 2



Band 3



$T_{1/2} = 0.36(2) \mu\text{s}$

Band 1:  $\nu[532]5/2^-$

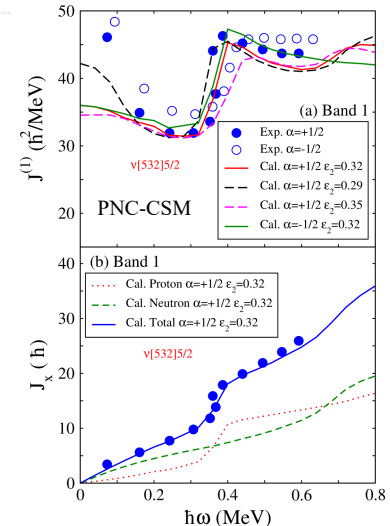
$\epsilon_2 = 0.32$

Band 2:  $\nu[413]5/2^+$

$\epsilon_2 = 0.32$

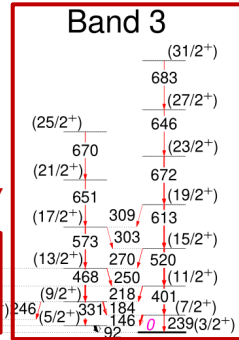
Band 3:  $\nu[411]3/2^+$

$\epsilon_2 = 0.32$

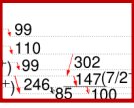


New Band

Band 3



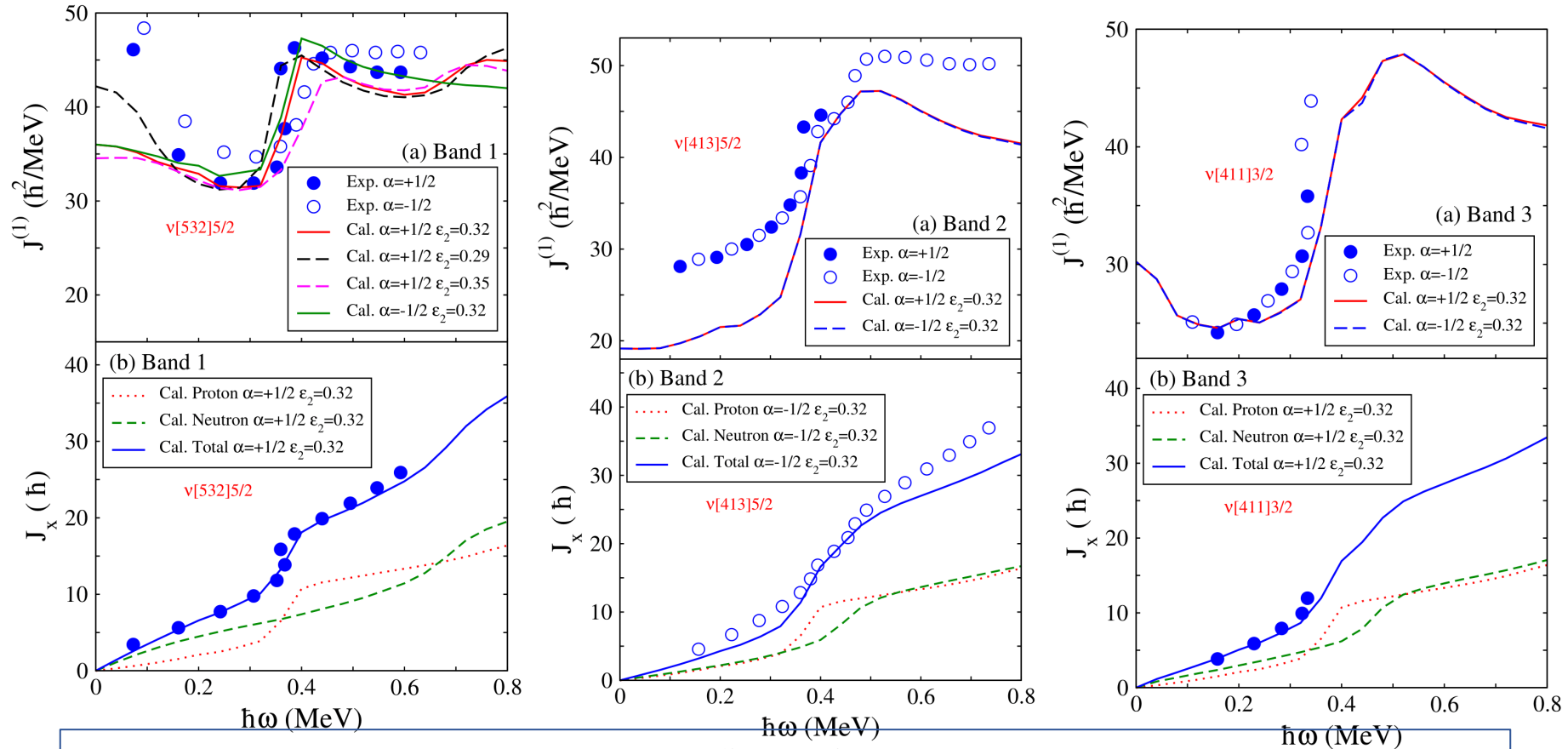
New  $\gamma$







# Results of PNC-CSM calculations of $^{119}\text{Ba}$



**Band 1:**  $v[532]5/2^-$  ( $\epsilon_2 = 0.32$ ) configuration.

**Band 2:**  $v[413]5/2^+$  ( $\epsilon_2 = 0.32$ ) configuration, not good agreement for  $J^{(1)}$  and for  $J_x$  at high spin, but good agreement for the crossing frequency.

**Band 3:**  $v[411]3/2^+$  ( $\epsilon_2 = 0.32$ ) configuration.

Published in Phys. Rev. C **104**, 014326, 2021



# Summary

**The neutron-deficient deformed  $^{119}\text{Cs}$ ,  $^{119}\text{Ba}$ , and  $^{118}\text{Cs}$  nuclei have been studied with the **JUROGAM 3 + MARA** setup.**

- two most complete level schemes from low to high spin in the odd-even and odd-odd proton-rich nuclei,  $^{119}\text{Cs}$  and  $^{118}\text{Cs}$ , were observed.
- one new rotational band and several low-lying states were newly identified in  $^{119}\text{Ba}$ .

**The identifications of the low-lying **isomers**.**

- $T_{1/2} = 0.36(2) \mu\text{s}$  and  $T_{1/2} = 55(5) \mu\text{s}$ , for the  $5/2^-$  and  $11/2^-$  band heads of the bands based on neutron and proton  $h_{11/2}$  orbitals in  $^{119}\text{Ba}$  and  $^{119}\text{Cs}$ , respectively.
- $T_{1/2} = 0.55(6) \mu\text{s}$  has been measured for the  $7^+$  state below the  $8^+$  band-head of the  $\pi h_{11/2} \otimes \nu h_{11/2}$  band in  $^{118}\text{Cs}$ .

**The configurations of the observed bands were assigned based on **PNC-CSM** calculations.**

- based on the analysis of the alignment properties of the bands, on systematics.

# Summary

**The chiral bands built on a configuration with only protons in the transient backbending regime was also observed for the first time in  $^{119}\text{Cs}$ .**

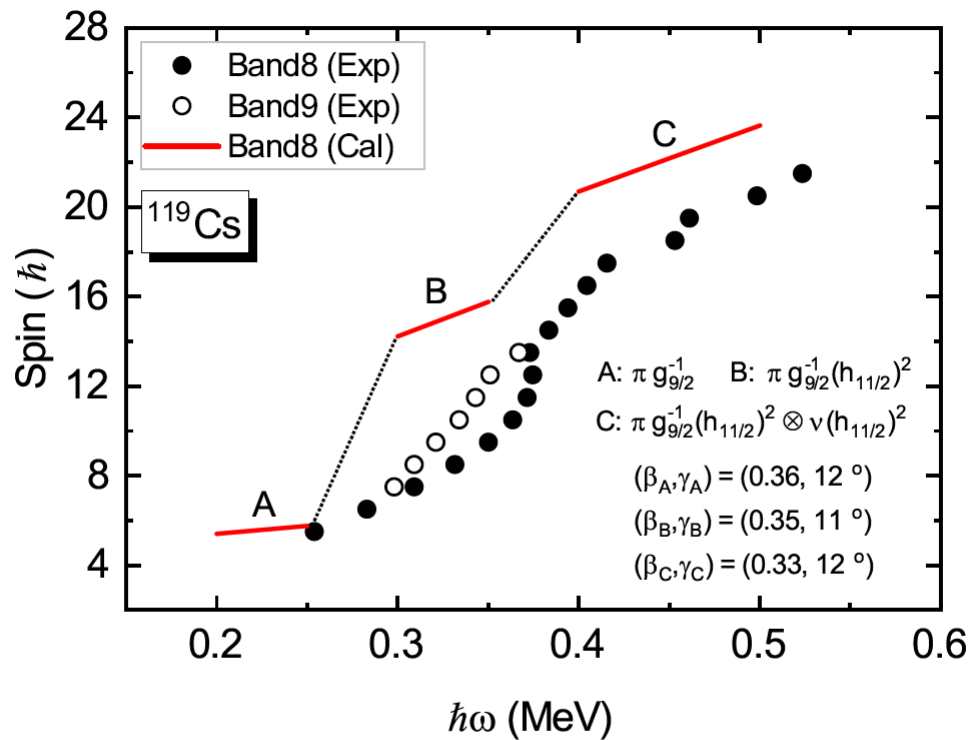
- two  $h_{11/2}$  protons revolving from the short to the intermediate axis of the triaxial core, and a strongly coupled  $g_{9/2}$  proton stucked along the long axis. The direction of the total angular momentum moves in 3D, giving rise to chiral bands that can be called  $R\chi D$  (Revolving Chiral Doublet) bands.

# Summary

**The chiral bands** built on a configuration with **only protons** in the transient backbending regime was also observed for **the first time** in  $^{119}\text{Cs}$ .

- two  $h_{11/2}$  protons revolving from the short to the intermediate axis of the triaxial core, and a strongly coupled  $g_{9/2}$  proton stuck along the long axis. The direction of the total angular momentum moves in 3D, giving rise to chiral bands that can be called  $R\chi D$  (Revolving Chiral Doublet) bands.

**Thanks for your attention!**



moderate

FIG. 2. (Color online) Comparison between the experimental spin versus rotational frequency and the TAC-CDFT calculations for bands 8 and 9 of <sup>119</sup>Cs.

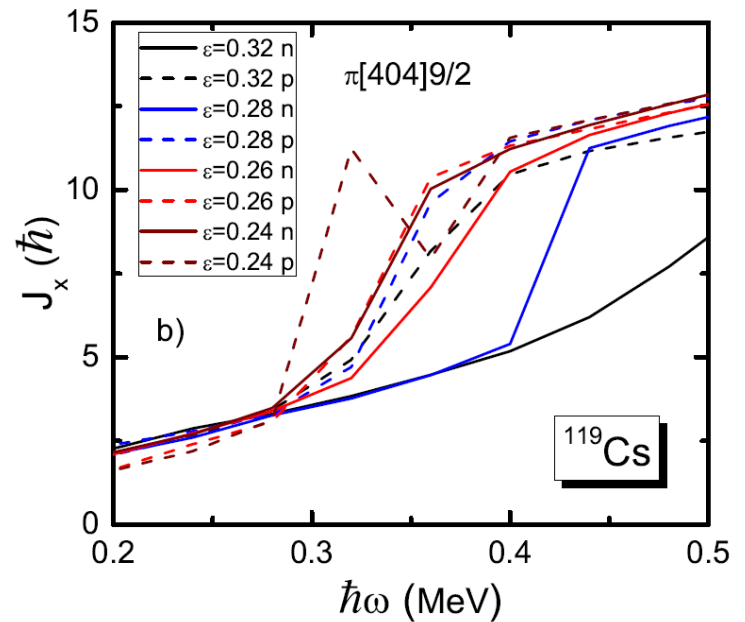
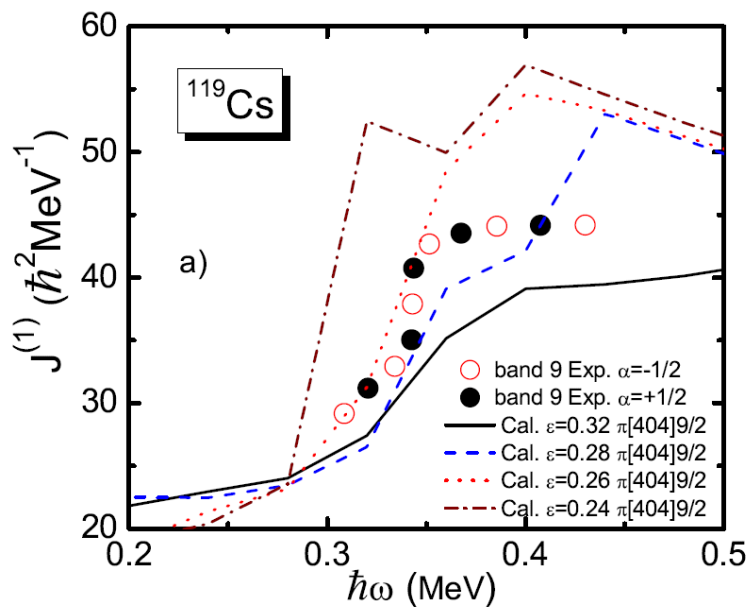


**Figure 5.30:** Moments of inertia  $J^{(1)}$  and projection of the angular momenta on the cranking axis  $J_x$  for Band 9 of  $^{119}\text{Cs}$  for different deformations. The states with signature  $\alpha = +1/2$  and  $\alpha = -1/2$  are drawn with filled and open symbols, respectively.

spin versus rotational frequency and the TAC-CDF calculations for bands 8 and 9 of  $^{119}\text{Cs}$ .



中国科学院近代物理研究所  
Institute of Modern Physics, Chinese Academy of Sciences

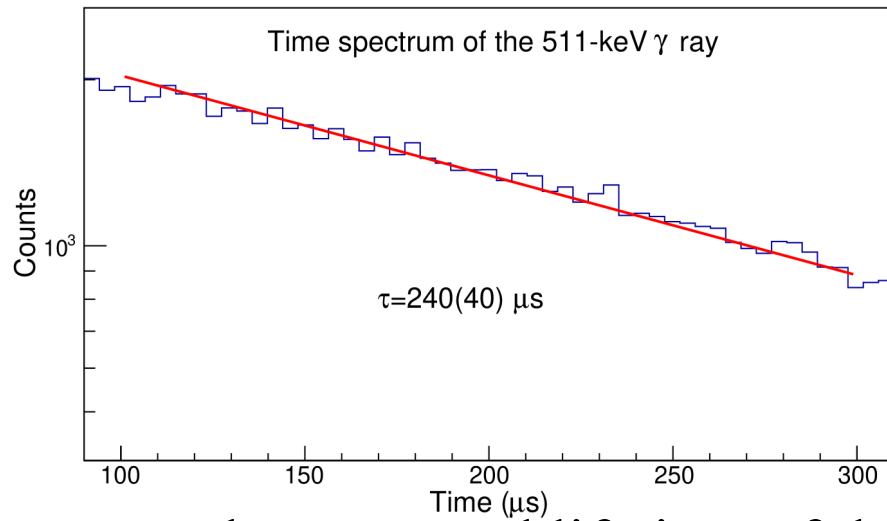
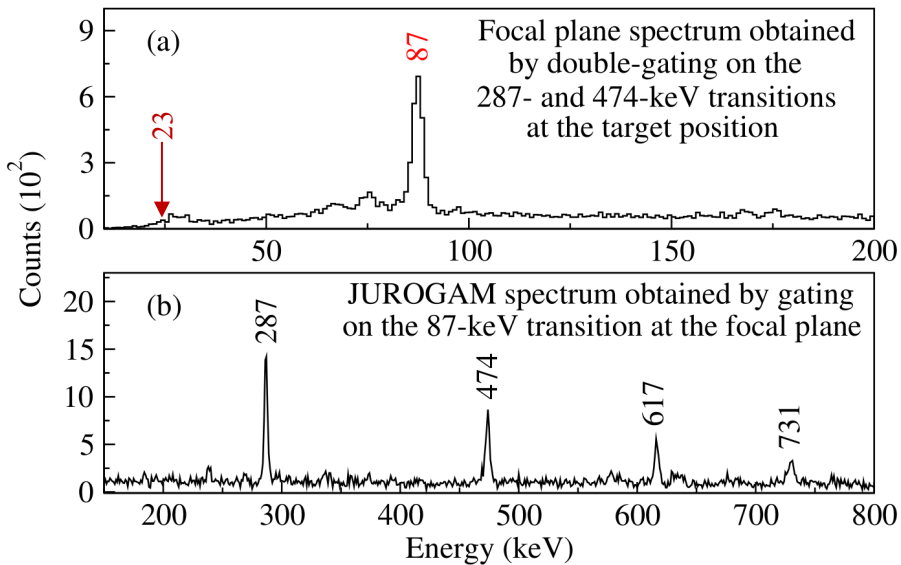


中国科学院大学  
University of Chinese Academy of Sciences

K. K. Zheng, C. M. Petrache, et al. EPJ A 59 (2022) 50  
K. K. Zheng, C. M. Petrache, et al. Phys. Rev. C104 (2021) 044325  
K. K. Zheng, C. M. Petrache, et al. Phys. Rev. C104 (2021) 044305  
K. K. Zheng, C. M. Petrache, et al. Phys. Lett. B 822 (2021) 136645  
K. K. Zheng, C. M. Petrache, et al. Phys. Rev. C104 (2021) 014326

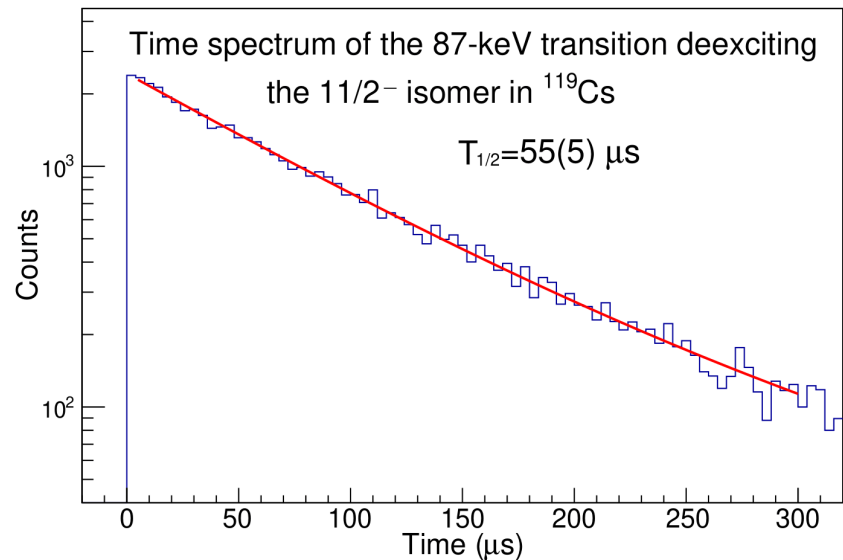
*Chirality and Wobbling in Atomic Nuclei, July 10 - July 14, 2023, Huizhou, China*

# Results: isomeric states of $^{119}\text{Cs}$



The time spectrum of the background 511-keV  $\gamma$  ray has a slight slope. Thus, we fit isomer spectra with two exponentials, one with a fixed lifetime of  $\tau = 240 \mu\text{s}$  deduced from the fit of the background.

$$y = N_0 e^{\frac{-t}{240 \mu\text{s}}} + N_1 e^{\frac{-t}{\tau}}$$



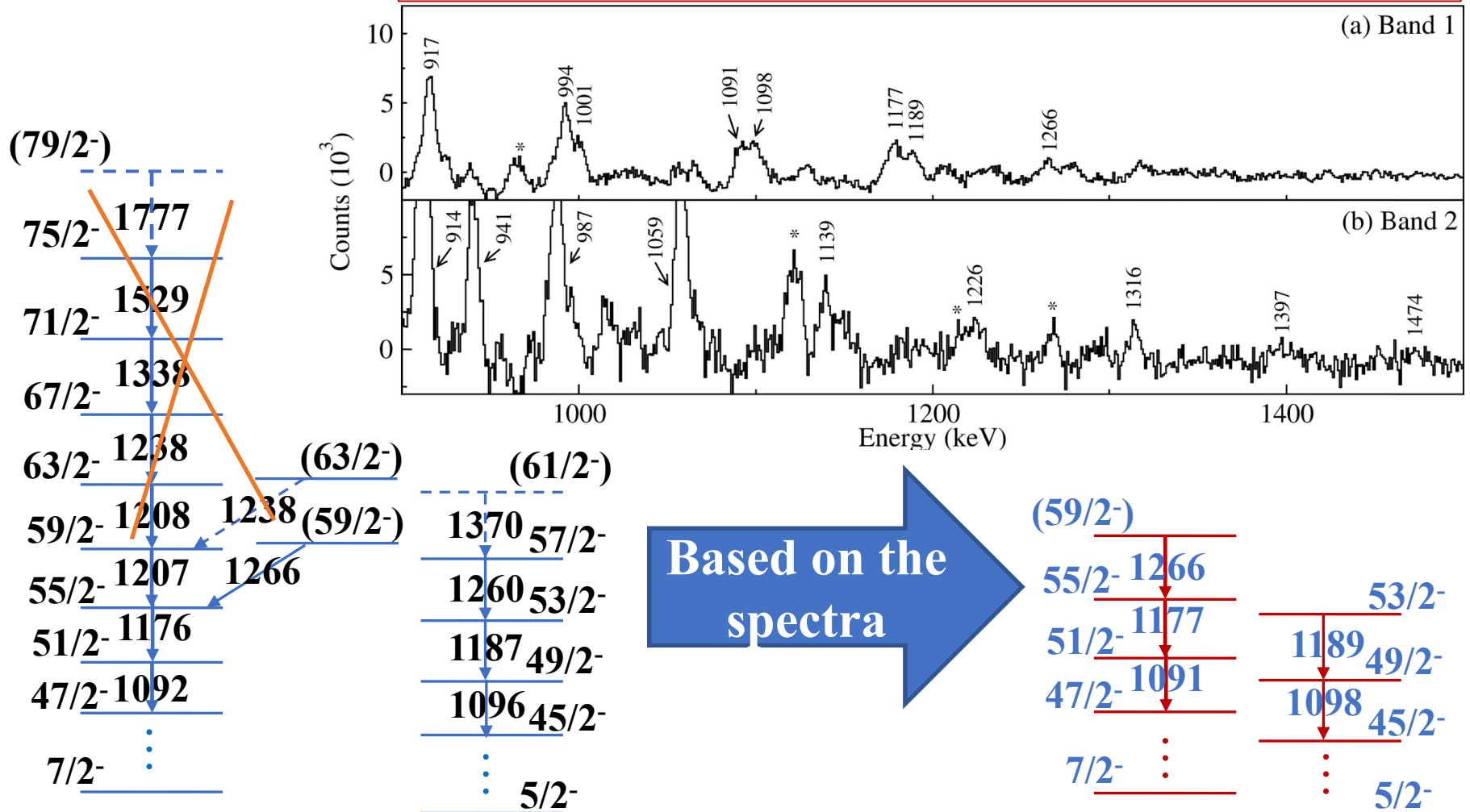
The extracted lifetime of the  $11/2^-$  state is  $T_{1/2} = 55(5) \mu\text{s}$ .





# Results: Neutron excitations in $^{119}\text{Ba}$

## $^{119}\text{Ba}$ : **double gates** spectra of high-spin states

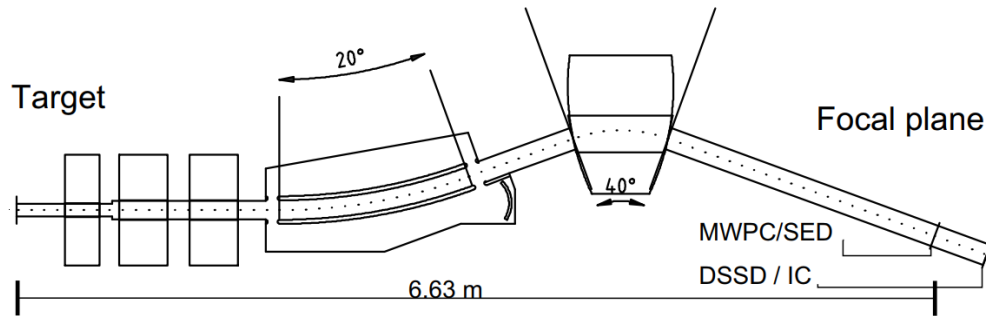


Band 1 : J. F. Smith, Phys. Rev. C **61**, 044329 (2000)

Band 1: Our work

# Experimental Setup: MARA

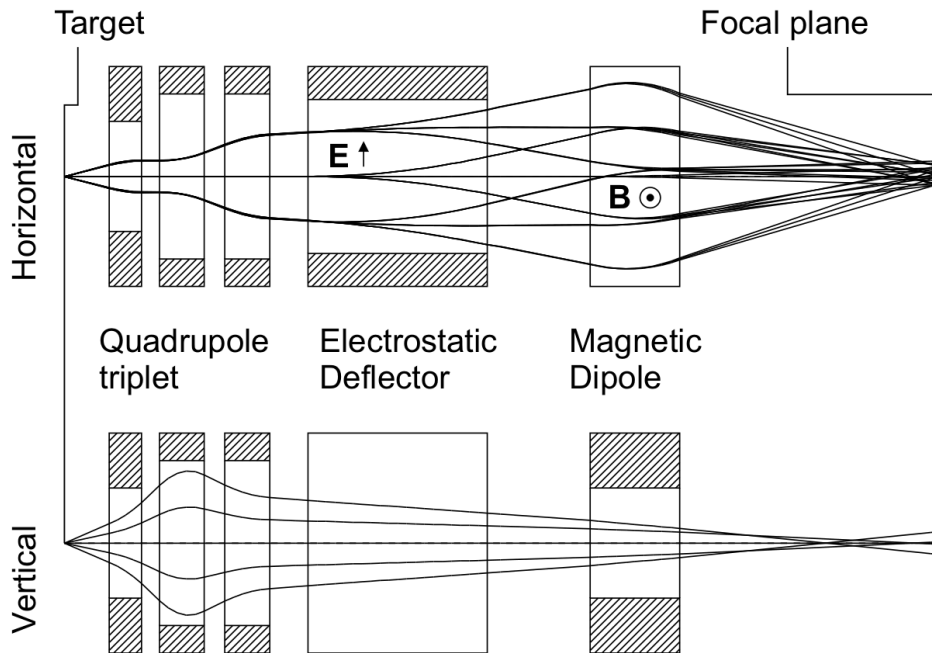
## Configuration: $QQQD_E D_M$ .



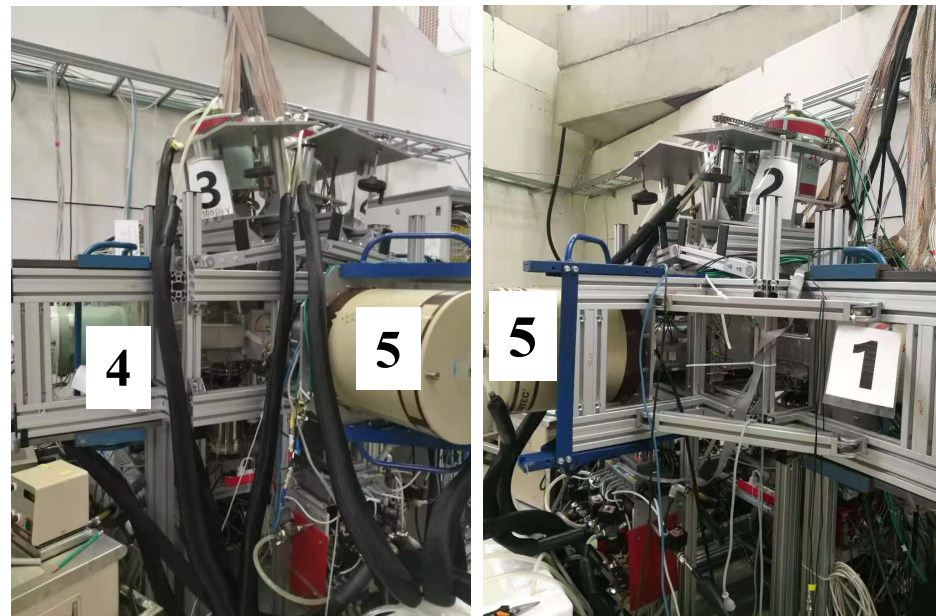
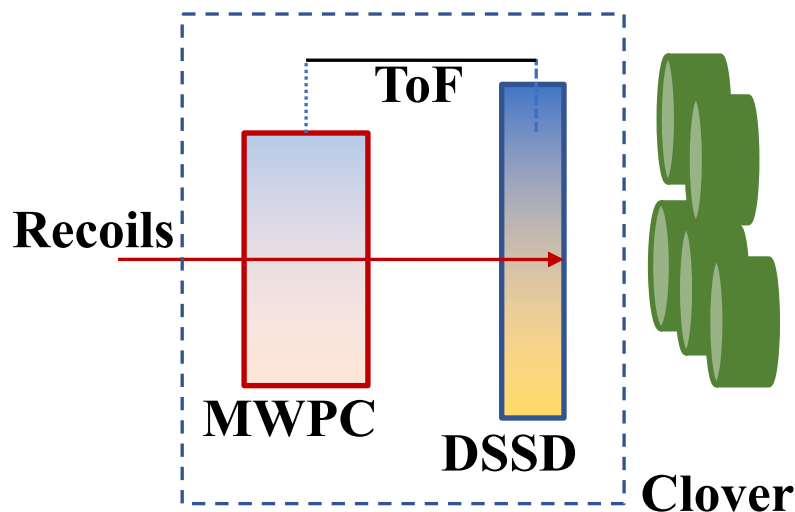
$QQQ$  is used to create a point-to-point focusing condition over the separator in both directions and to bend horizontally diverging charged particles to parallel trajectories before entering the electric field.

$D_E$  separates primary beam and recoils residues

$D_M$  provides a fixed energy focus for the separated ions with different  $m/q$  ratio.



# Experimental Setup: Focal plane



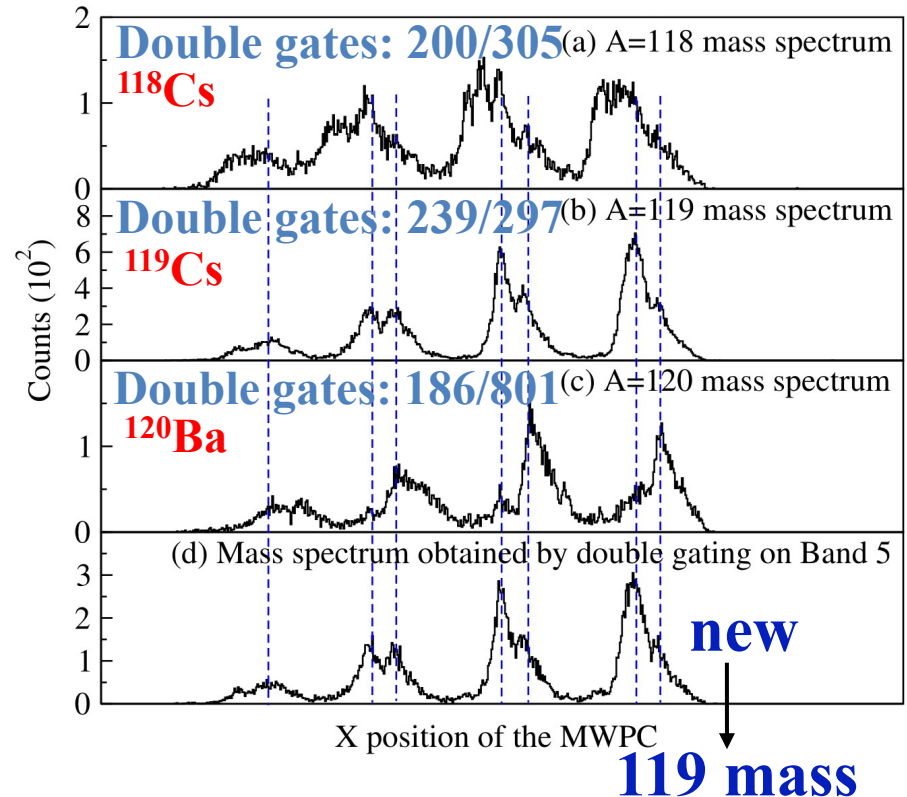
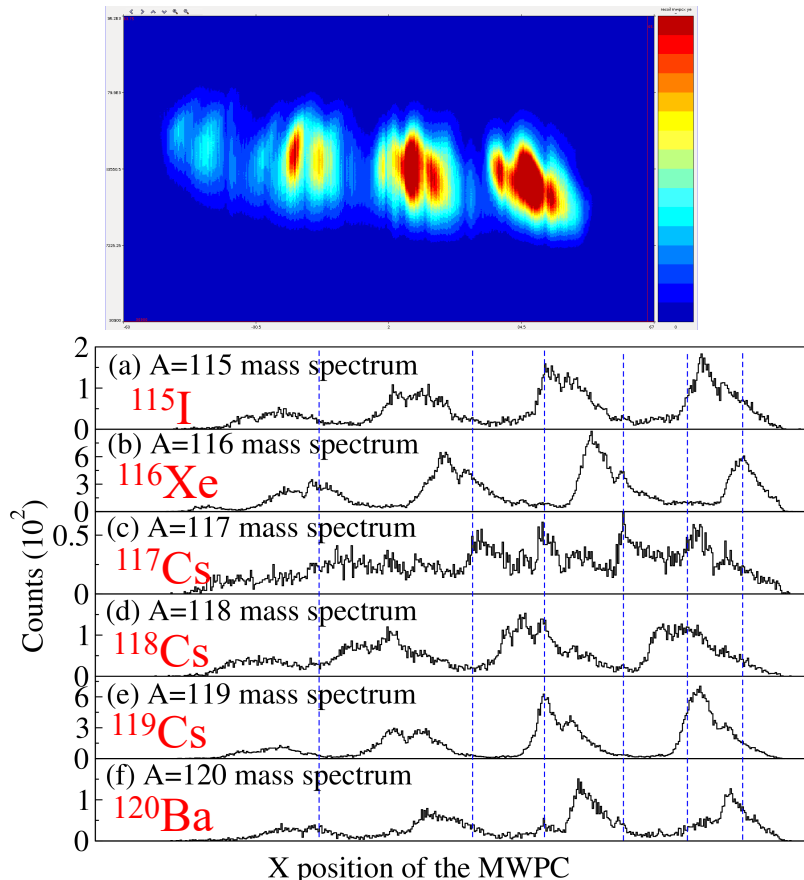
**The Time of Flight** (ToF) between the MWPC and DSSD was recorded. The ToF and the recoil energy deposited in the **DSSD** were used to **distinguish between fusion recoils and scattered beam**.

**Five clover detectors** surrounding the focal-plane detection system were used to detect  $\gamma$ -rays emitted by **long-lived isomers of the implanted recoils and the daughter nuclei produced by  $\beta$ -decay**.

# Results: The assignment of the bands to nuclei

The assignments of the bands to  $^{119}\text{Cs}$ ,  $^{119}\text{Ba}$ , and  $^{118}\text{Cs}$  are based on:

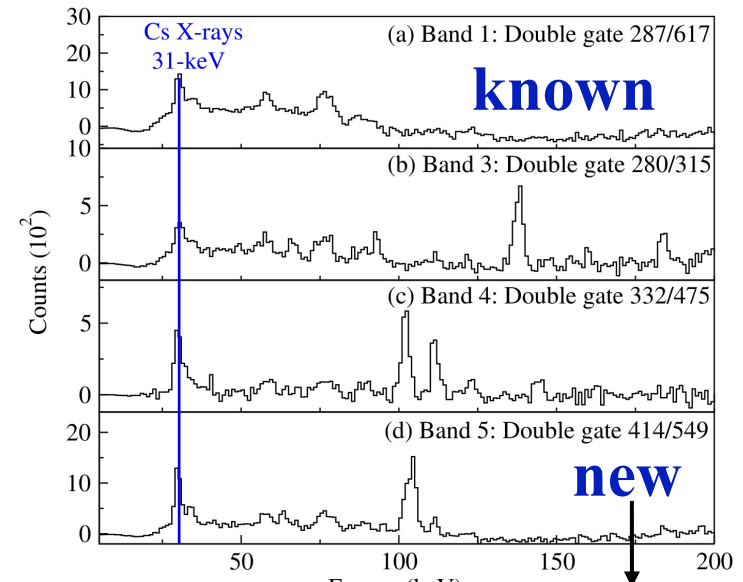
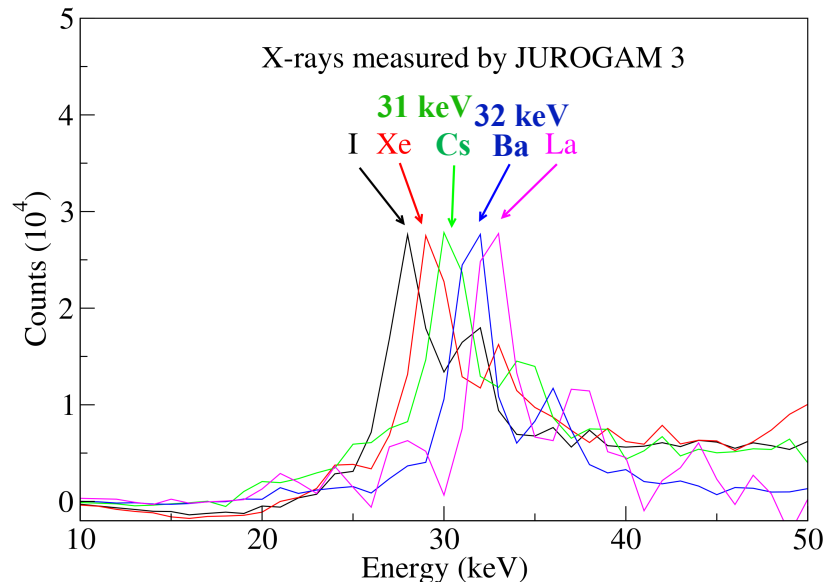
**1. The mass 119 and 118 detected at the MARA focal plane in coincidence with transitions detected in JUROGAM 3;**



# Results: The assignment of the bands to nuclei

The assignments of the bands to  $^{119}\text{Cs}$ ,  $^{119}\text{Ba}$ , and  $^{118}\text{Cs}$  are based on:

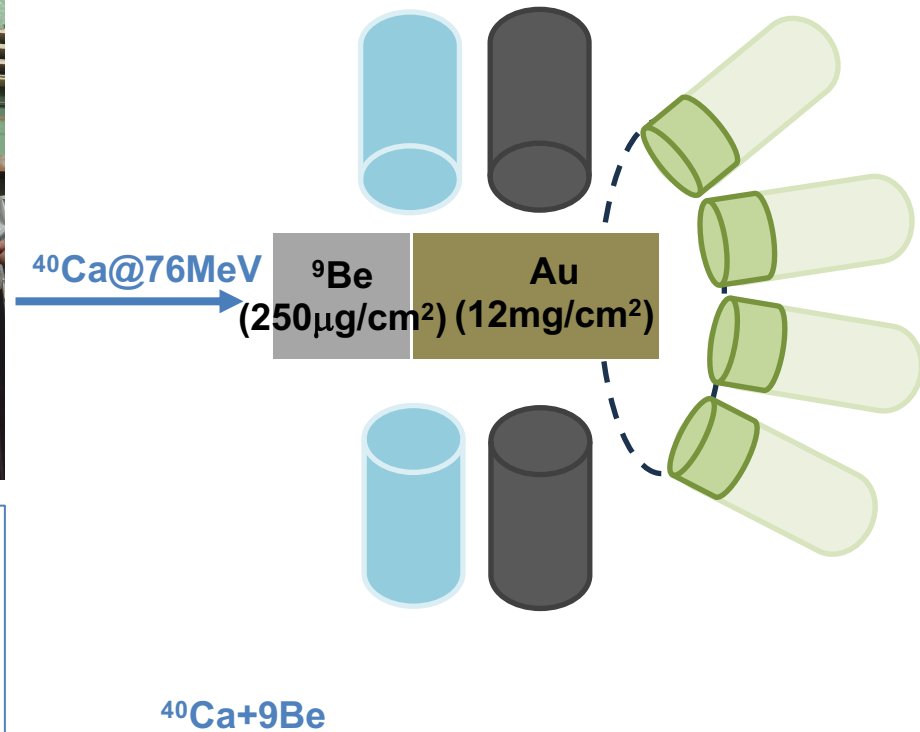
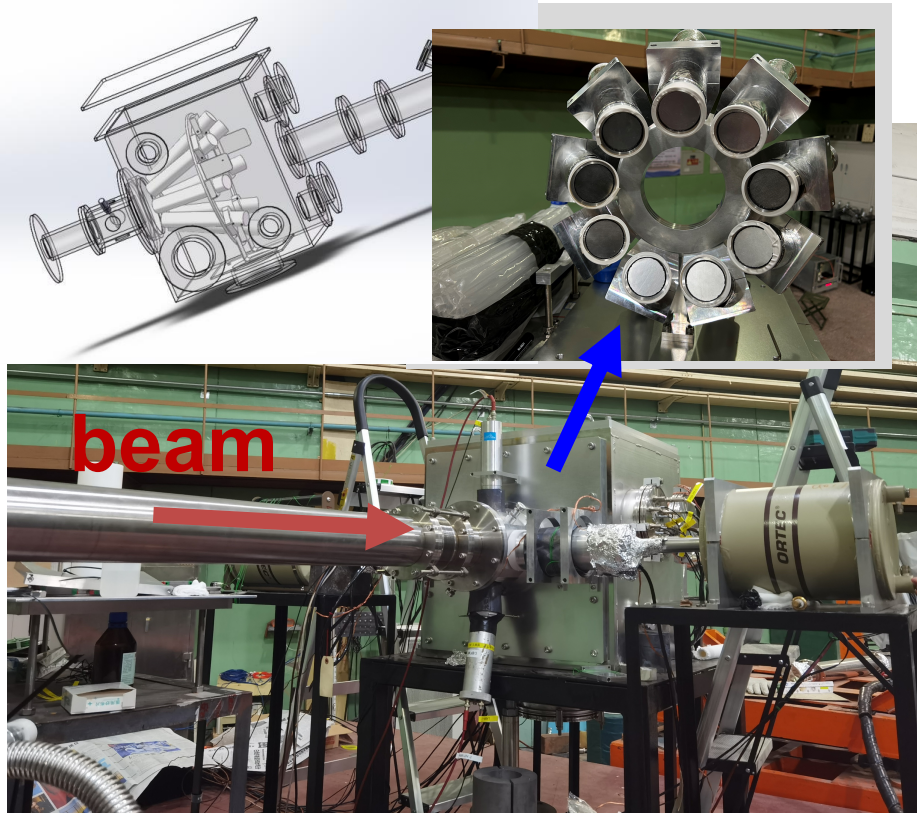
- 1. The mass 119 and 118 detected at the MARA focal plane** in coincidence with transitions detected in JUROGAM 3;
- 2. The 31 and 32 keV  $K_{\alpha}$  X rays** of cesium and barium nuclides detected in prompt coincidence with in-band transitions.



Combining information on the mass spectra and on the X-rays, we could assign new bands.



# Test ex



## Experimental Setup:

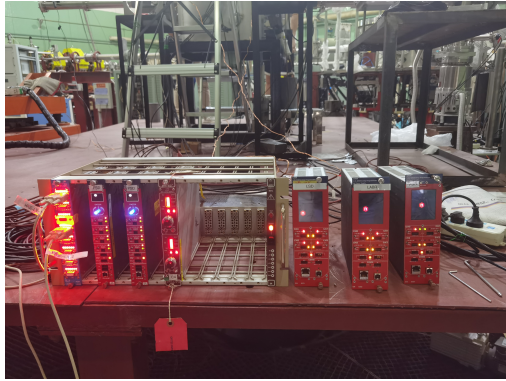
HPGe 2

LaBr<sub>3</sub> 4

Liquid scintillation detector 2

Laminated plastic scintillator 9

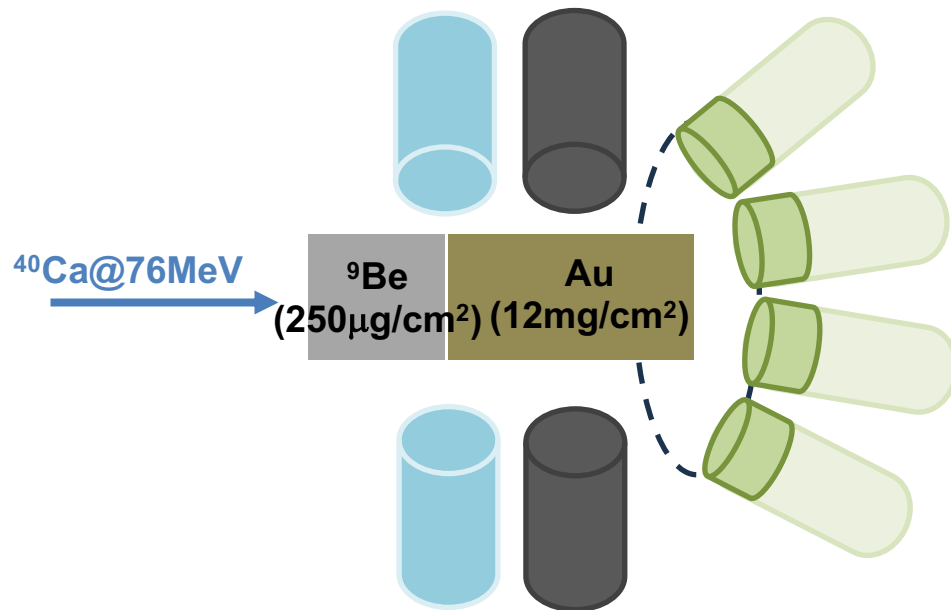
# Conclusion



Digital Acquisition System

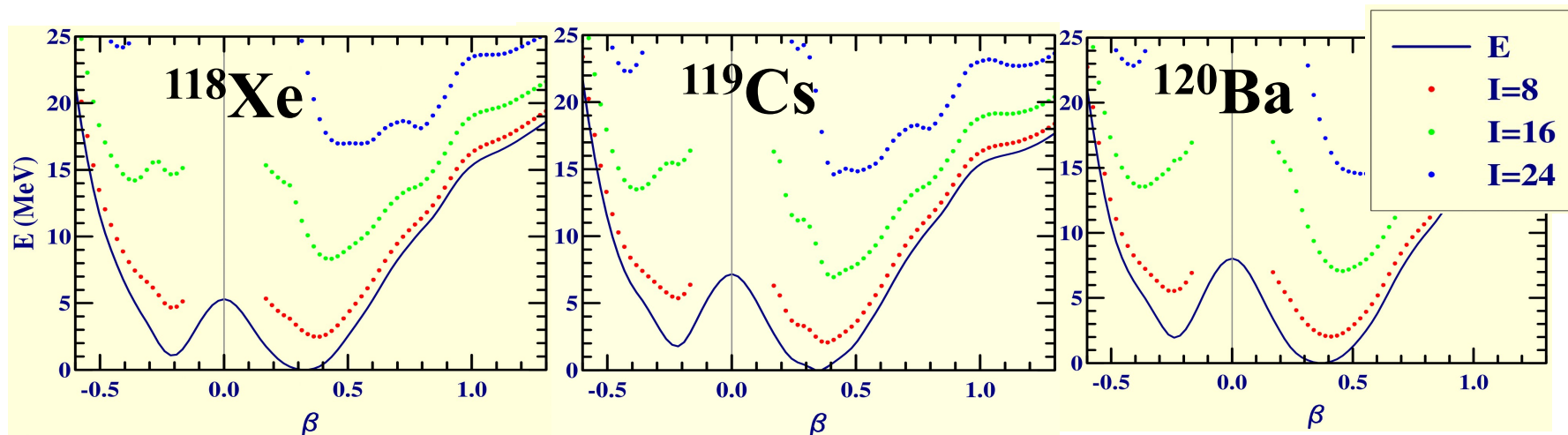
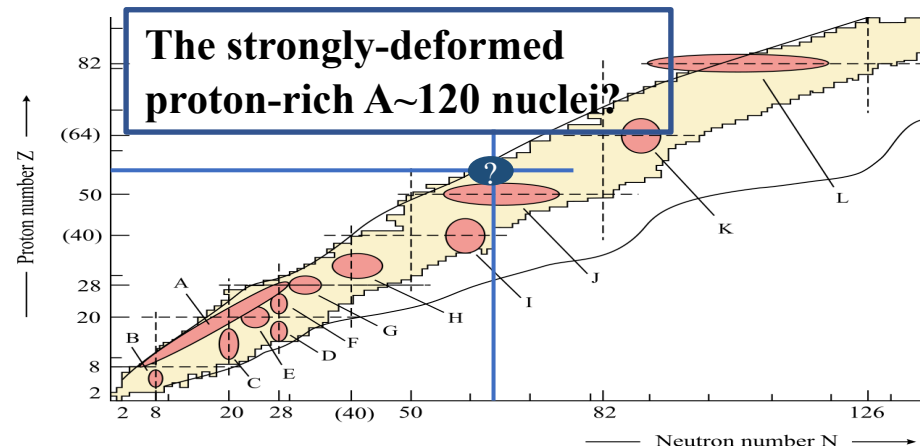


# Motivation



# Shape coexistence

In 1956, the **first experimental** evidence of **spherical-prolate shape** coexistence was observed in the  $^{16}\text{O}$  isotope. Many regions of shape coexistence are known.



**Two minima** in the potential energy of  $^{118}\text{Xe}$ ,  $^{119}\text{Cs}$ , and  $^{120}\text{Ba}$ , for positive and negative quadrupole deformation corresponding to **prolate and oblate shapes**, respectively.

H. Morinaga Phys. Rev. 101, 254. Kris Heyde. Rev. Mod. Phys. 83, 1467.

[http://www-phynu.cea.fr/science\\_en\\_ligne/carte\\_potentiels\\_microscopiques/carte\\_potentiel\\_nucleaire\\_eng.htm](http://www-phynu.cea.fr/science_en_ligne/carte_potentiels_microscopiques/carte_potentiel_nucleaire_eng.htm).

# Experimental Setup

**Location:** JYFL;

**Beam:**  $^{64}\text{Zn}$ , 255 MeV, 2-3 pnA;

**Target:**  $^{58}\text{Ni}$  (self-supporting enriched), 0.75 mg/cm<sup>2</sup>;

**Populated nuclei:**  $^{119}\text{Cs}$  (150 mb),  $^{119}\text{Ba}$  (20 mb) and  $^{118}\text{Cs}$  (40 mb).

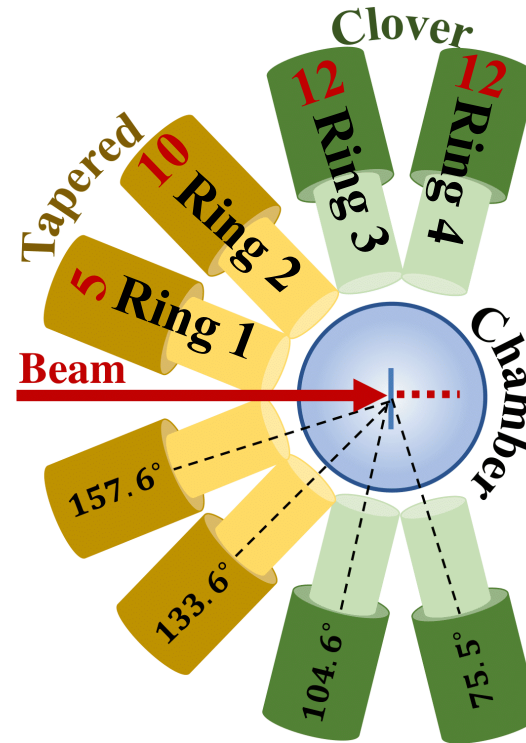
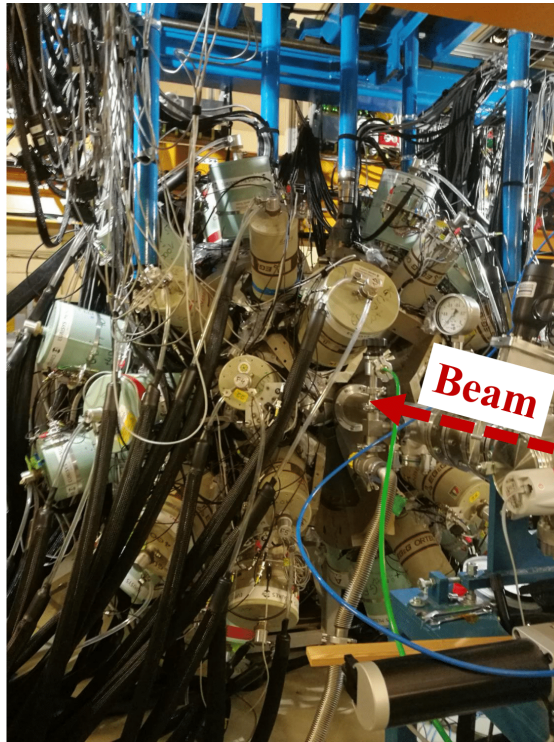


# Experimental Setup: JUROGAM 3

**Detector:** 15 tapered + 24 clover + 39 BGO shields;

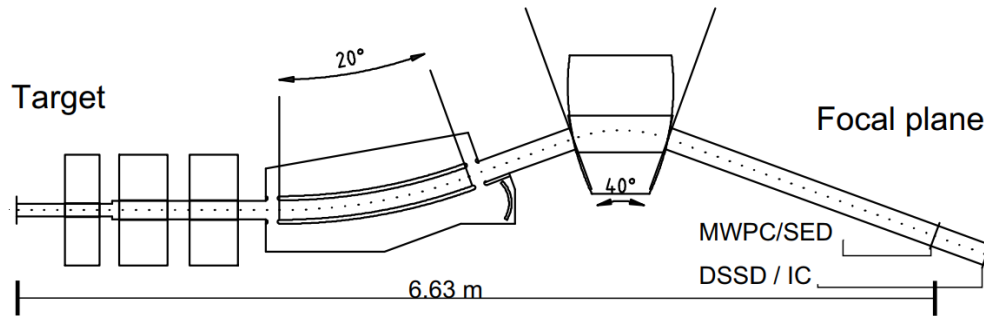
**Efficiency:** 5.2% at 1.3 MeV;

**Extraction:**  $R_{ac}$ ,  $R_{DCO}$ , linear polarization.



# Experimental Setup: MARA

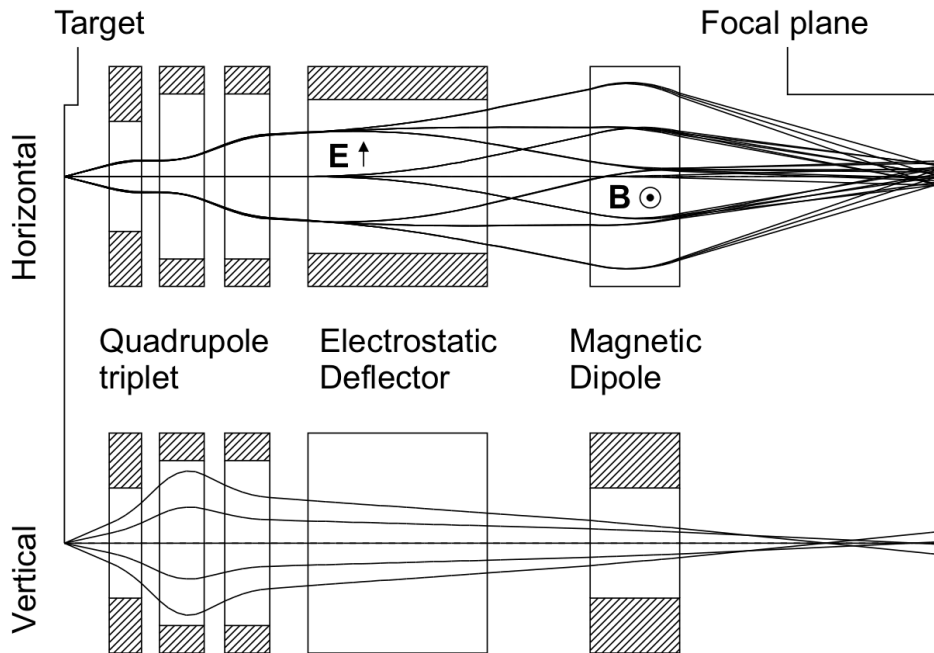
## Configuration: $QQQD_E D_M$



$QQQ$  is used to create a point-to-point focusing condition over the separator in both directions and to bend horizontally diverging charged particles to parallel trajectories before entering the electric field.

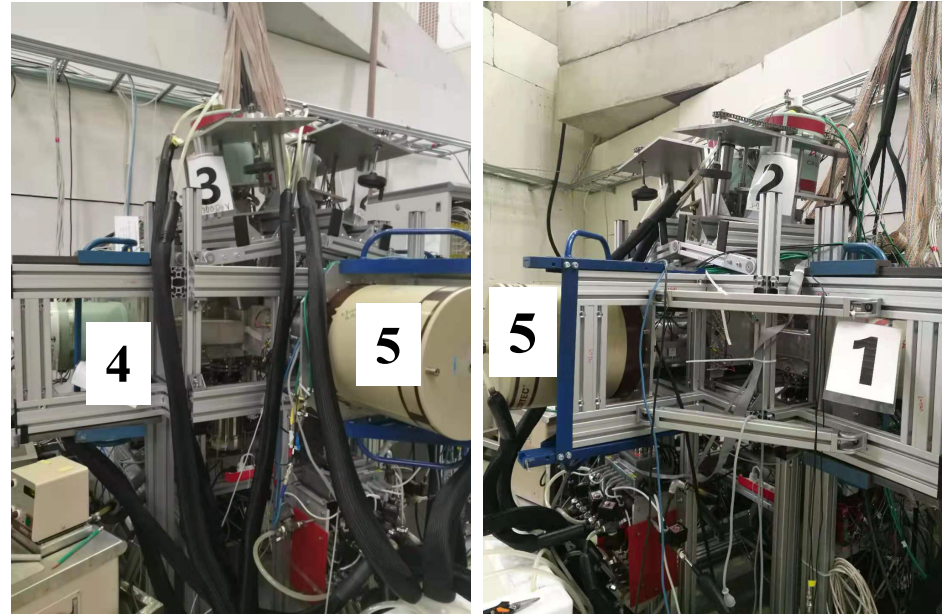
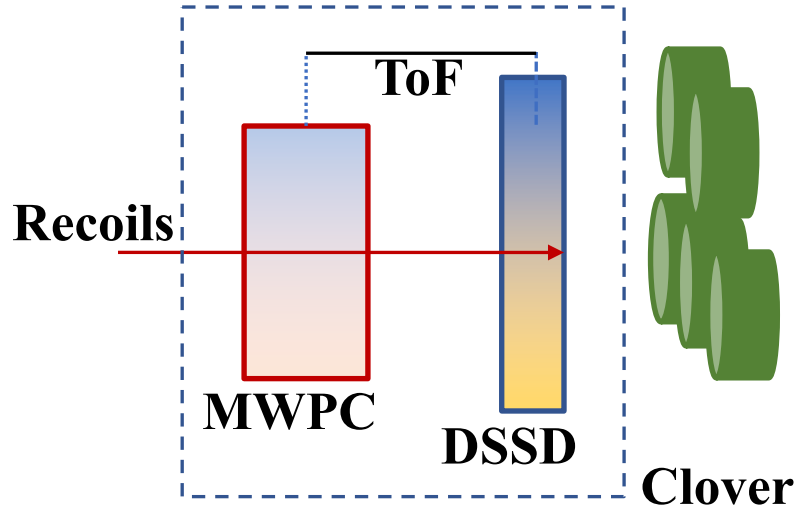
$D_E$  separates primary beam and recoils residues

$D_M$  provides a fixed energy focus for the separated ions with different  $m/q$  ratio.





# Experimental Setup: Focal plane



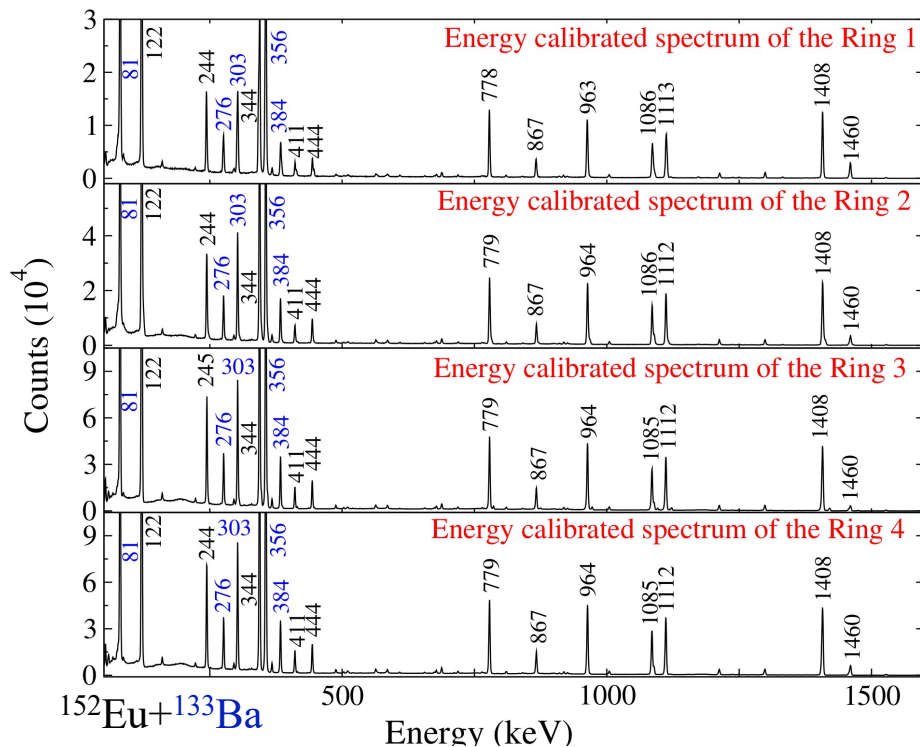
**The Time of Flight** (ToF) between the MWPC and DSSD was recorded. The ToF and the recoil energy deposited in the **DSSD** were used to **distinguish between fusion recoils and scattered beam**.

**Five clover detectors** surrounding the focal-plane detection system were used to detect  $\gamma$ -rays emitted by **long-lived isomers of the implanted recoils and the daughter nuclei produced by  $\beta$ -decay**.

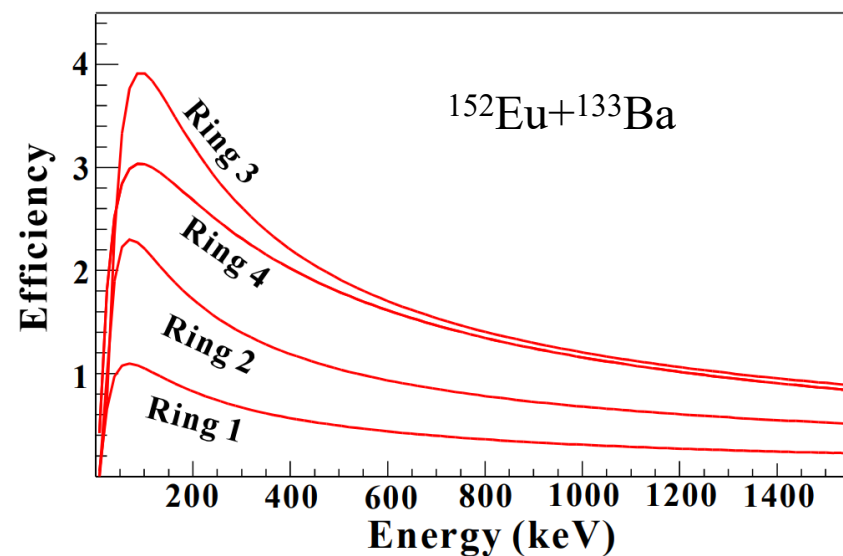
# Data analysis

## 1 Setting of the low-energy thresholds, energy calibrations, gain matching, and efficiency calibrations

The low-energy thresholds of most detectors were set to  $\approx 25$  keV.



The energy calibrated spectra of the 4 rings of the JUROGAM 3 array using the  $E_\gamma = a + bx + cx^2$  formula.



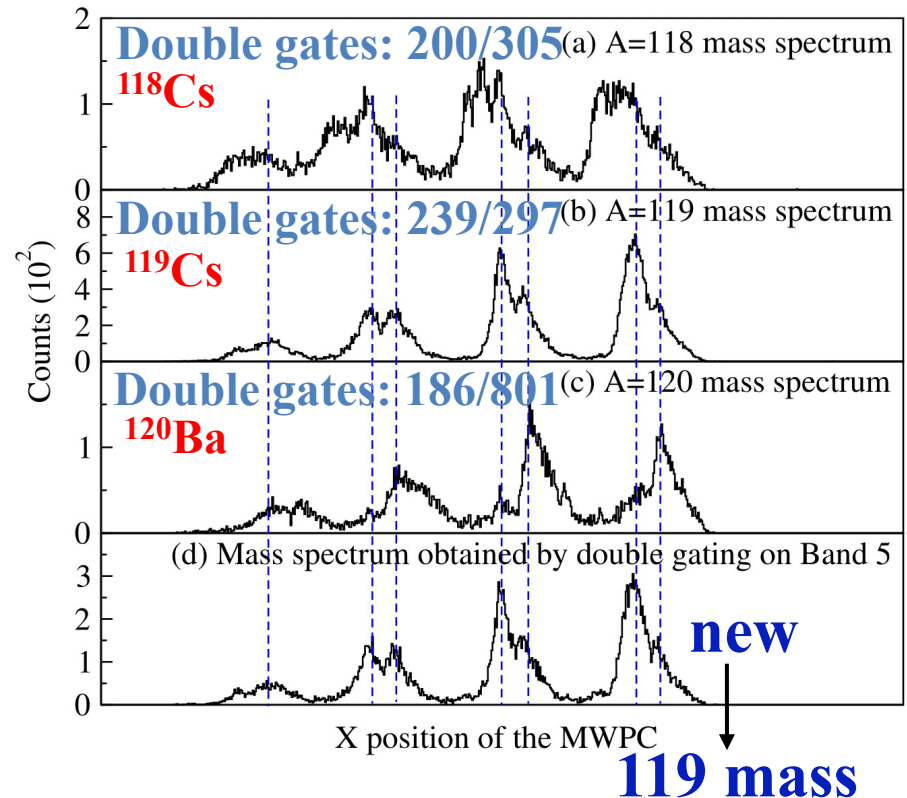
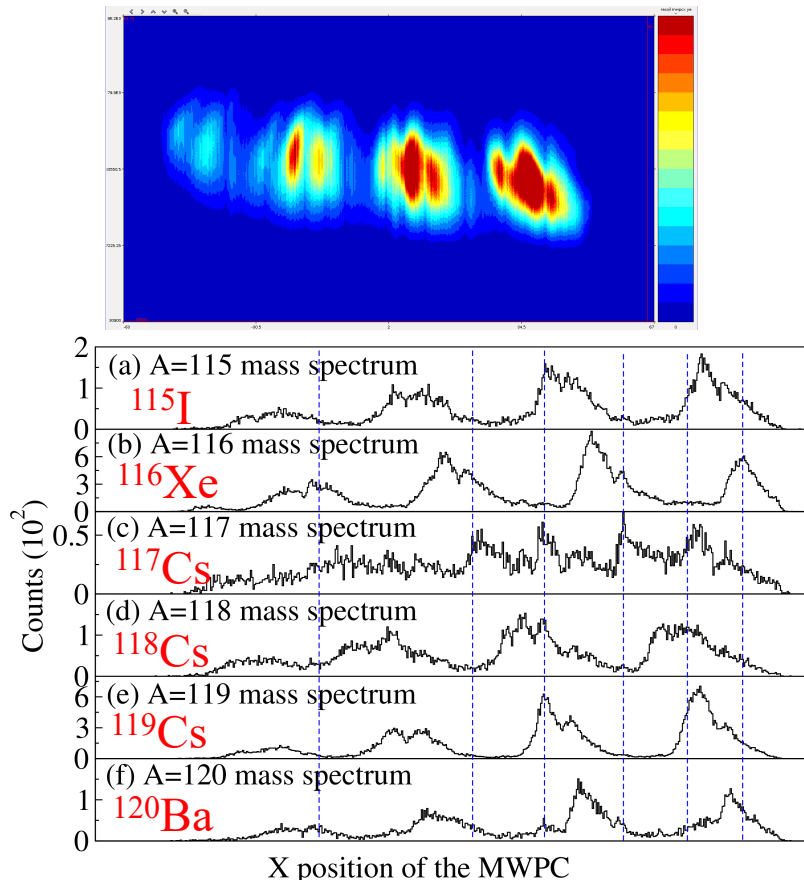
The efficiency curves of the 4 rings of the JUROGAM 3 array by fitting the  $\ln \epsilon = (A + Bx - e^{C+Dx})$  formula to the experimental points.



# Results: The assignment of the bands to nuclei

The assignments of the bands to  $^{119}\text{Cs}$ ,  $^{119}\text{Ba}$ , and  $^{118}\text{Cs}$  are based on:

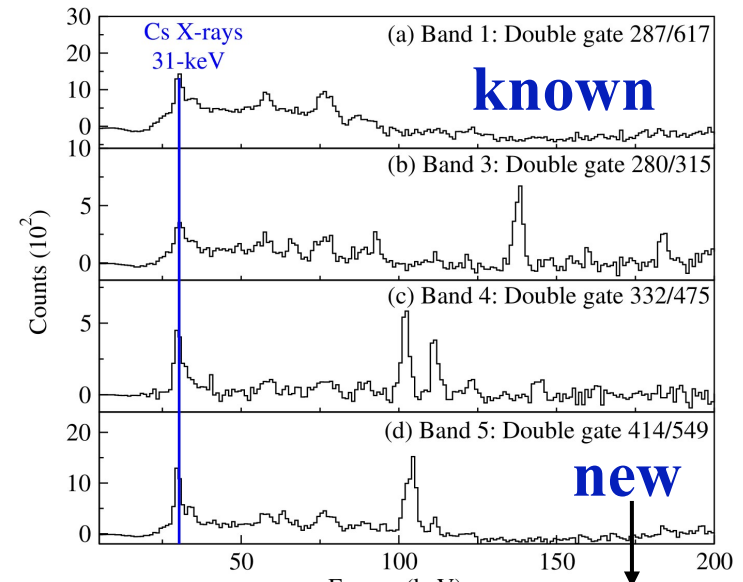
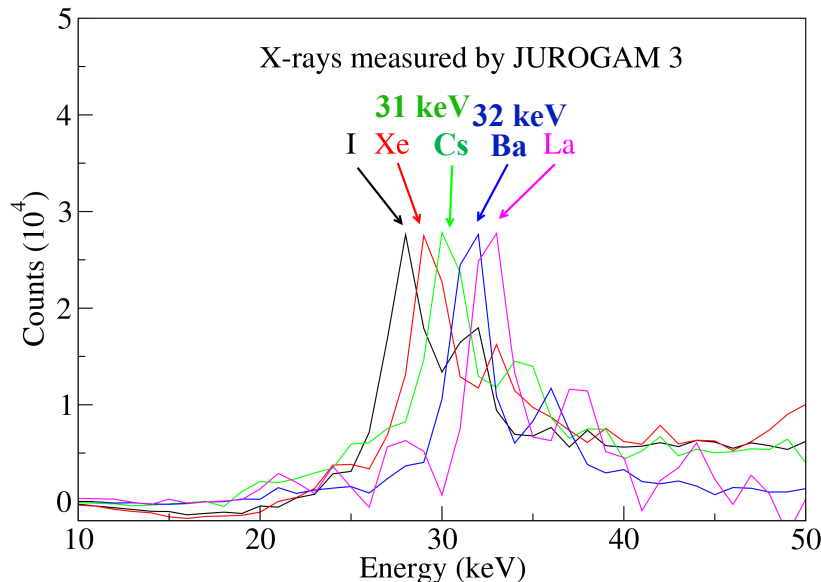
**1. The mass 119 and 118 detected at the MARA focal plane in coincidence with transitions detected in JUROGAM 3;**



# Results: The assignment of the bands to nuclei

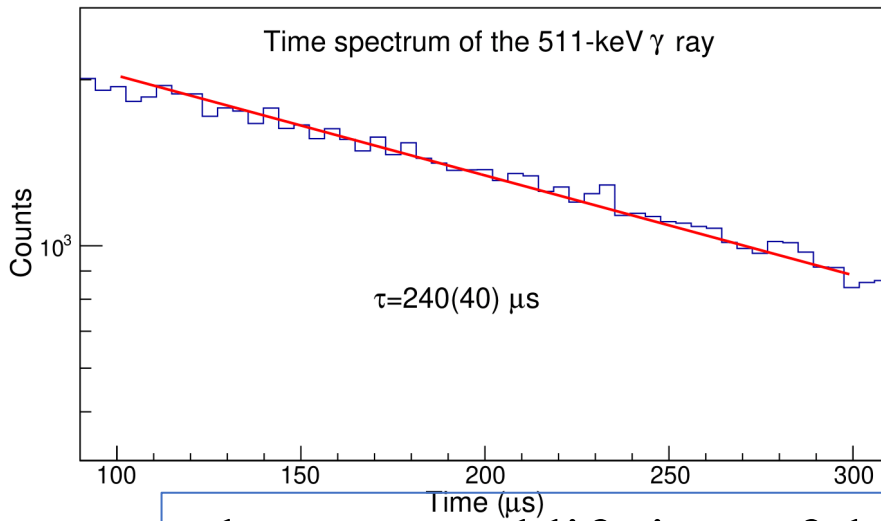
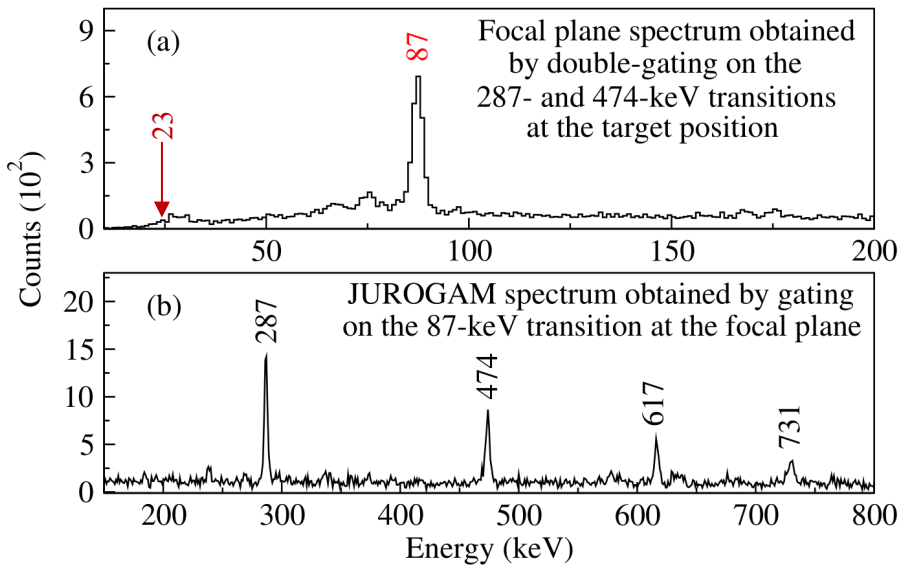
The assignments of the bands to  $^{119}\text{Cs}$ ,  $^{119}\text{Ba}$ , and  $^{118}\text{Cs}$  are based on:

- 1. The mass 119 and 118 detected at the MARA focal plane** in coincidence with transitions detected in JUROGAM 3;
- 2. The 31 and 32 keV  $K_{\alpha}$  X rays** of cesium and barium nuclides detected in prompt coincidence with in-band transitions.



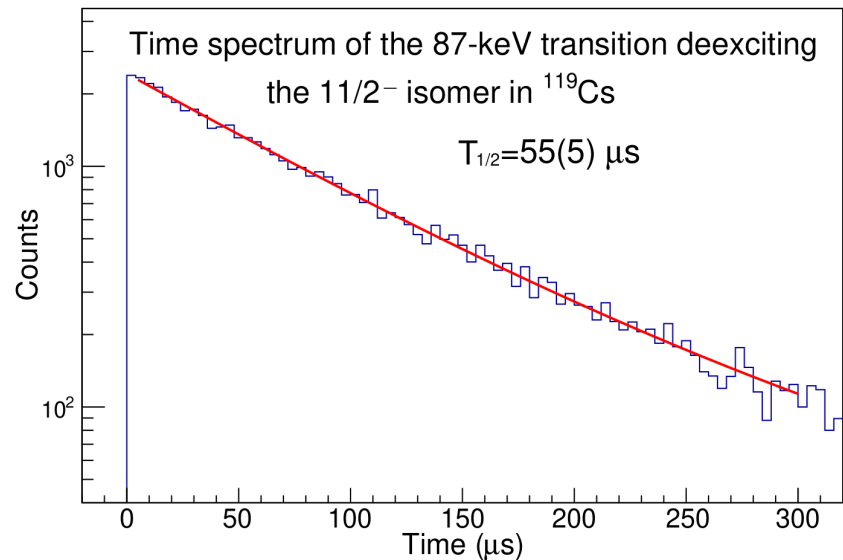
Combining information on the mass spectra and on the X-rays, we could assign new bands.

# Results: isomeric states of $^{119}\text{Cs}$



The time spectrum of the background 511-keV  $\gamma$  ray has a slight slope. Thus, we fit isomer spectra with two exponentials, one with a fixed lifetime of  $\tau = 240 \mu\text{s}$  deduced from the fit of the background.

$$y = N_0 e^{\frac{-t}{240 \mu\text{s}}} + N_1 e^{\frac{-t}{\tau}}$$



The extracted lifetime of the  $11/2^-$  state is  $T_{1/2} = 55(5) \mu\text{s}$ .

# Data analysis

2

## Doppler shift correction, add-back

$$E_{\gamma}(\theta) = E_{\gamma}(0) \frac{\sqrt{1 - \beta^2}}{1 - \beta \cos \theta}$$

If  $v \ll c$ ,  $\beta \ll 1$

$$E_{\gamma}(\theta) = E_{\gamma}(0)(1 + \beta \cos \theta)$$

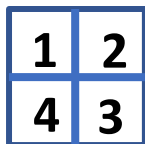
**a:**  $E_{\gamma}(0)$  is the energy of  $\gamma$ -ray emitted by the recoils at rest.

**b:**  $\theta$  is the detector angle which is defined with respect to the recoil velocity direction.

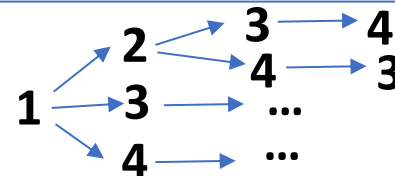
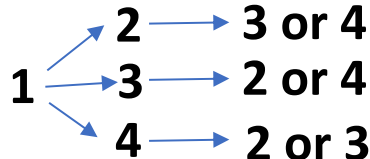
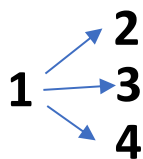
**c:**  $\beta = v/c$ .

In our experiment, we used a value  $\beta = 0.044$  for all  $\gamma$  rays detected in the JUROGAM 3 which resulted in the **best resolution** for high energy  $\gamma$  rays.

The clover detector can be operated in two modes: single crystal and **add-back mode**.



1

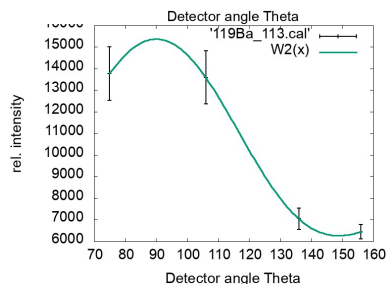
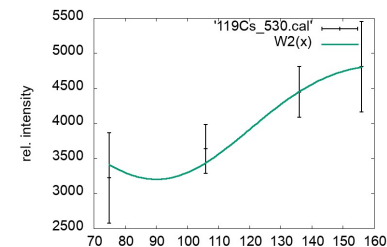


# Data analysis

4

Assignment the multipolarities by using  $R_{DCO}$  and  $R_{ac}$

**DCO ratio is defined as**  $R_{DCO} = \frac{I_{\gamma}(157.6^{\circ}, \approx 90^{\circ})}{I_{\gamma}(\approx 90^{\circ}, 157.6^{\circ})}$



**Gating on a quadrupole:**

**Gating on a dipole:**

$R_{DCO} \approx 1$  (pure quadrupole)  
 $R_{DCO} \approx 0.46$  (pure dipole)

$R_{DCO} \approx 2.1$  (pure quadrupole)  
 $R_{DCO} \approx 1$  (pure dipole)

**$R_{ac}$  is defined as**

$$R_{ac} = \frac{I_{\gamma}(133.6^{\circ} + 157.6^{\circ})}{I_{\gamma}(75.5^{\circ} + 104.5^{\circ})}$$

$R_{ac} \approx 1.4$  (pure quadrupole)  
 $R_{ac} \approx 0.8$  (pure dipole)

**→ It's very useful for weak transitions**

- A. Krämer-Flecken, Meth. Phys. Res. A 275, 333 (1989)
- C. J. Chiara et al., Phys. Rev. C 75, 054305 (2007)

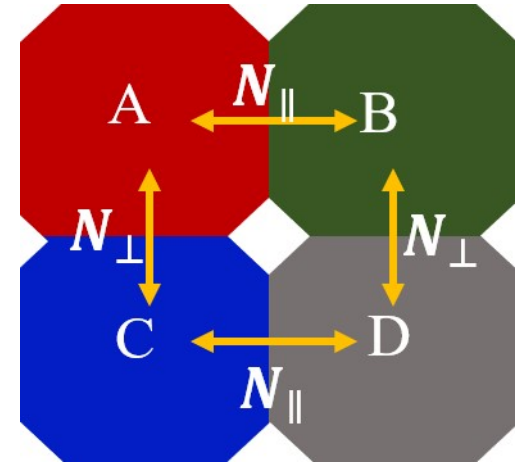
# Data analysis

The asymmetry  $A$  is defined as

$$A = \frac{aN_{\perp} - N_{\parallel}}{aN_{\perp} + N_{\parallel}}$$

where  $a$  is a correction coefficient

$$a(E_{\gamma}) = 1.113(7) - 5.4(8) \times 10^{-5} E_{\gamma}$$



**A positive asymmetry  $A$  implies electric nature, while a negative asymmetry implies magnetic nature.**

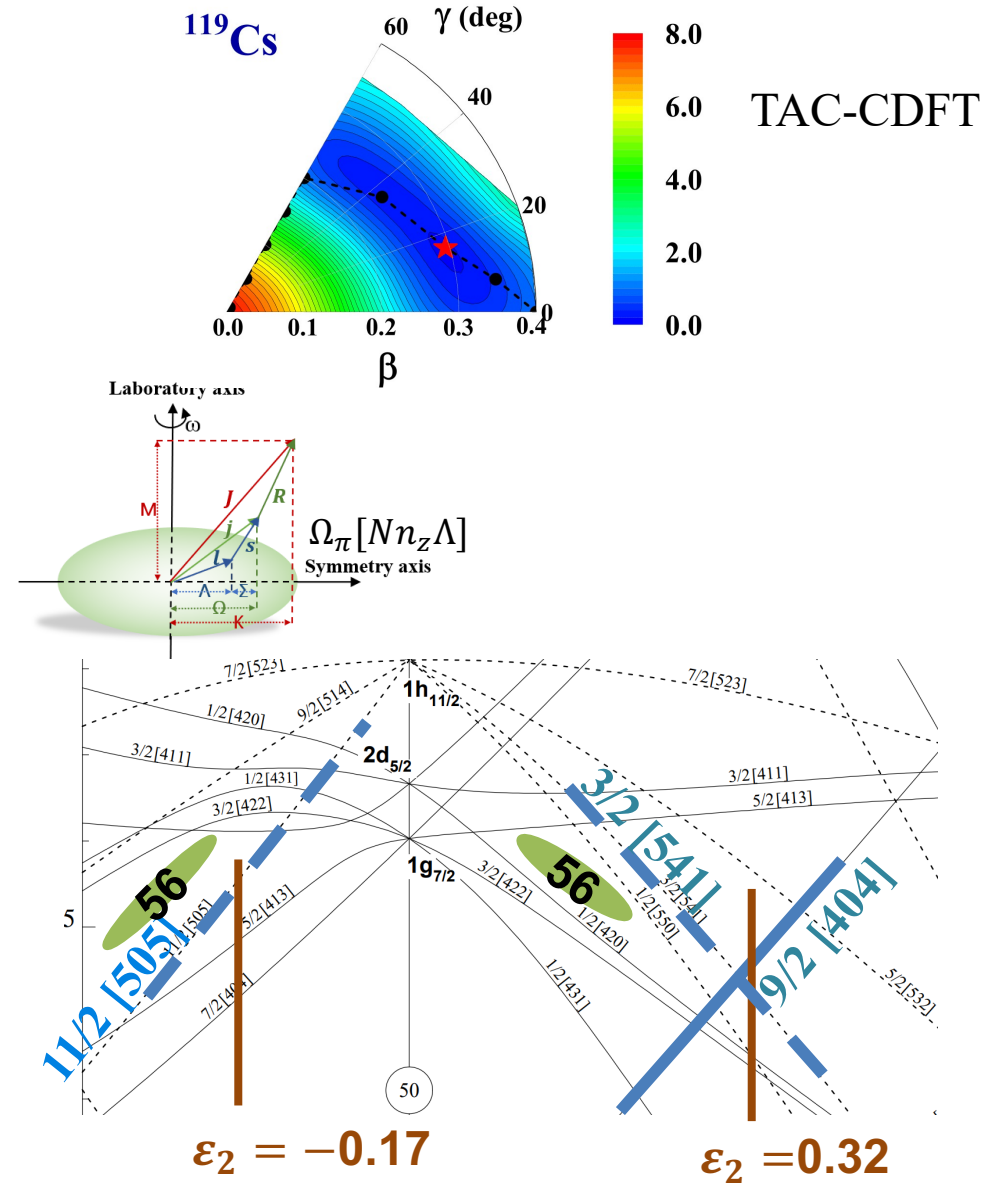
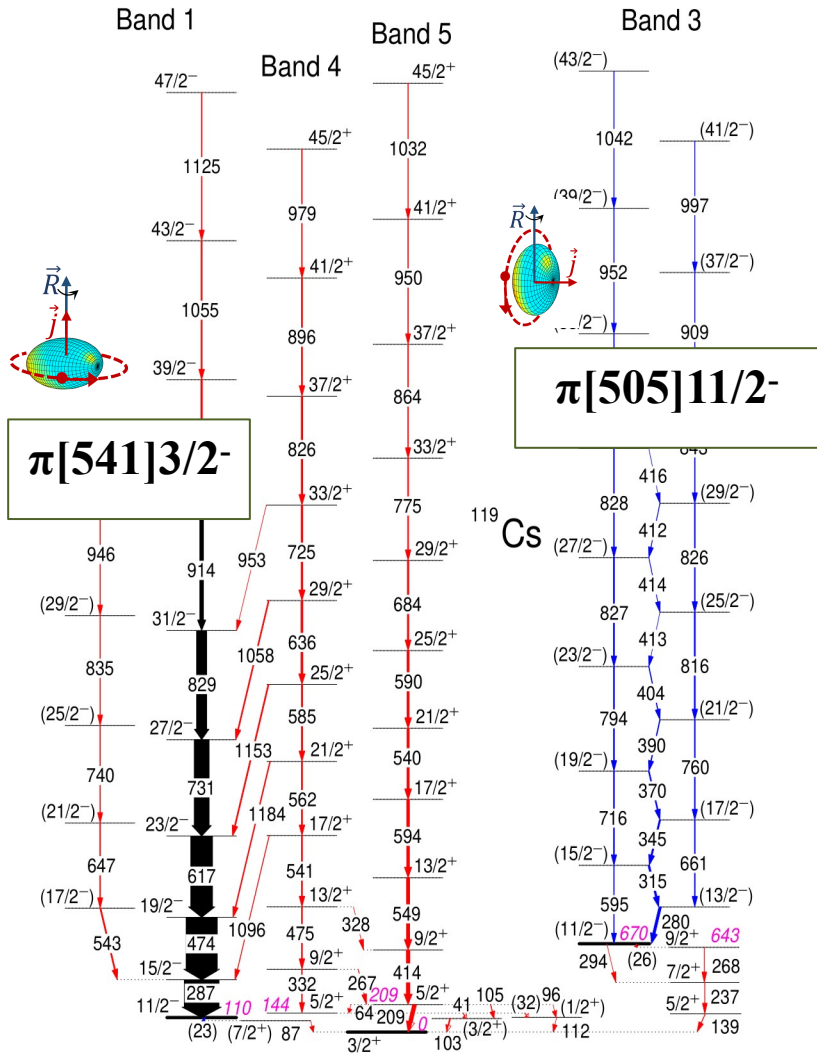
K. Starosta, Nucl. Instrum. Meth. Phys. Res. A423, 16 (1999)

A. Herzán, Phys. Rev. C 92, 044310 (2015)

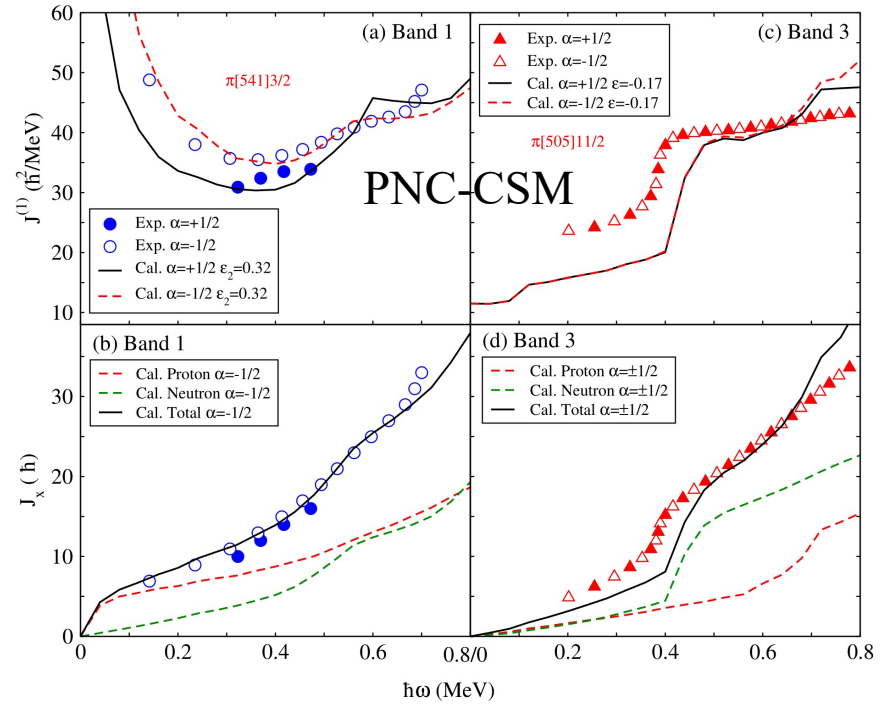
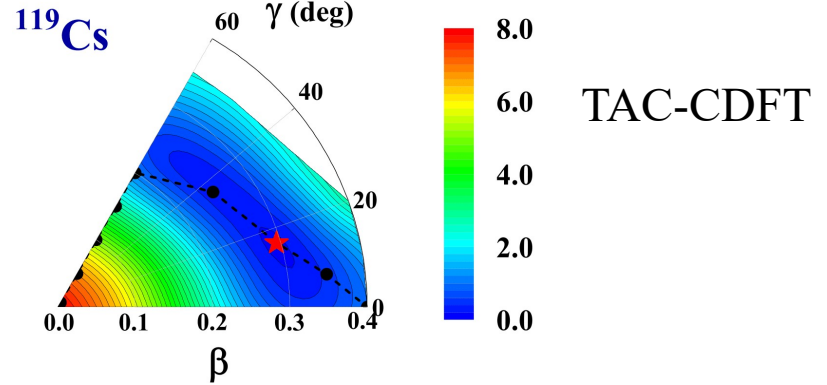
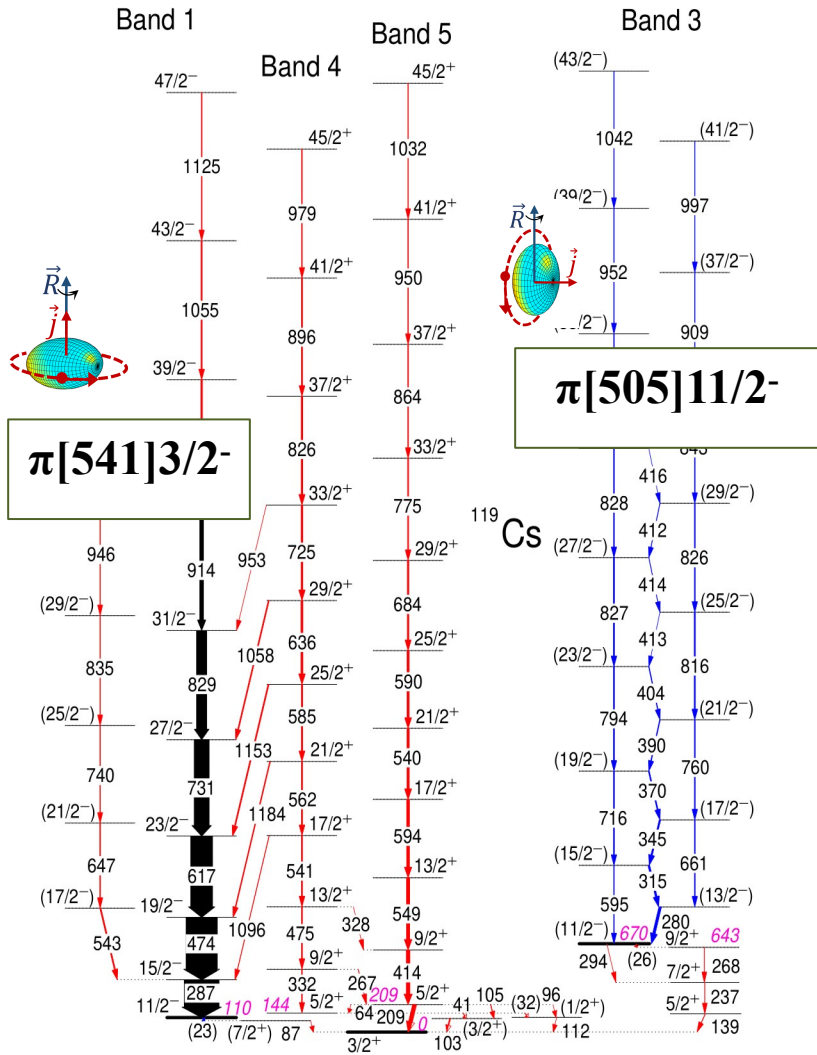
- Introduction
- Experimental details
- **Results and discussion**
  - $^{119}\text{Cs}$
  - $^{119}\text{Ba}$
  - $^{118}\text{Cs}$
- Conclusion



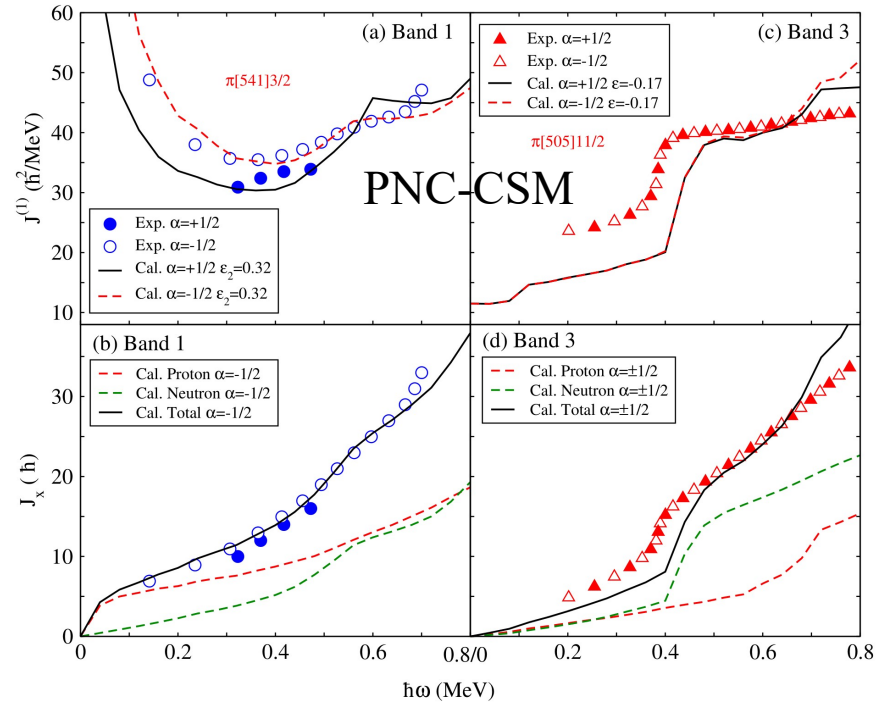
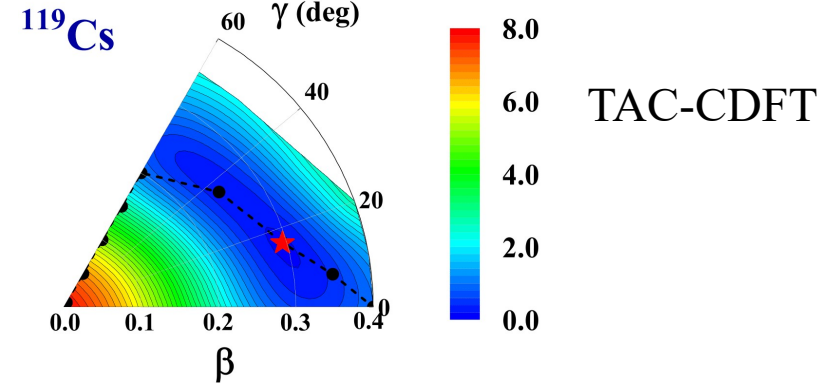
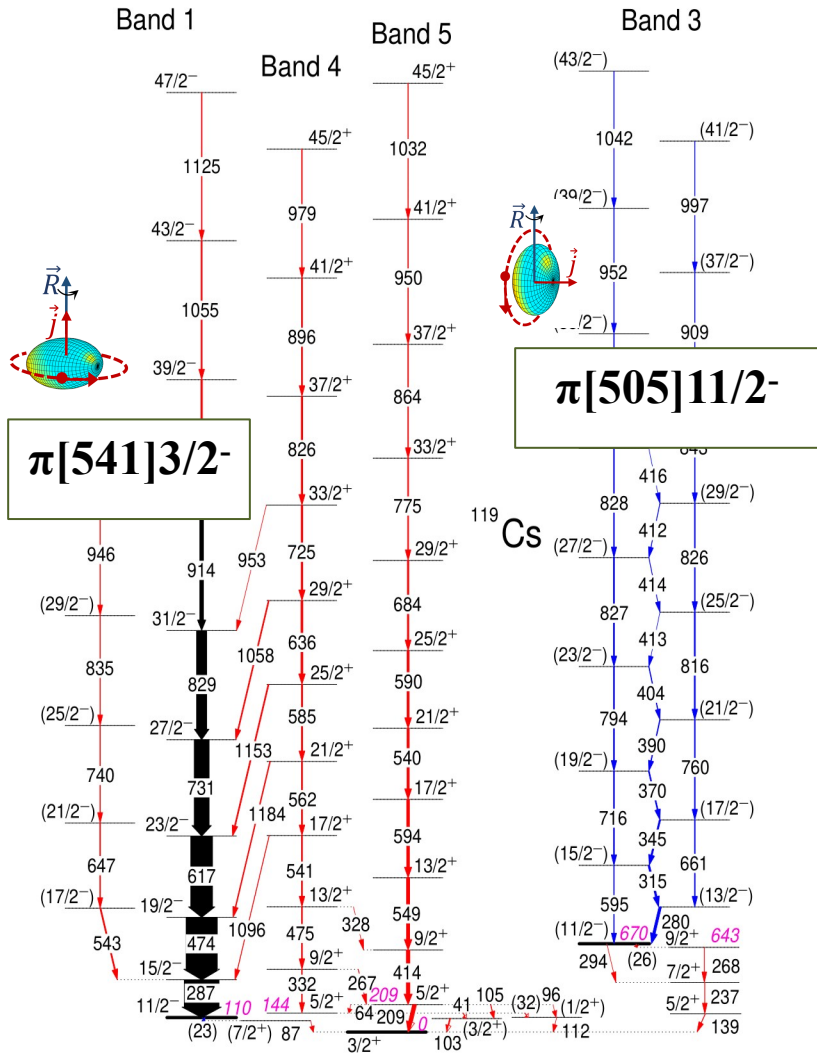
# Oblate-prolate shape coexistence in $^{119}\text{Cs}$



# Oblate-prolate shape coexistence in $^{119}\text{Cs}$

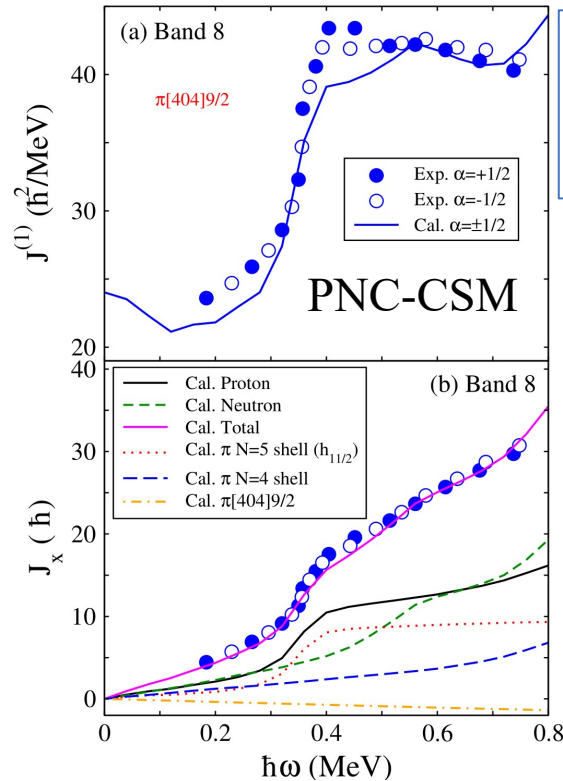


# Oblate-prolate shape coexistence in $^{119}\text{Cs}$

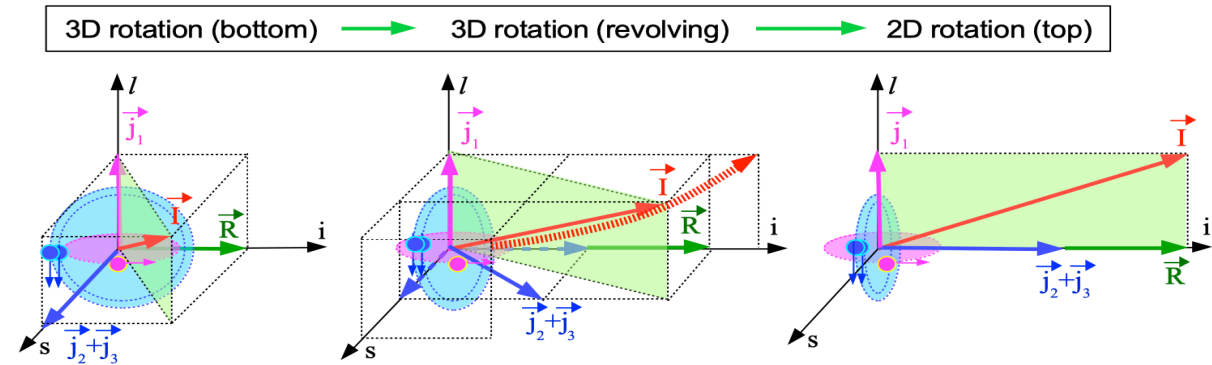


We observed for the first time the **oblate-prolate shape coexistence** in the 120 mass region.

# Proton based revolving chiral bands in $^{119}\text{Cs}$



Bands 8, 9 are built on the **three-proton configuration** in the backbending region, one in the **high- $\Omega$  [404]9/2** orbital and two in **low- $\Omega$   $h_{11/2}$**  orbitals.



Gamma band with Chiral character

We observed for **the first time such chiral doublet band:**

the configuration is formed by only protons;

the total angular momentum is revolving in 3D;

the triaxiality is not maximum ( $10^\circ$ - $15^\circ$ );

one proton keeps aligned along the long axis, while the other two are changing their orientation.



# Acknowledgments

## Neutron excitations in $^{119}\text{Ba}$

K. K. Zheng,<sup>1,2</sup> C. M. Petrache<sup>3</sup>,<sup>1</sup> Z. H. Zhang,<sup>4</sup> M. Luoma,<sup>4</sup> J. Ojala,<sup>4</sup> J. Pakarinen,<sup>4</sup> J. Uusitalo,<sup>4</sup> G. Zimba,<sup>4</sup> B. Cederwall,<sup>6</sup> B. M. Nyakó,<sup>8</sup> D. Sohler,<sup>1</sup> Université

Evidence of oblate-prolate shape coexistence in the strongly-deformed nucleus  $^{119}\text{Cs}$

KK Zheng<sup>a,b</sup>, CM Petrache<sup>a,\*</sup>, ZH Zhang<sup>c</sup>, PW Zhao<sup>d</sup>, YK Wang<sup>d</sup>, A. Astier<sup>a</sup>, J. Pakarinen<sup>e</sup>, M. Luoma<sup>e</sup>, J. Ojala<sup>e</sup>, G. Zimba<sup>e</sup>, M. Sandzelius<sup>e</sup>, J. Sarén<sup>e</sup>, W. Zhang<sup>g</sup>, M. Doncel<sup>f</sup>,

## Complete set of proton excitations in $^{119}\text{Cs}$

K. K. Z  
M. Lu  
J. Uusita

Rich band structure and multiple long-lived isomers in the odd-odd  $^{118}\text{Cs}$  nucleus

K. K. Zheng,<sup>1,2</sup> C. M. Petrache,<sup>1</sup> Z. H. Zhang,<sup>3</sup> A. Astier,<sup>1</sup> B. F. Lv,<sup>1,\*</sup> P. T. Greenlees,<sup>4</sup> T. Grahn,<sup>4</sup> R. Julin,<sup>4</sup> S. Juutinen,<sup>4</sup> M. Luoma,<sup>4</sup> J. Ojala,<sup>4</sup> J. Pakarinen,<sup>4</sup> J. Partanen,<sup>4,†</sup> P. Rahkila,<sup>4</sup> P. Ruotsalainen,<sup>4</sup> M. Sandzelius,<sup>4</sup> J. Sarén,<sup>4</sup> H. Tann,<sup>4,5</sup> J. Uusitalo,<sup>4</sup> G. Zimba,<sup>4</sup> B. Cederwall,<sup>6</sup> Ö. Aktas,<sup>6</sup> A. Ertoprak,<sup>6</sup> W. Zhang,<sup>6</sup> S. Guo,<sup>2,7</sup> M. L. Liu,<sup>2,7</sup> X. H. Zhou,<sup>2,7</sup> I. Kuti,<sup>8</sup> B. M. Nyakó,<sup>8</sup> D. Sohler,<sup>8</sup> J. Timár,<sup>8</sup> C. Andreoiu,<sup>9</sup> M. Doncel,<sup>5</sup> D. T. Joss,<sup>5</sup> and R. D. Page<sup>5</sup>

<sup>1</sup>Université Paris-Saclay, CNRS/IN2P3, IJCLab, 91405 Orsay, France

<sup>2</sup>Key Laboratory of High Precision Nuclear Spectroscopy and Center for Nuclear Matter Science, Institute of Modern Physics, Chinese Academy of Sciences, Lanzhou 730000, People's Republic of China

<sup>3</sup>Mathematics and Physics Department, North China Electric Power University, Beijing 102206, China

<sup>4</sup>University of Jyväskylä, Department of Physics,

P.O. Box 35, FI-40014, University of Jyväskylä, Finland

<sup>5</sup>Oliver Lodge Laboratory, Department of Physics,

University of Liverpool, Liverpool L69 7ZE, United Kingdom

<sup>6</sup>KTH Department of Physics, S-10691 Stockholm, Sweden

<sup>7</sup>School of Nuclear Science and Technology, University of Chinese Academy of Science, Beijing 100049, People's Republic of China

<sup>8</sup>Institute for Nuclear Research (Atomki), 4001 Debrecen, Hungary

<sup>9</sup>Department of Chemistry, Simon Fraser University, Burnaby, BC V5A 1S6, Canada

# Thanks for your attention

# Cross section

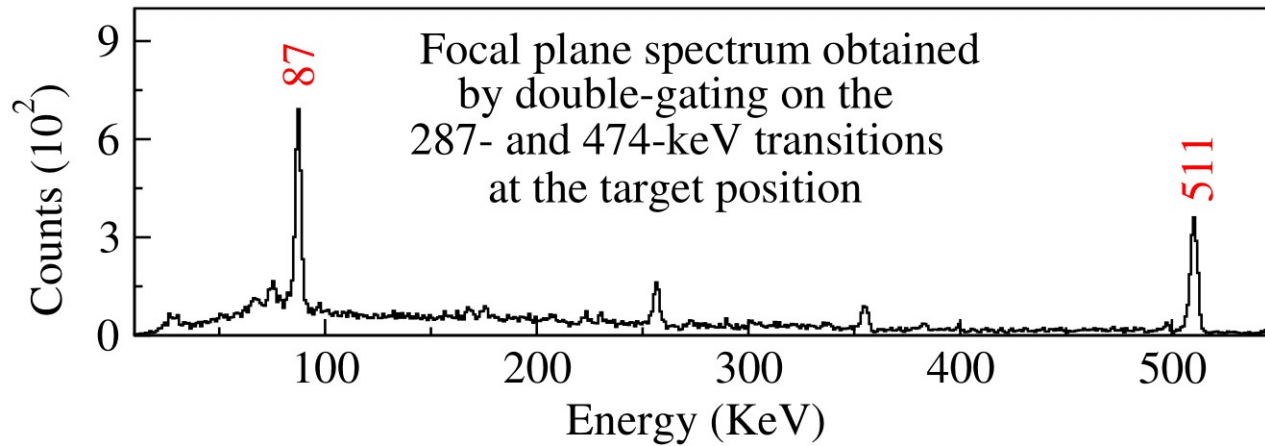
Mass	114	115	116	117	118	119	120	121
$^{52}\text{Te}$	2 mb							
$^{53}\text{I}$		20 mb						
$^{54}\text{Xe}$		2 mb	20 mb	6 mb	90 mb			
$^{55}\text{Cs}$				6 mb	35 mb	140 mb		
$^{56}\text{Ba}$					1 mb	20 mb	100 mb	
$^{57}\text{La}$							4 mb	7 mb

Changed states: 27, 28, 29, 30

m/q overlap: 120/116 119/115 118/114

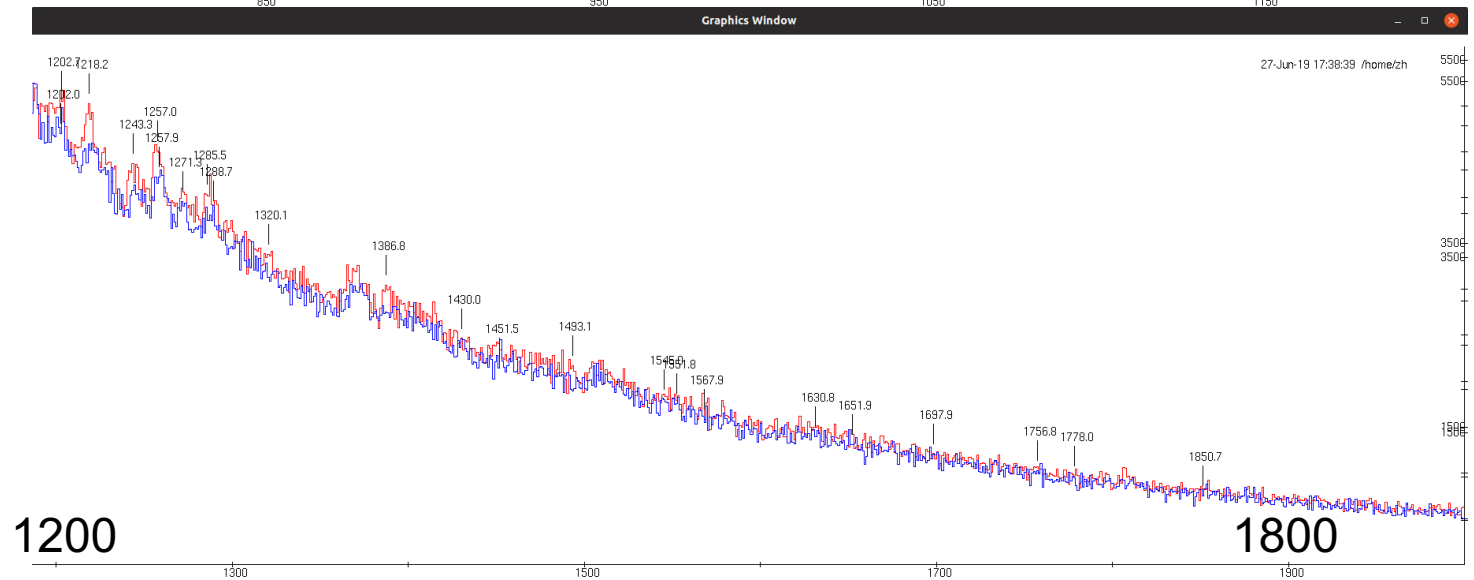
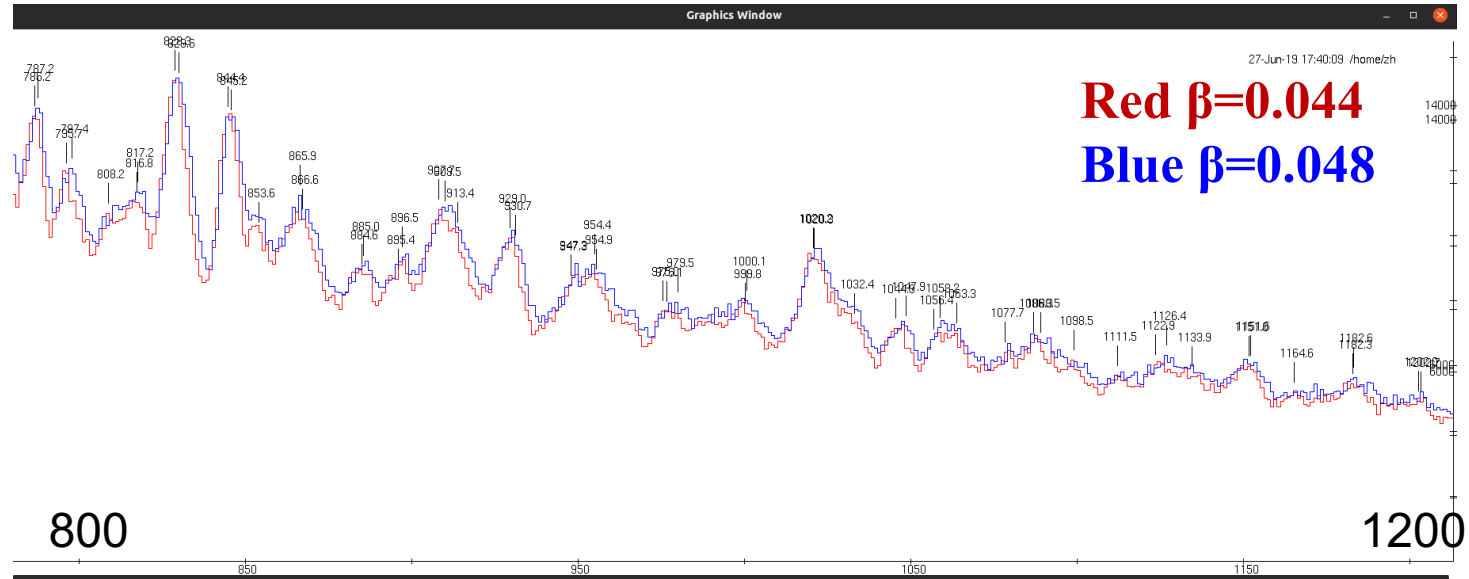
# isomer of $^{119}\text{Cs}$

## Background 511-keV

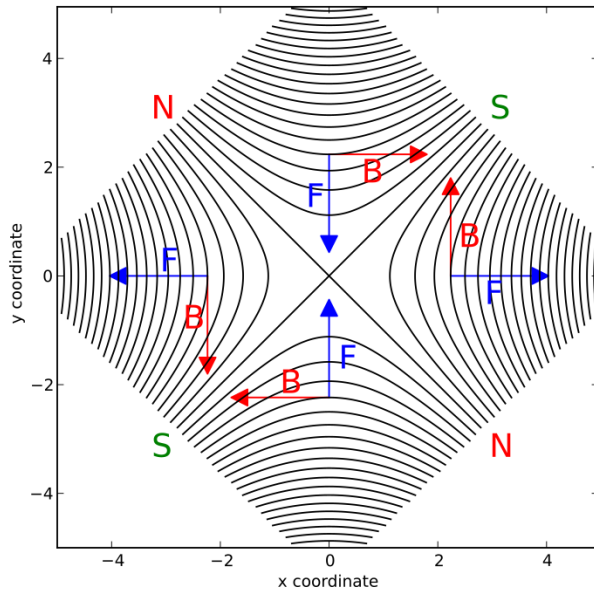




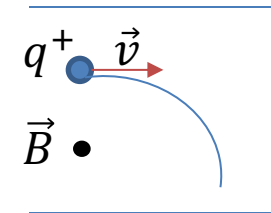
# Doppler shift correction



# QQQ D<sub>E</sub> D<sub>M</sub>



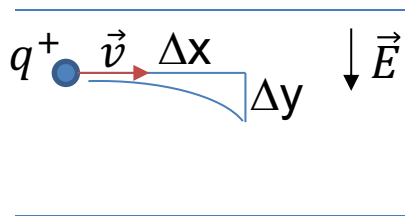
$$\vec{F} = q \vec{v} \times \vec{B}$$



Centrifugal = Lorentz force

$$m \frac{v^2}{\rho} = qvB$$

$$\frac{p}{q} = B\rho$$



$$m\ddot{y} = qE$$

$$\Delta y = \frac{qE}{m} \left( \frac{\Delta x}{v} \right)^2$$

$$\Delta y \propto \frac{1}{mv^2} \propto \frac{1}{E_c}$$

# $\kappa$ and $\mu$

The term  $V'$  of the Nilsson potential is of the form

$$V' = -\kappa(N)\hbar\omega_0\{2l_i \cdot s + \mu(N)(l_i^2 - \langle l_i^2 \rangle_N)\}$$

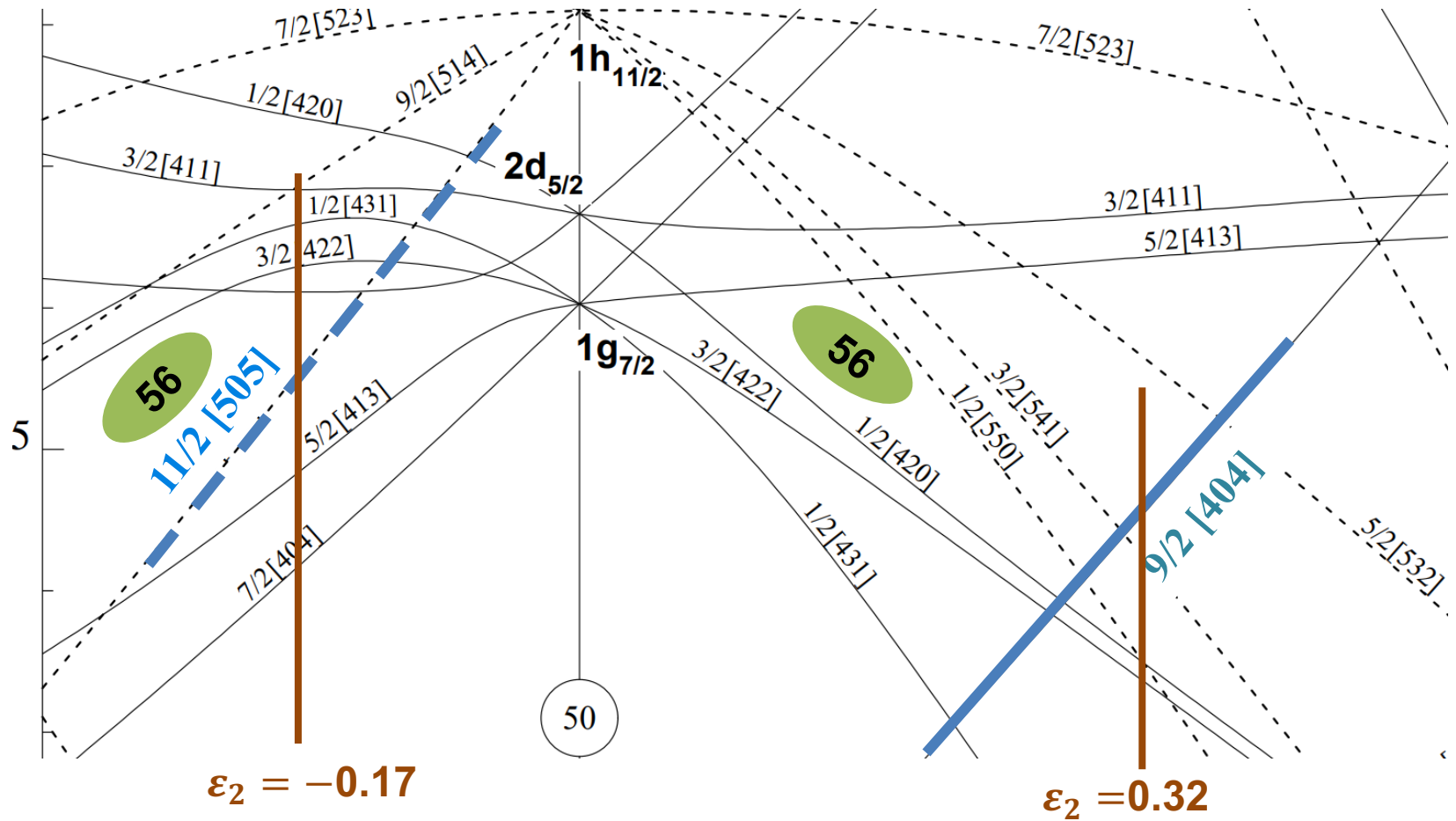
*T. Bengtsson, I. Ragnarsson / Rotational bands*

TABLE I

The modified oscillator parameters,  $\kappa$  and  $\mu$ , which have been used in this work

$N_{\text{rot}}$	Protons		Neutrons	
	$\kappa$	$\mu$	$\kappa$	$\mu$
0	0.120	0.00	0.120	0.00
1	0.120	0.00	0.120	0.00
2	0.105	0.00	0.105	0.00
3	0.090	0.30	0.090	0.25
4	0.065	0.57	0.070	0.39
5	0.060	0.65	0.062	0.43
6	0.054	0.69	0.062	0.34
7	0.054	0.69	0.062	0.26
8	0.054	0.69	0.062	0.26

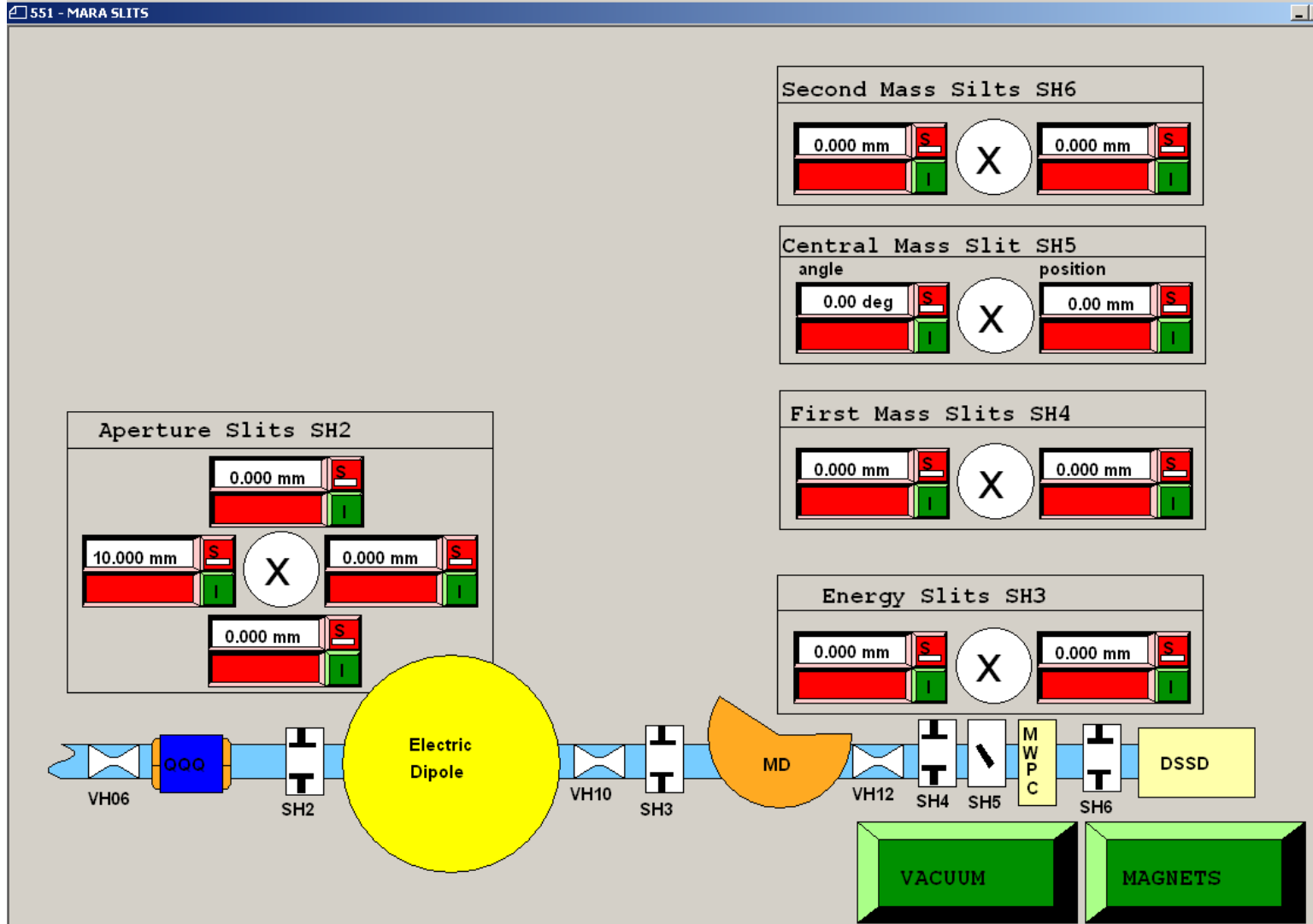
# Nilsson Diagram (Proton)



# MARA

<b>Quadrupole triplet</b>	<b>Q<sub>1</sub></b>	<b>Q<sub>2,3</sub></b>
Optical length	25 cm	35 cm
Bore diameter	10 cm	15 cm
Maximum field gradient	10 T/m	10 T/m
Nominal field relative to $B\rho$	0.4698 T/ $B\rho$	0.5859, 0.2387 T/ $B\rho$
<b>Sector fields</b>	<b>Electrostatic</b>	<b>Magnetic</b>
Radius of curvature, $\rho$	4.000 m	1.000 m
Bending angle, $\phi$	20°	40°
Vertical gap	14 cm	20 cm (active)
Horizontal gap	10 cm (active)	10 cm
Maximum rigidity	14.2 MV	1 Tm
Inclination of EFB (entrance and exit)		8°
EFB curvature radii (entrance and exit)		2.0 m
Height of the gap in the anode	1.5 cm (extending from $\approx 10^\circ$ to $\approx 19^\circ$ )	
<b>Drift lengths</b>	<b>Length [cm]</b>	
Target – Q <sub>1</sub>	35	
Q <sub>1</sub> – Q <sub>2</sub>	14	
Q <sub>2</sub> – Q <sub>3</sub>	16	
Q <sub>3</sub> – Deflector EFB	30	
Deflector EFB – Dipole EFB	80	
Dipole EFB – Focal plane	205.8	

# Slits



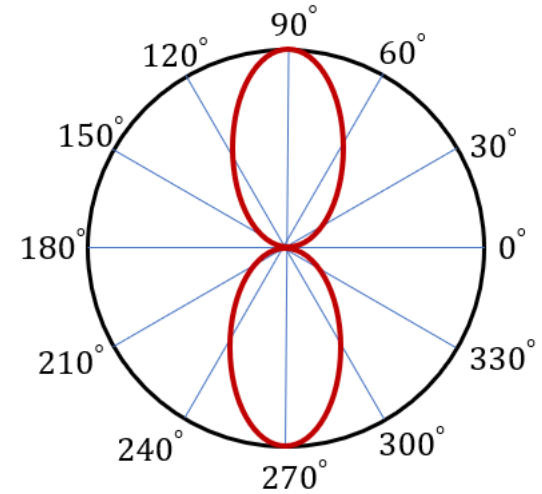


# PDCO

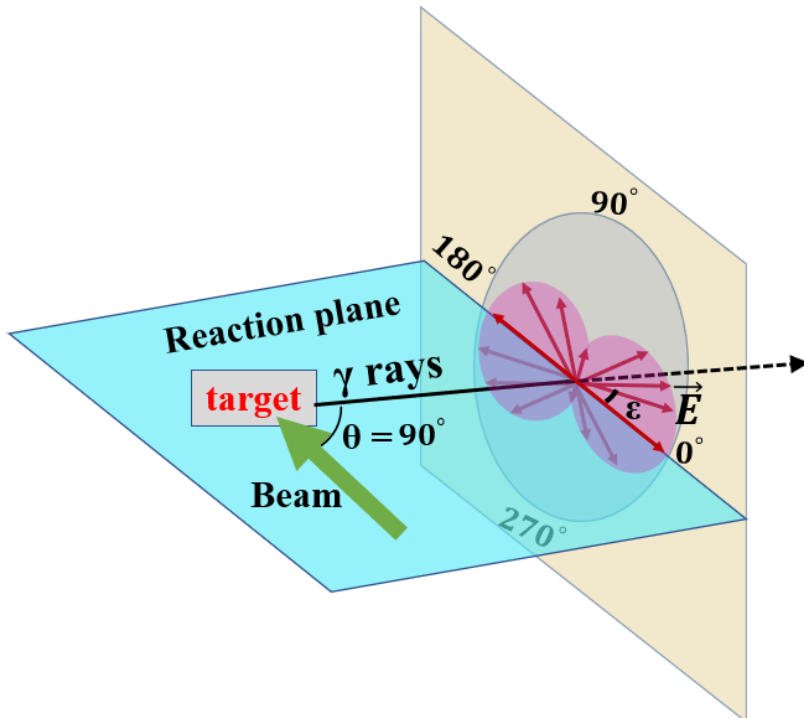
For an axially oriented nucleus, the transitions have a linear polarization defined by

$$p(\theta) = \frac{w(\theta, \epsilon = 0^\circ) - w(\theta, \epsilon = 90^\circ)}{w(\theta, \epsilon = 0^\circ) + w(\theta, \epsilon = 90^\circ)}$$

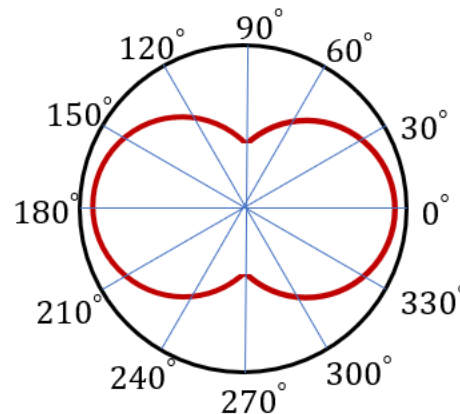
$$W(\theta, \epsilon) = \frac{d\Omega}{8\pi} \sum_{\lambda=\text{even}} B_\lambda U_\lambda [A_\lambda P_\lambda(\cos \theta) + 2A_{2\lambda} P_{2\lambda}^{(2)}(\cos \theta) \cos 2\epsilon]$$



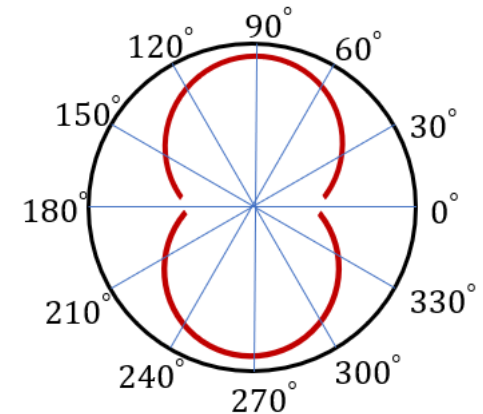
$p(\theta)$  for  $E_1$   $E_2$  or  $M_1$



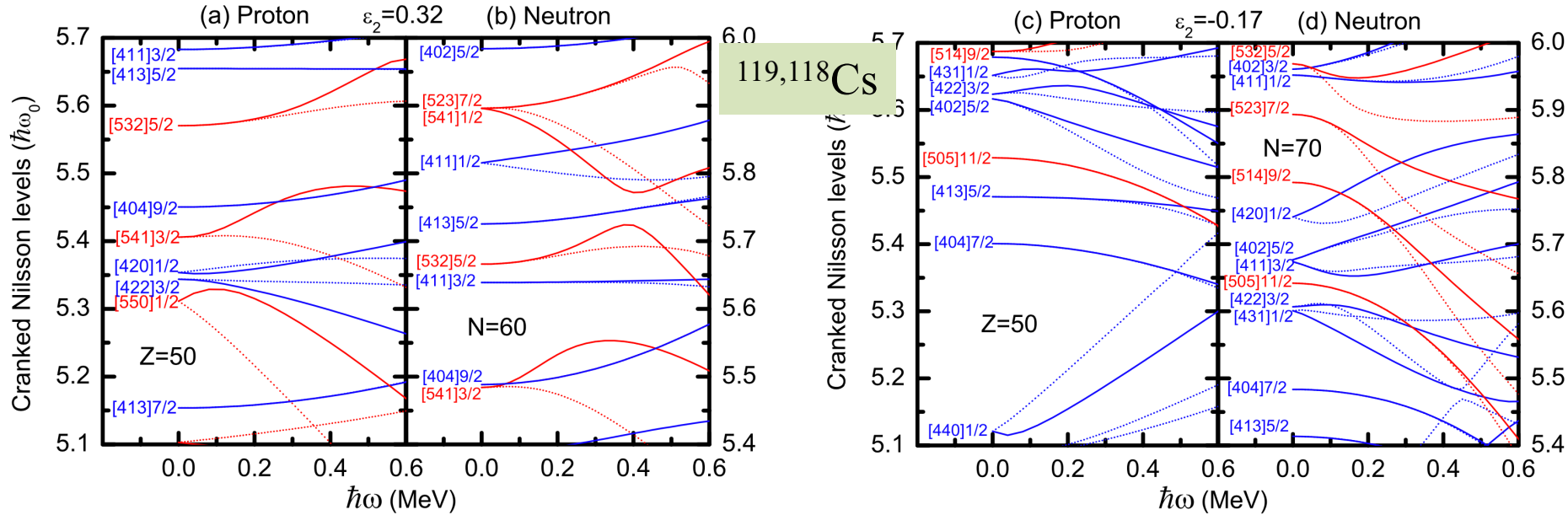
$W^{E_1 \text{ or } E_2}(\theta = 90^\circ, \epsilon)$



$W^{M_1}(\theta = 90^\circ, \epsilon)$

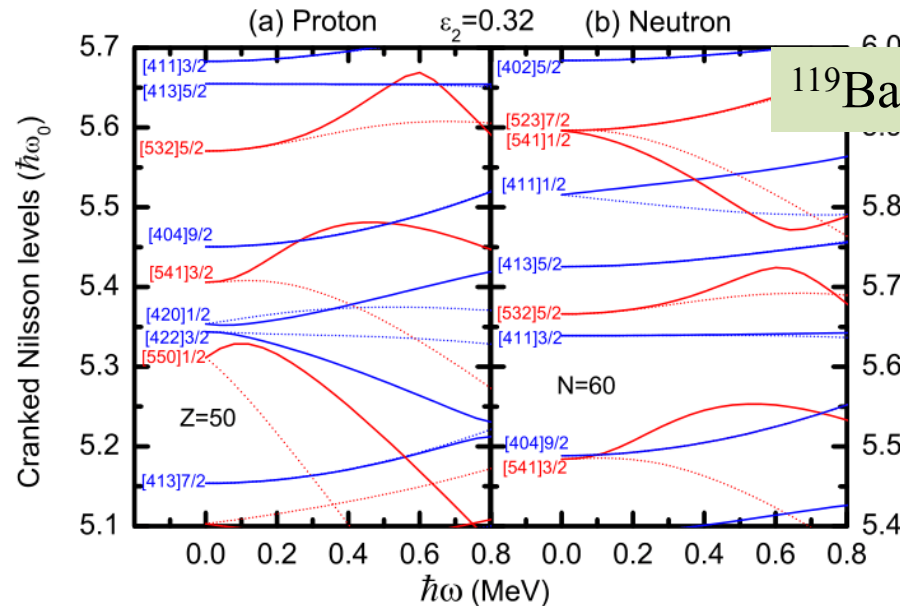


# Cranked Nilsson levels



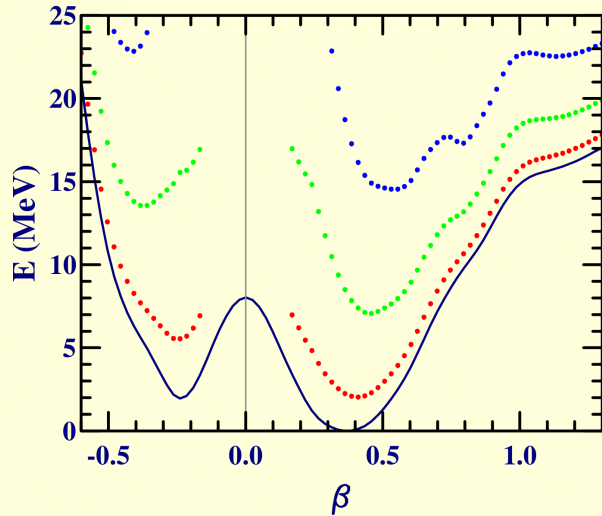
Positive parity

Negative parity



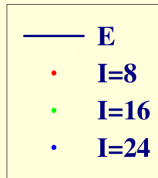
# Shape coexistence

<sup>120</sup>Ba<sub>64</sub>



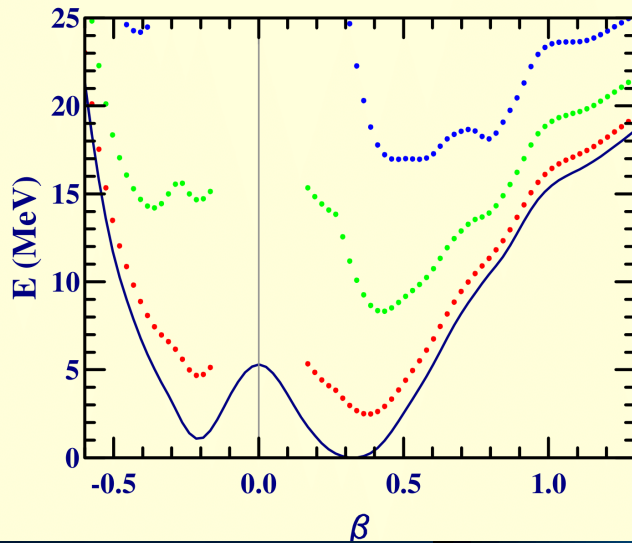
**Binding energy**

HFB=990.940 MeV  
Exp=993.63 MeV



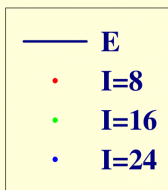
HFB-D1S Bruyères-le-Châtel

<sup>118</sup>Xe<sub>64</sub>

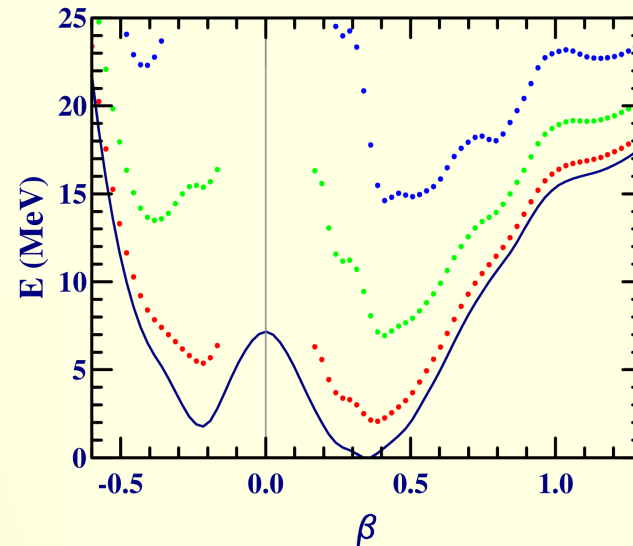


**Binding energy**

HFB=984.825 MeV  
Exp=987.88 MeV

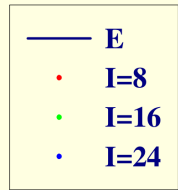


<sup>119</sup>Cs<sub>64</sub>



**Binding energy**

HFB=987.262 MeV  
Exp=989.77 MeV



HFB-D1S Bruyères-le-Châtel

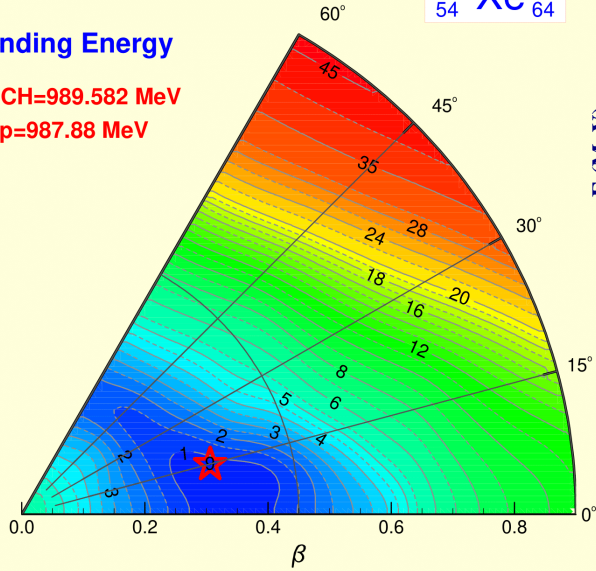
# Shape coexistence

cea

Binding Energy

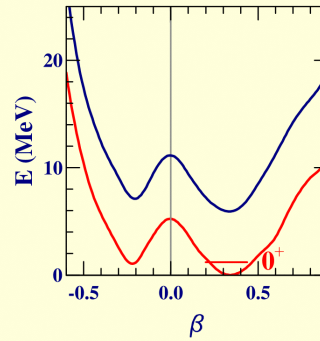
5DCH=989.582 MeV  
Exp=987.88 MeV

$^{118}_{54}\text{Xe}_{64}$



HFB-D1S Bruyères-le-Châtel

— HFB+ZPE  
— HFB

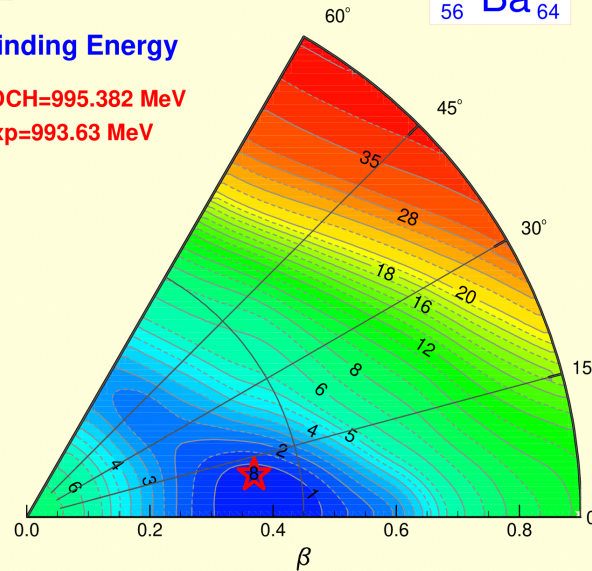


cea

Binding Energy

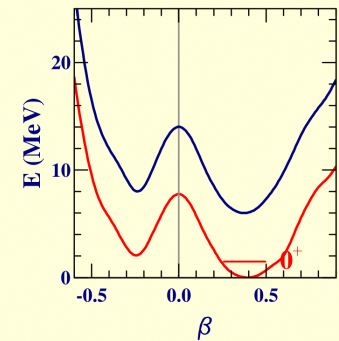
5DCH=995.382 MeV  
Exp=993.63 MeV

$^{120}_{56}\text{Ba}_{64}$

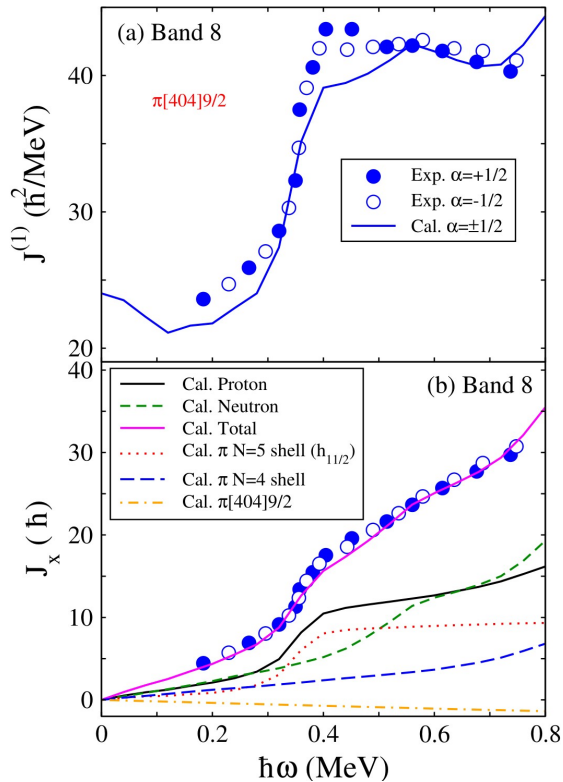


HFB-D1S Bruyères-le-Châtel

— HFB+ZPE  
— HFB



# Proton based revolving chiral bands in $^{119}\text{Cs}$



K value :  $K=4.5(\text{B8},\text{B9})$ ;  
 $K=0.5 (\text{B10})$ .

The Harris parameters:

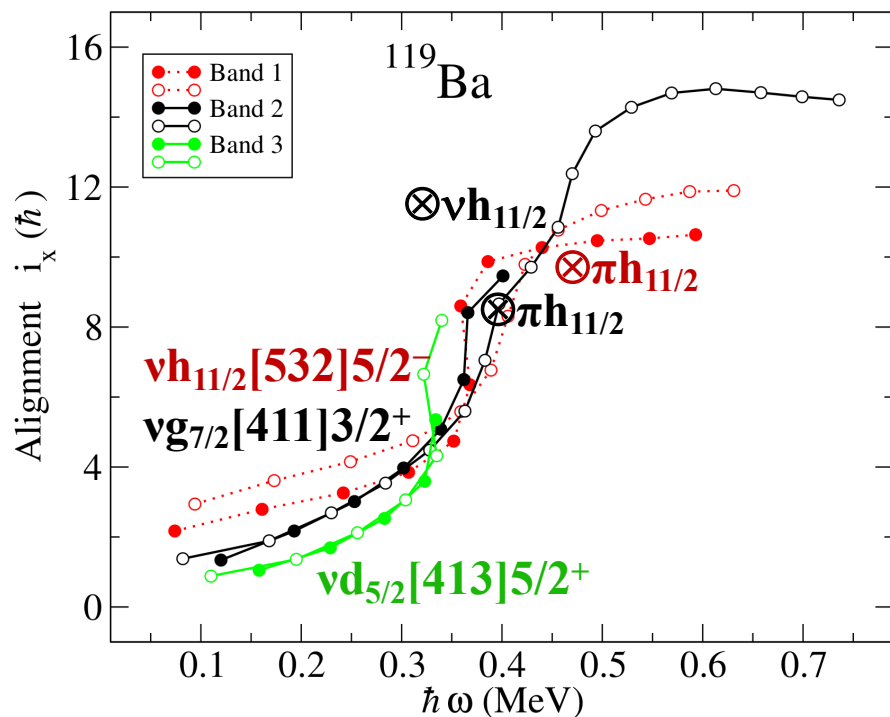
$$J_0 = 17 \hbar^2 \text{MeV}^{-1}$$

$$J_1 = 25 \hbar^4 \text{MeV}^{-3}.$$

The gain of angular momentum is  $\approx 8\hbar$ , alignment of a pair of  $h^{11/2}$  particle, negligible contribution of the strongly-coupled  $[404]9/2^+$  proton orbital.

Bands 8, 9 are nearly degenerate, have similar moments of inertia and  $B(\text{M1})/B(\text{E2})$  ratios of reduced transition probabilities.

# Results: alignment analysis of $^{119}\text{Ba}$



The **K** values: 2.5, 2.5, and 1.5 for Bands 1, 2, and 3.

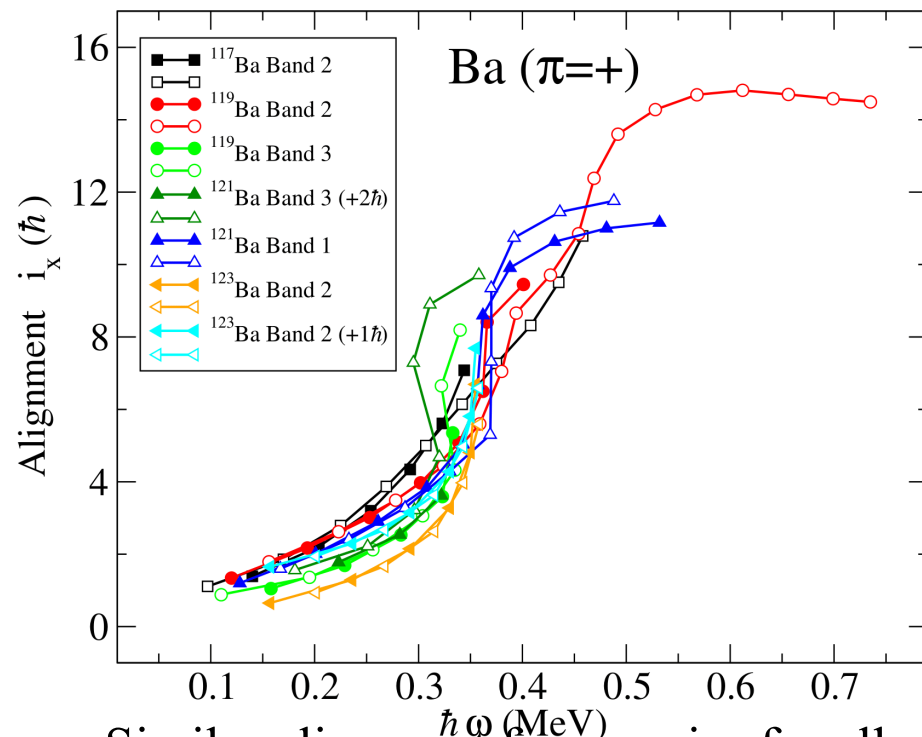
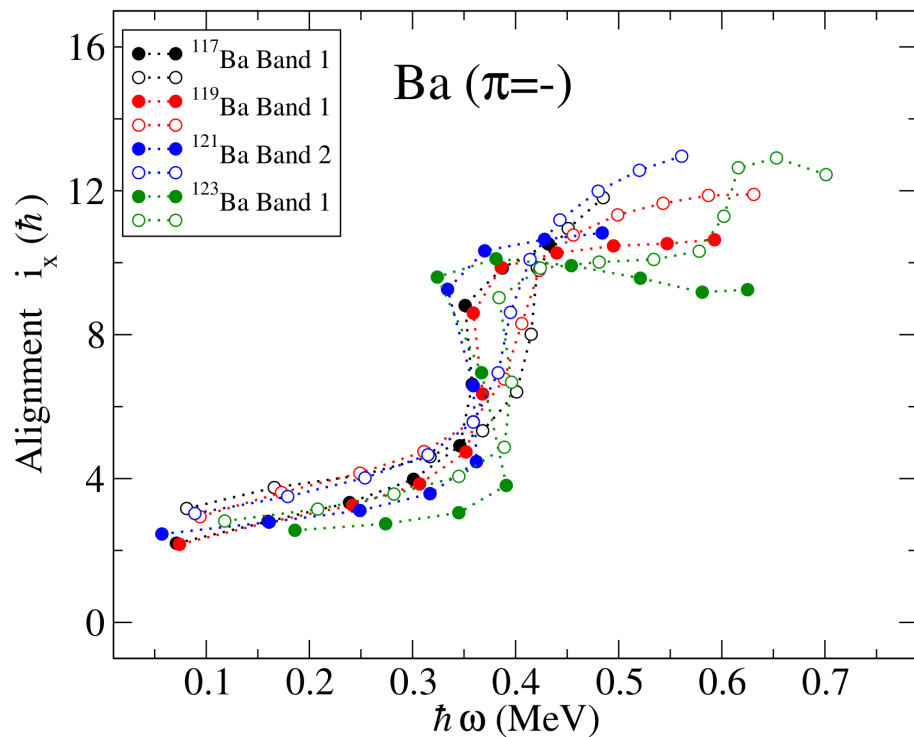
**Band 1:** a large signature splitting  
**Bands 2, 3:** zero signature splitting.

**Bands 1, 2:** alignment occurs at rotational frequency of  $\hbar\omega \approx 0.35$  MeV  
**Band 3:** more sharp, lower deformation

As Bands 2 and 3 are assigned to the  $vd_{5/2}[413]5/2^+$  and  $vg_{7/2}[411]3/2^+$  configurations, respectively, one would expect a higher alignment in Band 3, which is in contrast with the experimental alignment which is smaller than in Band 2. However, as the two configurations assigned to Bands 2 and 3 are **strongly mixed**, the K-values are difficult to define. An intermediate  $K = 2$  value would lead to very similar alignments of the two bands.



# Results: alignment analysis of $^{119}\text{Ba}$



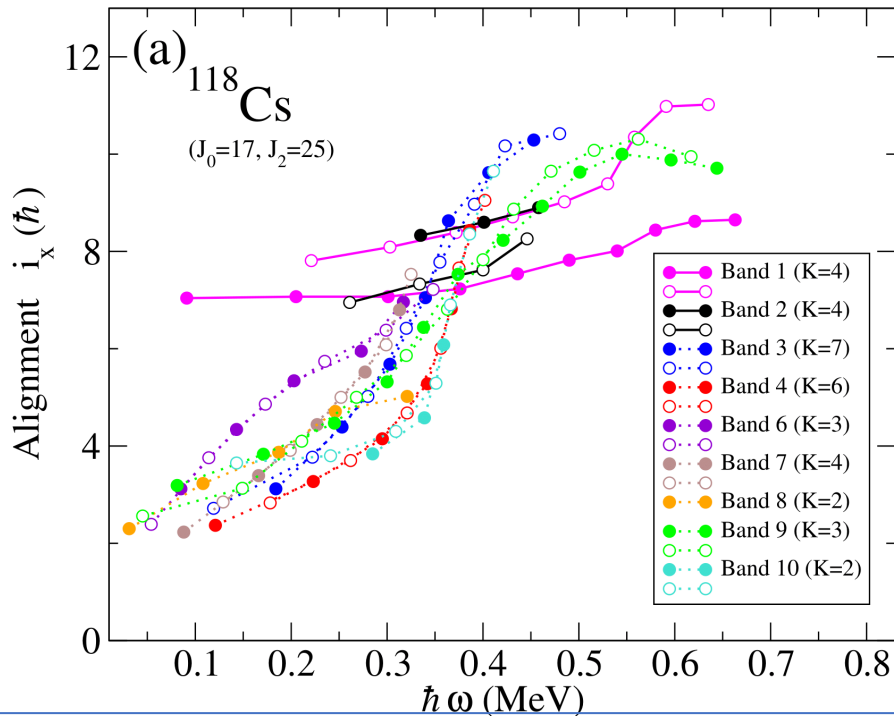
$\alpha = -1/2$  signature partners are sharper than that of the  $\alpha = +1/2$ . This sharpness increases with the neutron number; Only in the negative-parity signature of Band 1 in  $^{123}\text{Ba}$  a second alignment at  $\hbar\omega \approx 0.6$  MeV has been observed.

Similar alignment frequencies for all bands excepting Bands 3 of  $^{119}\text{Ba}$  and  $^{121}\text{Ba}$  (sharper).

$^{119}\text{Ba}$ ,  $\alpha = -1/2$  signature partners of Band 3 was observed after the second alignment up to high spin.

$^{117}\text{Ba}$ , the alignment of the negative-signature partner of Band 2 is more gradual, and no second alignment was

# Results: alignment analysis of $^{118}\text{Cs}$



**Bands 1, 2:** the alignment exhibited in Band 1 is around  $7\hbar$ , in agreement with the  $\pi[541]3/2 - \otimes \nu[532]5/2 -$  configuration previously assigned. the alignments exhibited by the two signature partners are very similar.

**Bands 3, 4:** The alignment of Band 3 is around  $2.5\hbar$  at low frequency, exhibits an alignment gain of  $\approx 8\hbar$  at  $\hbar\omega \approx 0.35$  MeV, and saturates at  $i_x \approx 10\hbar$  at high frequency.

**Bands 6, 7:** exhibiting smooth up-bends with steeper slopes than in the other bands. They are composed of degenerate signature partners, and are not connected by any transition.

**Bands 8, 9, 10:** interconnected by several transitions. the alignment exhibited by Bands 8 and 9 are similar, but more gradual than those of Bands 3 and 4. An alignment gain of  $\approx 7\hbar$  at  $\hbar\omega \approx 0.35$  MeV is exhibited, which saturates at high frequency at  $i_x \approx 10\hbar$ , like in Band 3.